universität
wien

DISSERTATION

Titel der Dissertation

„Role of MEK1 in the crosstalk

between signaling cascades"

Verfasserin

Mag. Katarina Zmajkovicova

angestrebter akademischer Grad

Doctor of Philosophy (PhD)

Wien, 2013

ACKNOWLEDGEMENTS

ABSTRACT

Signaling cascades control virtually all cellular processes. A signal that is received at the surface of a cell by receptors is transmitted by numerous signaling modules in the cell's interior to finally trigger an appropriate response. In mammals, the most intensely studied MAPK cascade is the RAS/RAF/MEK/ERK signaling module. It regulates many fundamental aspects of cell biology including proliferation, differentiation, apoptosis, and migration. However, signaling cascades should not be viewed as linear pipelines isolated from each other. In fact, intense crosstalk and mutual regulation exists among different pathways to ensure tight control and fine-tuning of the signals. The aim of the thesis is to study the crosstalk of the ERK pathway with the PI3K/AKT pathway via MEK1 kinase and its implications *in vivo*. These pathways negatively regulate each other, but the mechanism involved is incompletely understood.

Both ERK and AKT pathways are involved in correct functioning of the immune system and establishment of peripheral tolerance.

We now identify MEK1 as an essential regulator of lipid/protein phosphatase PTEN, through which it controls phosphatidylinositol-3-phosphate accumulation and AKT signaling. MEK1 ablation stabilizes AKT activation and, *in vivo*, causes a lupus-like autoimmune disease and myeloproliferation. Mechanistically, MEK1 is necessary for PTEN membrane recruitment as part of a ternary complex containing the multidomain adaptor MAGI1. Complex formation is independent of MEK1 kinase activity but requires phosphorylation of T292 on MEK1 by activated ERK. Thus, inhibiting the ERK pathway reduces PTEN membrane recruitment, increasing phosphatidylinositol-3-phosphate accumulation and AKT activation.

The presented work provides mechanistic insights in the crossregulation of the MEK/ERK and AKT signaling. Our data also offer a conceptual framework for the observation that activation of the PI3K pathway frequently mediates resistance to MEK inhibitors, and for the promising results obtained by combined MEK/PI3K inhibition in preclinical cancer models.

ZUSAMMENFASSUNG

Sämtliche Prozesse innerhalb einer Zelle werden durch intrazelluläre Signalkaskaden kontrolliert. Extrazelluläre Signale aus der Umgebung werden nach Bindung und Aktivierung von Rezeptoren an der Zelloberfläche oder im Inneren der Zelle durch eine Vielzahl von Signalmolekülen weitergeleitet, was letztlich zu einer spezifischen Antwort der Zelle führt. Der MAPK Signalweg, bestehend aus den Signalmolekülen RAS/RAF/MEK/ERK, reguliert grundlegende zelluläre Funktionen wie Proliferation, Differentierung, Apoptose und Migration und wurde daher in der Vergangenheit speziell in Säugern intensiv untersucht. Neueste Studien haben gezeigt, dass Signaltransduktionswege in Zellen nicht isoliert voneinander betrachtet werden dürfen. Die Kontrolle der Signalweiterleitung, abgestimmt auf die jeweils biologischen Erfordernisse einer Zelle, gleicht viel eher einem Netzwerk von verschiedenen Kaskaden, die miteinander interagieren und sich gegenseitig beeinflussen. Ziel der vorliegenden Arbeit ist die Interaktion des ERK Signalweges mit dem PI3K/AKT Signalweg über die MEK1 Proteinkinase sowie die Auswirkungen dieser Interaktion *in vivo* zu untersuchen. Schon seit längerem konnte beobachtet werden, dass sich die beiden Signaltransduktionswege wechselseitig negativ regulieren. Eine Erklärung dafür aus mechanistischer Sicht konnte bisher noch nicht vorgelegt werden. Sowohl der ERK als auch der AKT Signalweg spielen eine bedeutende Rolle für die Funktion des Immunsystems und sind dabei unter anderem für die Induktion und Aufrechterhaltung der peripheren Toleranz zur Vermeidung von Autoimmunerkrankungen wichtig. Unsere Untersuchungen konnten zeigen, dass die MEK1 Proteinkinase ein essentieller Regulator der Lipid/Protein-Phosphatase PTEN ist. MEK1 kontrolliert dabei über die Akkumulation von Phosphatidylinositol-3-phosphat den AKT Signalweg. Fehlen von MEK1 stabilisiert die AKT Aktivierung und äußert sich phänotypisch in Form einer SLE-ähnlichen Autoimmunerkrankung begleitet von Zeichen der Myeloproliferation *in vivo*. Weiters konnte gezeigt werden, dass MEK1 Teil eines ternären Proteinkomplexes bestehend aus MEK1, PTEN und dem Adaptormolekül MAGI1 ist. Dieser Komplex rekrutiert als Folge der Zellstimulation PTEN an die cytoplasmatische Seite der Zellmembran. Die Bildung dieses Multi-Proteinkomplexes benötigt eine Phosphorylierung am T292 von MEK1 durch aktiviertes ERK und ist völlig unabhängig von MEK1 Kinaseaktivität. Die Inhibition des ERK Signalweges führt somit über die Reduktion von PTEN an der Zellmembran zur Akkumulation von Phosphatidylinositol-3-phosphat sowie zur Aktivierung von AKT. Neben der Aufklärung des biochemischen Mechanismus bezüglich der Interaktion und wechselseitigen Regulation zwischen dem MEK/ERK und AKT Signalweg, erklären die vorliegenden Daten weiters, dass die Resistenz gegenüber MEK Inhibitoren häufig durch die Aktivierung des PI3K Signalweges bedingt ist, was wiederum die Bedeutung einer Kombination von MEK/PI3K Inhibitoren für künftige zielgerichtete Therapieansätze in der Krebsbehandlung hervorhebt.

TABLE OF CONTENT

I. INTRODUCTION

1.1 Aim of the doctoral research

In our laboratory, we have a long standing interest in deciphering the signaling via the RAF/MEK/ERK pathway and its connections to other cellular signaling modules. We are particularly interested in the RAF and MEK kinases and their unique, isoform-specific functions *in vivo*. This project is focused on the MEK1 kinase. The lab has recently identified its essential role in controlling the strength and duration of the ERK signal in the context of MEK1/MEK2 heterodimers [1].

As a follow-up of this study, we wanted to investigate the possible role of MEK1 in the crosstalk to other signaling pathways. Preliminary results (obtained by Gloria Reyes and Federica Catalanotti) suggested that MEK1 negatively controls the PI3K/AKT pathway via an unknown mechanism. The knockout (KO) of MEK1 results in an increased and prolonged AKT activation in mouse embryonic fibroblasts. The main aim of this project was to clarify the mechanism behind the crosstalk and identify the molecular partners involved in this regulatory process.

The second aim of the study was to study the phenotype of *Mek1^{f/f} Sox2-cre* mice (MEK1 KO mice). In these mice, Mek1 is deleted in all embryonic tissues, but not in the trophoblast in order to rescue placental development and therefore the embryonic lethality of the Mek1$^{-/-}$ mice [1]. The MEK1 KO mice have no obvious phenotype. However, we noticed an increased mortality rate and symptoms of a systemic autoimmune inflammatory disease in these mice (Veronika Jesenberger). Therefore, we set out to characterize the precise phenotype of these mice and the molecular mechanisms behind it.

The first part of the introduction describes the state-of-the-art about ERK and AKT signaling. The second part covers the basic background of immune tolerance, autoimmunity and the signaling involved in the pathogenesis of autoimmune diseases.

1.2 Cellular signaling and MAPK pathways

Cells need to communicate with their environment and with other cells to ensure their own correct functioning and the functioning of the whole organism. A signal that is received at the surface of a cell by receptors is transmitted by numerous signaling modules into the cell's interior to finally trigger the appropriate response. One of the challenges in cell biology is to decipher the precise mechanism and order of events in cellular signaling. A large number of signal transduction molecules have been already discovered, which are organized into signal transducing pathways such as the mitogen activated protein kinase (MAPK) pathways. MAPK cascades are evolutionary conserved in all eukaryotes and regulate many fundamental aspects of cell biology including proliferation, differentiation, apoptosis, and migration. There are four known MAPK pathways in vertebrates; ERK, JNK, p38 and ERK5. Each MAPK pathway contains a three-tiered kinase cascade comprising a MAP kinase kinase kinase (MAPKKK), a MAP kinase kinase (MAPKK) and the MAPK [2]. In mammals, the most intensely studied MAPK-cascade is the RAS/RAF/MEK/ERK signaling module.

1.3 RAS/RAF/MEK/ERK pathway

Activation of the pathway starts with the binding of a ligand to its receptor, often a receptor tyrosine kinase (RTK) (Fig 1). Growth factor stimulation promotes RTK dimerization and cross-phosphorylation on tyrosine residues [3]. The phospho-tyrosines serve as docking sites for signaling molecules and adaptor proteins that contain SH2 (Src homology region 2) or PTB (phosphotyrosine-binding) domains. Their binding leads to the recruitment of the RAS specific GEF Son of Sevenless (SOS). Once RAS is GTP-loaded and activated at the membrane, it can mediate RAF activation. RAF kinases further phosphorylate MEK kinases and these are able to prosphorylate and activate extracellular regulated kinase (ERK). ERK targets a large variety of substrates in the cytoplasma, cytoskeleton, nucleus and other cellular compartments [4]. Amplitude and duration of the signal are critical for cell signaling decisions [5]. Additional levels of complexity and fine-tuning within the cascade are provided by homo- and heterodimerization of the components (RAF, MEK and ERK isoforms) [6], as well as by their interaction with scaffolding proteins mediating their compartmentalization; and by the regulation through phosphatases and as well as through crosstalk to other pathways [7].
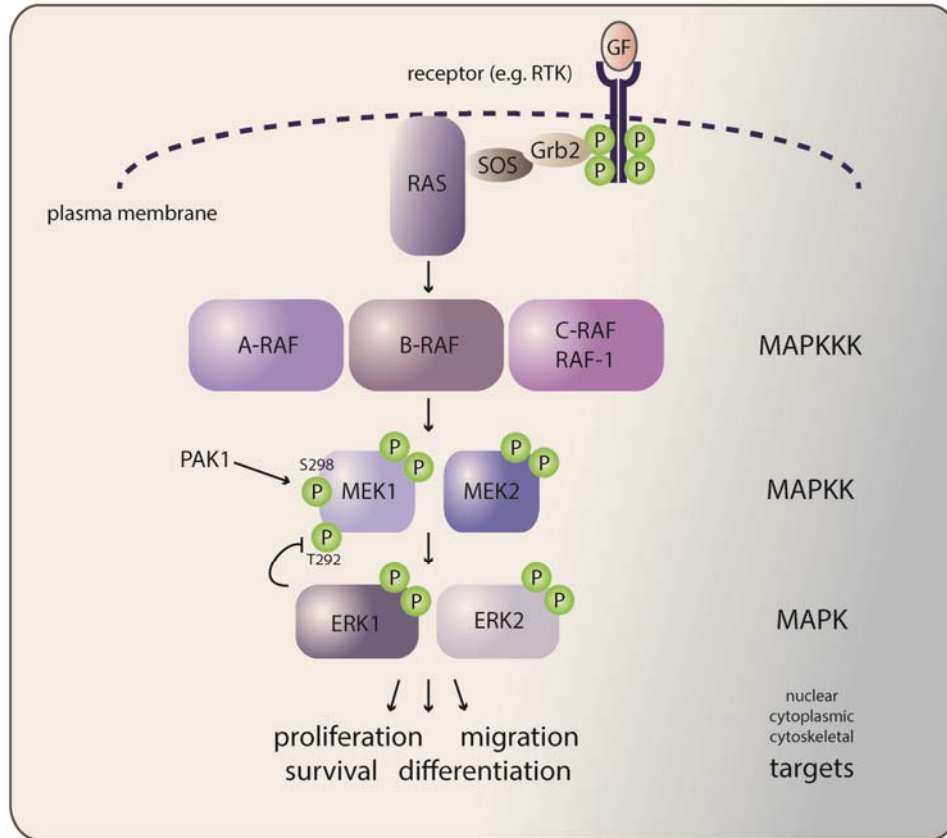
Fig 1. Model of the RAF/MEK/ERK pathway. Signaling by a receptor (in this case a receptor tyrosine kinase, RTK) induces recruitment of the adaptor and GEF proteins Grb2 and SOS, leading to activation of small GTPase Ras. The signal is then transferred to three-tiered cytosolic kinase cascade. Activated RAF kinases (MAPK kinase kinase, MAPKKK) phosphorylate and activate MEK (MAPK kinase), which in turn activates ERK (MAPK). ERK phosphorylates a large array of cytosolic, cytoskeletal and nuclear targets.

Due to the high prevalence of upregulated ERK signaling in human tumors, the members of the pathway are considered as attractive drug targets and considerable effort is placed in development of effective inhibitors [8]. Activating germline mutations in genes within the pathway or associated genes cause a group of genetic syndromes including Cardio-Facio-Cutaneous syndrome (B-RAF, MEK1, MEK2, K-RAS), Noonan syndrome (PTPN11, K-RAS, SOS1, C-RAF) and Costello syndrome (H-RAS, K-RAS). These autosomal dominant multiple congenital anomaly syndromes are characterized by a distinctive facial appearance, heart defects, musculocutaneous abnormalities, and mental retardation [9].

1.4 MEK kinases

MEK1 and MEK2 are ubiquitously expressed dual-specificity protein kinases that mediate phosphorylation of tyrosine and threonine residues in the activation segment of ERK1 and ERK2. ERKs are the only known physiological substrates of MEK kinases. While lower organisms (e.g. *D. melanogaster* or *C. elegans*) have only one *mek* gene,

vertebrates have two *mek* genes (1 and 2) [10]. MEK1 and MEK2 can form homo- as well as heterodimers. In our laboratory, we have previously shown that MEK1/MEK2 heterodimers control the strength and duration of the ERK signal [1]. The two MEK isoforms share almost 80% identity in the sequence, yet they have unique roles in signaling. The distinct functions of MEK1 and MEK2 were best demonstrated *in vivo* using conventional knockout (KO) mice. While MEK2-/- mice are viable, fertile and have no obvious phenotype [11], MEK1-/- mice die around day 9 of gestation due to trophoblast defects [1, 12]. Embryonic lethality can be circumvented by conditional deletion of MEK1 in the epiblast, which yields viable and fertile mice [1].
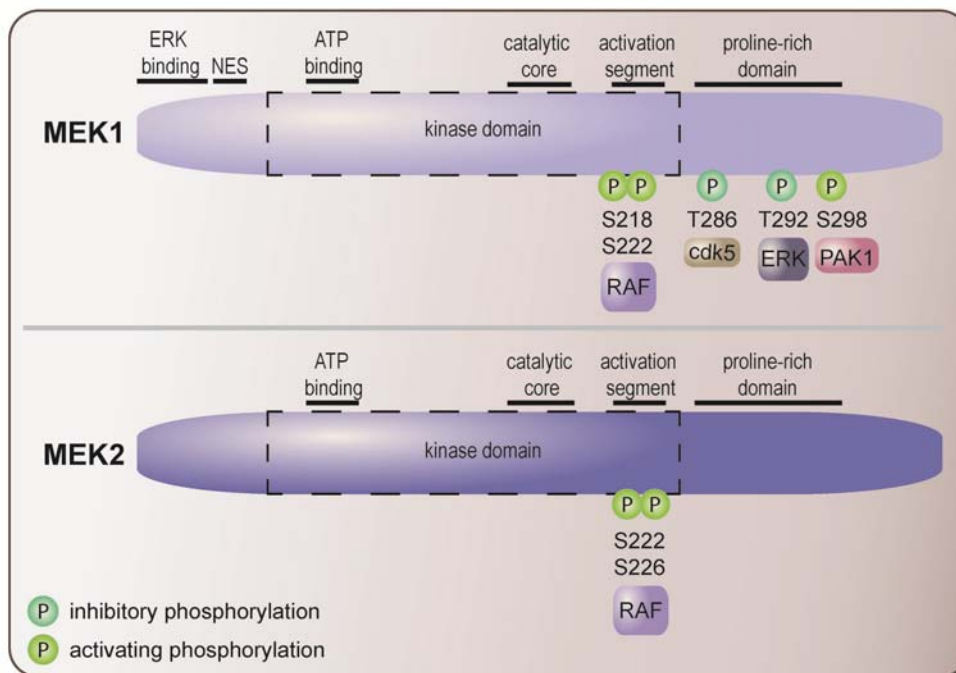
Fig 2. A simplified model of MEK1 and MEK2 domain organization. The model also shows the best characterized phosphorylation sites and the kinases that phosphorylate them. NES, nuclear export signal.

Structurally, MEK proteins consist of a regulatory N-terminal sequence containing a nuclear export signal and an ERK-binding site; a typical protein kinase domain composed of N-lobe and C-lobe; and a short C-terminal sequence (Fig 2). Despite being very similar, MEK1 and MEK2 differ in two regions. The first is located in the N-terminus and it is responsible for docking and nuclear export of ERK and PPARγ [13]. The second divergent region is an approximately 40 amino-acid long, proline-rich domain in the C-terminal part of the protein (only 40% identity). It contains potential sites for interaction with SH3 domains and the regulatory phosphorylation sites T286, T292 and S298 [10].

MEK activation requires the phosphorylation of two serine residues in the activation segment of the kinase domain [14]. These residues are S218 / S222 in MEK1 and S222 / S226 in MEK2. Selective phosphorylation of MEK1 S298 by the p21-activated kinase (PAK1) is the initial and essential event for MEK and ERK activation in adhesion signaling [15, 16]. Although an analogous site is present in MEK2, MEK2 is not phosphorylated by PAK1. MEK1 can also be inhibited by phosphorylation. The threonine residue found at position 292 is involved in negative feedback regulation by ERK. Upon heterodimerization, MEK1, but not MEK2, is subject to phosphorylation by ERK on T292, which makes MEK1 essential for the downregulation of the MEK-ERK pathway [17, 18]. Threonine 286 is phosphorylated by CDK5, which is active mainly in postmitotic neurons [19]. Numerous other phosphorylated residues have been detected on MEK kinases using phospho-proteomic analyses, but their biological functions remain largely unknown. Other post-translational modifications of MEK1 and MEK2 include SUMOylation on Lys104 (108 in MEK2). SUMOylation of MEK proteins inhibits MEK-induced ERK phosphorylation by disrupting the MEK-ERK complex [20].

1.5 Scaffolds

When considering the complexity of the ERK pathway, the many stimuli capable of activating it, and the number of resulting specific responses, it is obvious that a mechanism must exist to channel pathway output in the desired outcome. This signaling specificity can be achieved by spatio-temporal regulation of pathway components, at least partly mediated by adaptor and scaffold proteins that assemble signaling complexes at defined subcellular localizations and/or control the duration of a signal [21]. The differential binding of the members of the ERK pathway to scaffolding proteins is achieved in different ways. One possibility are isoform-specific differences in protein structure; another way to ensure differential regulation are posttranslational modifications, as in the case of residues phosphorylated in MEK1, but not MEK2. The differences in the scaffolding partners then contribute to the diversification and fine-tuning of signaling outputs. While many MAPK scaffolds have already been discovered, it is likely that other remain to be identified.

MEK-binding scaffolds (Fig 3)

KSR. Kinase suppressor of RAS (KSR) is the best characterized MAPK scaffold and binds to C-Raf, B-Raf, MEK1/2 and ERK 1/2 [21]. Interestingly, MEK is constitutively associated with KSR, while other components of the pathway bind in response to extracellular stimuli. Optimal expression levels of KSR are needed for maximal ERK

response, meaning that a precise stoichiometry of the complexes has to be maintained for optimal signal transmission [22].
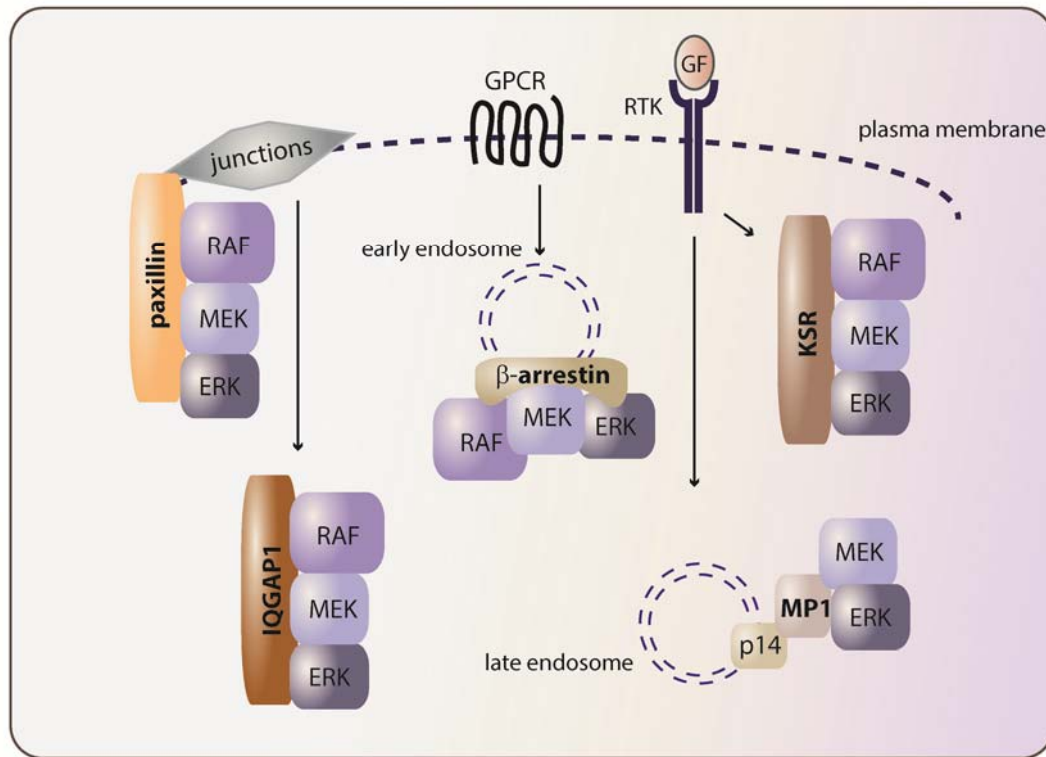
Fig 3. A model of spatial regulation of MEK signaling by protein scaffolds. Signaling at cellular junctions mediates assembly of RAF, MEK and ERK-containing complexes with paxillin and IQGAP1. GPCR activation leads to binding between β-arrestin and RAF/MEK/ERK, which then signal from internalized early endosomes. KSR is a scaffolding protein involved in assembly of the RAF/MEK/ERK pathway after RTK stimulation. MEK1 can also bind to MP1/p14 complex, which mediates the ERK signaling from late endosomes.

Paxillin. Similar to KSR, paxillin has been reported to constitutively bind MEK, and is able to recruit RAF and ERK after activation by growth factors, to facilitate local activation of ERK at focal adhesions [23].

IQGAP1. MEK and ERK kinases also bind to the multidomain protein IQGAP1. Both MEK1 and MEK2 are capable to interact with IQGAP via its IQ domain. Very high and very low intracellular IQGAP1 concentrations impaired stimulation of MEK and ERK by EGF, as in the case of KSR [24].

β-arrestins. Besides their role in desensitization/termination of G-protein-coupled receptor (GPCR) signaling, β-arrestins also function as MAPK scaffolds. They bind all three members of the pathway, RAF, MEK and ERK and this complex promotes ERK

signaling on early endosomes [25, 26]. MEK1 and MEK2 can bind directly to β-arrestins via their N-terminus [27].

MP1. MEK Partner 1 (MP1) was identified in a yeast two-hybrid screen as specific binding partner of MEK1 [28]. MP1 is recruited to late endosomes by p14 and is required for efficient ERK signaling on these organelles [29, 30]. The complex is involved in the regulation of endosomal traffic and cellular proliferation [31].

hDlg. Human disc-large homolog (hDlg), a scaffold protein implicated in neuronal synapses and epithelial junctions, was reported to bind MEK2, but not MEK1. The interaction occurs via PDZ2 domain of hDlg and C-terminal RTAV sequence of MEK2 [32]. The functional role of this interaction has not yet been identified.

1.6 Crosstalk

Signaling cascades should not be viewed as linear pipelines isolated from each other. In fact, intense crosstalk and mutual regulation exist among different pathways to ensure tight control and fine-tuning of the signals. The ERK pathway crosstalks to numerous other signaling cascades. A few examples of these are the activation of PI3K/AKT pathway by RAS, C-RAF's ability to regulate motility and differentiation via Rok-α and apoptotic signaling through MST2 and ASK1 kinases, the Rac1/CDC42/PAK1 module impacting on MEK1; and many others [33, 34]. Broadening our knowledge about crossregulation of signal transduction will not only contribute to better understanding of cellular processes and communication, but can also translate into improved treatments for diseases, such as cancer, which involve deregulated signaling. It is known that targeting one cascade by chemical inhibitors can activate others, as in the example of MEK/ERK and PI3K/AKT pathways [35]. Such mechanisms can lead to the rapid emergence of drug resistances. This phenomenon can be overcome by the combined inhibition of these two pathways, which shows increased potency and efficacy in preclinical cancer models in comparison to single-agent treatments. In two example studies, the combination of PI3K inhibitors with RAF/MEK inhibitors leads to decreased proliferation of tumor cells and their increased apoptosis [36, 37].

Previous studies have suggested a specific role of MEK(1) in the regulation of the AKT pathway. In a report by Menger and McCance, the overexpression of MEK1, but not MEK2 led to downregulation of AKT signaling [38]. In other studies, the use of MEK inhibitors or silencing of MEK resulted in increased phosphorylation of AKT [39-41]. However, the exact molecular mechanism of the crosstalk has not yet been elucidated.
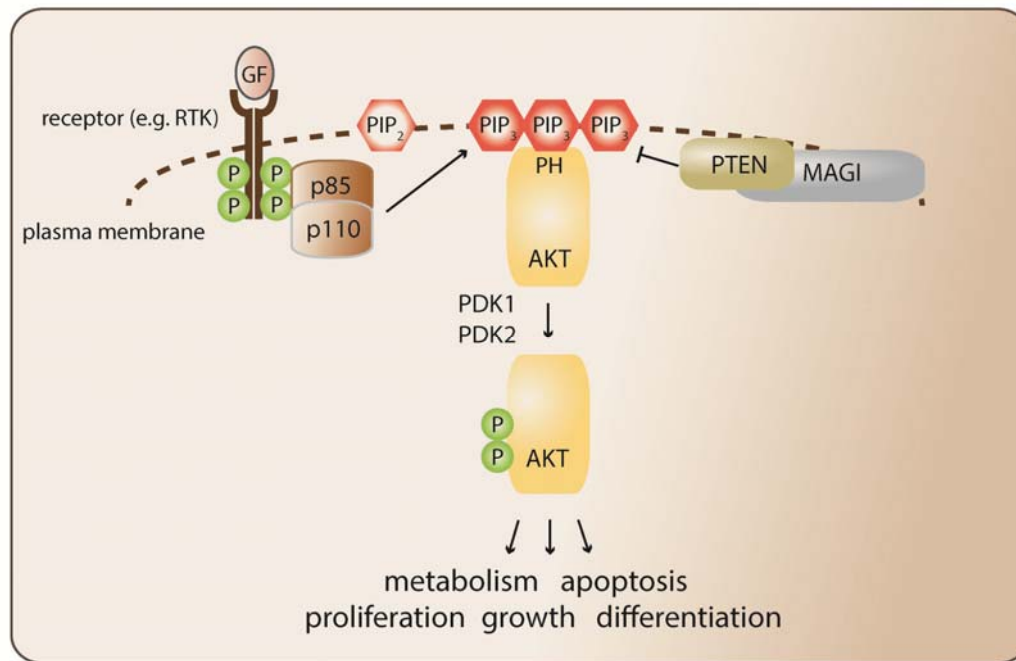
Fig 4. Schematic representation of signaling via PI3K/AKT pathway. The signal from activated receptor (in this case RTK) recruits phosphatidylinositol-3-kinase (PI3K) composed of p85 and p110 subunits. The activated PI3K phosphorylates PIP_2 generating PIP_3. PIP_3 serves as second messenger lipid in the cellular membrane and recruits the AKT kinase via its PH domain. AKT becomes phosphorylated and activated by PDK1 and PKD2 at the membrane. The activated form of AKT phosphorylates its numerous targets in the cytoplasm and thereby regulates cellular metabolism, growth, proliferation, differentiation and cell death. The activity of the pathway is negatively regulated by the phosphatase PTEN, which dephosphorylates PIP_3 generating PIP_2.

1.7 PI3K/AKT pathway

PI3K/AKT regulates an extraordinarily diverse group of cellular functions, including cell growth, proliferation, differentiation, motility, survival and intracellular trafficking. The AKT kinase (also known as PKB) is activated by various extracellular stimuli (such as growth factors) in a phosphatidylinositol 3-kinase (PI3K)-dependent manner (Fig 4). PI3Ks, composed of heterodimers of a regulatory (p85) and catalytic (p110) subunits, phosphorylate phosphatidylinositol-4,5-bisphosphate (PIP_2), producing phosphatidylinositol-3,4,5-bisphosphate (PIP_3) [42]. PIP_3 serves as a second messenger lipid and docking site for a group of proteins containing lipid-binding domains, such as the PH (pleckstrin-homohogy) domain of AKT. PIP_3 accumulation allows the translocation of AKT from the cytoplasm to the plasma membrane, where AKT is activated by a multistep process that requires phosphorylation of both T308 in the activation loop of the kinase domain and S473 within the hydrophobic motif of the regulatory domain mediated by PDK1 and PDK2 respectively [43]. Activated AKT is then able to phosphorylate numerous substrates and regulates cell growth (via mTOR), cell cycle and glucose metabolism (via GSK3β), apoptosis (via BAD, FKHR), differentiation

(via FOXO) and other processes [44]. The negative regulation of the pathway is ensured by the phosphatases PTEN and SHIP, which counteract PI3K activity by converting PIP_3 back to PIP_2, thereby terminating AKT activation [45].

1.8 PTEN

Phosphatase and tensin homologue on chromosome 10 (PTEN) is a lipid and protein phospahatase discovered by two independent groups as a candidate tumor-supressor gene located on chromosome 10 and encoding a 403 aminoacid-long protein [46, 47]. Next to p53, PTEN is one of the most frequent targets of loss of function mutations in human cancer. The principal function of PTEN is to catalyze dephosphorylation of PIP_3 [48]. Disruption of PTEN function therefore leads to increased AKT signaling and therefore of AKT-mediated survival as well as cell growth and proliferation [49, 50]. However, PTEN also acts as a tyrosine phosphatase targeting focal adhesion kinase (FAK), hereby regulating cell migration, spreading and focal adhesions [51].

PTEN expression and function is tightly controlled, and inactivating somatic genomic and epigenetic changes in the PTEN gene result in tumorigenesis [46, 52]. Germline mutations in PTEN cause a number of different disorders, such as Cowden syndrome (CS), Bannayan-Riley-Ruvalcaba syndrome and other. CS is characterized by multiple hamartomas and increased risk of breast, thyroid and endometrial cancers [53]. Regulation of PTEN expression, activity, stability, function and localization is a complex issue. The levels of PTEN expression are tightly regulated by a variety of mechanisms including transcriptional networks [54, 55], miRNAs and the recently discovered competing endogenous RNAs (ceRNAs) [56, 57]. The activity, localization and stability of PTEN protein is further controlled by posttranslational modifications such as acetylation [58], ubiquitination [59, 60], sumoylation [61], oxidation [62] and phosphorylation [63-65] (Fig 5). To access its lipid substrate, cytosolic PTEN must associate with membranes, at least transiently. Some posttranslational modifications, such as phosphorylation of the PTEN C-tail, cause a conformational change from a 'closed' to an 'open' protein conformation (Fig 6). In the open state, PTEN has increased activity and ability to contact membranes e.g. via membrane-bound scaffolds (such as MAGI proteins, see below) [66]. Also ubiquitination influences the subcellular localization of PTEN, but in this case it serves as a signal for nuclear import [60]. An increasing number of studies provides evidence about nuclear functions of PTEN, ranging from maintaining centromere stability and double-strand-break repair to cell cycle progression [67].
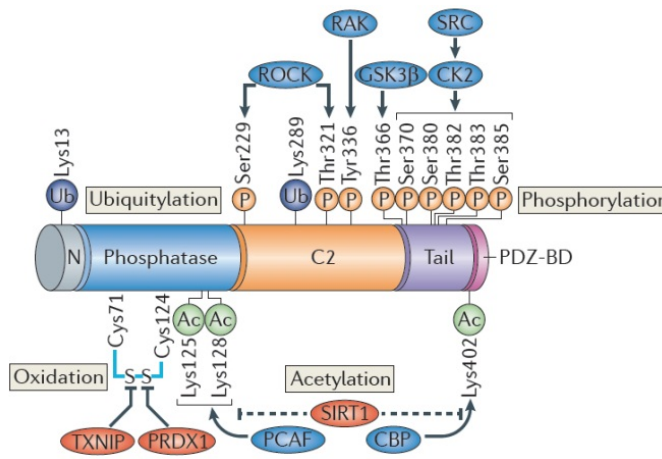
Fig 5. Posttranslational modifications of PTEN protein and their role in PTEN regulation. Phosphorylation of C- terminal tail of PTEN by the indicated kinases modulates PTEN tumor suppressive function, cell membrane association and stability. PCAF promotes PTEN acetylation at K125 and K128, whereas CBP acetylates K402. TXNIP and PRDX1 prevent the acetylation-mediated inactivation of PTEN. The formation of a disulphide bond between C124 and C71 by oxidation also reduces the catalytic activity of PTEN. Ubiquitylation of PTEN (K13, K289) regulates PTEN tumor suppressive function, subcellular localization and stability. Adapted from [68].
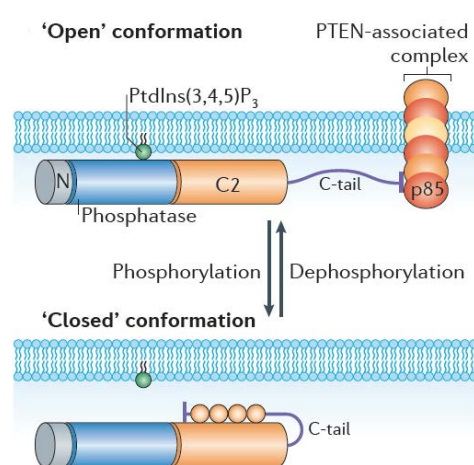
Fig 6. A model for the conformational regulation of membrane recruitment of PTEN. Phosphorylation of the C-terminal tail of PTEN promotes an electrostatic interaction between the acidic tail, the basic amino terminus and the C2 domain ('closed' conformation), and this conformation masks the membrane binding of PTEN. In the 'open' conformation, the basic N terminus is exposed and can bind to the acidic surface of the membrane and the PDZ domain interacts with the PTEN-associated complex at the membrane. Adapted from [68].

Disruption of the PTEN gene leads to early embryonic lethality [69]. PTEN +/- heterozygous mice are born alive, but exhibit neoplasms in multiple organs including endometrium, mammary gland, prostate, gastrointestinal tract, thyroid, thymus, lymph nodes, lung and liver. Even subtle variations in PTEN expression can determine cancer susceptibility, as evidenced by the study of mice expressing decreasing levels of PTEN (PTEN$^{+/+}$, PTEN$^{hy/+}$, PTEN$^{+/-}$ and PTEN$^{hy/-}$ [70, 71]. The tumor spectrum also depends on the specific mutant PTEN allele and it differs between PTEN$^{\Delta 4-5}$ (premature stop codon, complete loss-of-function allele), PTEN^{C124R} (lacks both lipid and protein phosphatase activity) and PTEN^{G129E} (lacks only lipid phosphatase activity) knock-in mice [72]. Additionally, PTEN heterozygous mice develop systemic autoimmune disease [73]. On the contrary, increased PTEN levels render mice cancer-resistant. This is due to changes in metabolism, characterized by increased energy expenditure and reduced body fat accumulation. Cells from these mice show reduced glucose and glutamine uptake, increased mitochondrial oxidative phosphorylation and are resistant to oncogenic transformation [74].

PTEN is composed of several distinct domains, the most prominent of which is the phosphatase domain. In addition, PTEN contains an N-terminal PIP$_2$-binding domain, a lipid-binding C2 domain, a flexible C-tail containing regulatory phosphorylation sites and a C-terminal PDZ domain [68] (Fig 5). The PDZ domain provides an interaction site with other PDZ domain-containing molecules, such as the MAGI scaffolding proteins MAGI1, MAGI2 and MAGI3 [75-77]. This interaction facilitates PTEN's localization at the cellular membrane [76, 78, 79].

1.9 MAGI proteins

Membrane-associated guanylate kinase with inverted domain structure (MAGI) proteins belong to the family of membrane-associated guanylate kinases (MAGUKs). The MAGI subfamily has three members named MAGI1, MAGI2 and MAGI3, which differ mainly in their tissue expression pattern. While MAGI1 and -3 are ubiquitous, MAGI2 is mostly restricted to brain [75, 80, 81]. MAGIs are differentially spliced in a number of isoforms, whose specific functions have not yet been fully characterized [81, 82]. MAGIs consist of multiple protein interaction motifs such as a guanylate kinase-like domain, two WW domains and five to six PDZ domains [80] (Fig 7). The main function of these proteins is the stabilization of cellular contacts and the scaffolding of signaling complexes. A number of interaction partners have been identified. As an example, MAGI1 was shown to interact with proteins involved in adhesion (JAM4, AMOTL1/2, ESAM, nephrin), signaling molecules (Dll1, Rap1, β-catenin), transmembrane proteins (megalin, cadherin23, Kir4.1) and actin-binding proteins (actinin, synaptopodin) [76, 78, 79, 83-91]. Recently, the members of MAGI family have been identified as tumor-supressor proteins and were found to be mutated in breast cancer, prostate cancer and melanoma [92-95]. Their function in various tissues and cell types as well as the specific roles of the individual splicing isoforms remain largely unaddressed.
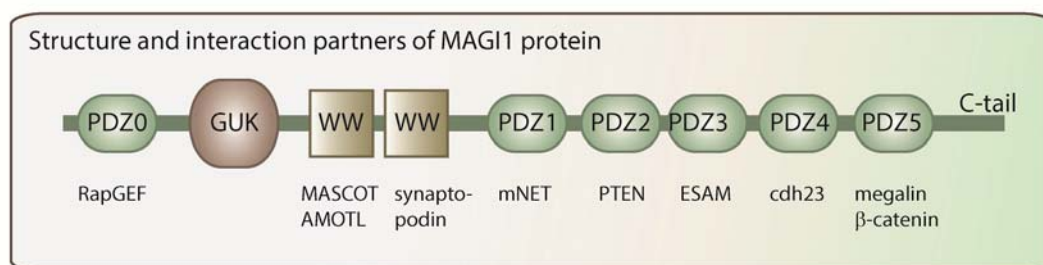
Fig 7. A model of domain structure of MAGI1 protein. The indicated binding partners are depicted below the domain that they bind to.

1.10 Immunity and mechanisms of immune tolerance

The immune system is composed of a series of defense mechanisms that provides protection against infection and other harms to an organism. These mechanisms can be classified in two large groups called nonspecific, innate immunity and specific, acquired (or adaptive) immunity. The vast repertoire of the adaptive immune system has evolved to recognize virtually all potentially dangerous molecules and at the same time to avoid the production of lymphocytes which react with the components of the organism itself. Therefore, mechanisms inducing tolerance against self-antigens must exist to avoid self-damaging immune reaction.

1.11 Basic mechanisms of tolerance establishment

The main principles governing induction of immunity and tolerance are the principles of clonal selection and clonal deletion. When an antigen receptor binds to a constitutively presented antigen within a certain defined time-frame in the development of a lymphocyte, this will lead to the death of such lymphocyte clone [96].

T cells develop in the thymus and B cells in the bone marrow. Lymphocytes precursors enter these primary lymphoid organs in order to differentiate and rearrange the Tcr and Ig loci (VDJ recombination). This results in a diverse array of (potentially self-reactive) receptors capable of binding antigens. As new lymphocytes are generated throughout our life, there is a continuous need to establish tolerance to self. Thus, lymphocytes need to pass through 'checkpoints' which enforce it [97] (Fig 8).

Central tolerance in T cells is established in the thymus by the process of negative selection. Thus, when developing high-avidity T cells react with self-antigen presented by corticomedullary macrophages in the thymus, they are deleted. Peripheral tolerance is mostly maintained by a process called 'activation-induced cell death', in which repeated activation of the TCR in the absence of adequate co-stimulation leads to apoptosis [96].

Another T cell involved directly in the maintenance of immune tolerance are T_{reg} T cells. These professional tolerance-inducing cells are characterized by expression of the Foxp3 transcription factor. They can be generated in the thymus (natural T_{regs}) or in the periphery (induced T_{regs}) and are capable of actively suppressing immune responses. Imbalance or depletion of this population leads to severe inflammatory diseases and autoimmunity [98].
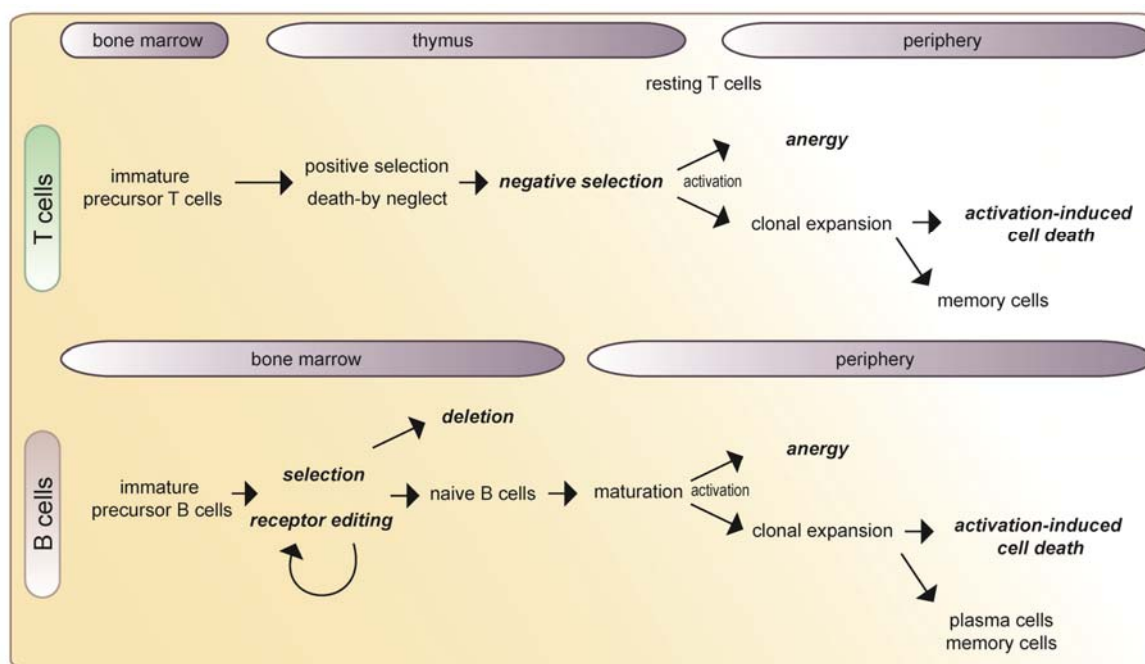
Fig 8. A simplified model of T and B cell development with the emphasis on central and peripheral tolerance establishment. The steps directly involved in tolerance are highlighted in ***bold italics***. T cell precursors migrate from the bone marrow to the thymus. Here they undergo selection processes termed 'positive selection', 'negative' selection and 'death-by-neglect'. Negative selection deletes clones with too high affinity for self-antigens. In the periphery, tolerance is maintained either by anergy (non-resposiveness to a stimulus) or by activation-induced cell death of T cells which undergo repeated stimulation rounds. Similar mechanisms operate in B cells, which undergo selection in the bone marrow. Self-reactive clones are either deleted or they might undergo receptor editing and change their antigen specificity. Further deletion occurs in the periphery during maturation processes. As the T cells, also B cells can become unresponsive (anergy) or die after stimulation (activation-induced cell death).

Similar mechanisms operate in B cells. B cell tolerance is maintained by clonal deletion (death of self-reactive cells), B cell anergy (induced by recognition of an antigen in the absence of a co-stimulatory signal), activation-induced cell death and receptor editing. Most autoreactive B cells are removed during the transition from pre-B cells to immature B lymphocytes during their interaction with stromal cells in the bone marrow [99]. A further round of autoreactive B cells deletion occurs during the transition from immature to mature B cells [100]. B cell tolerance can be also controlled by receptor editing. This process results in change of specificity of previously autoreactive BCR [101].

1.12 Autoimmunity

The term 'autoimmune disorders' comprises a whole spectrum of diseases ranging from organ-specific (e.g. autoimmue hepatitis) to systemic diseases (Sjögren's syndrome, lupus erythematosus). Autoimmunity starts with an initial immune response against a few epitopes of a self-antigen. Over time, this response eventually diversifies to other epitopes of the same molecule or even to other antigens.

Several genetic and environmental factors determine the susceptibility of humans to autoimmune diseases and their clinical manifestations, i.e. the severity of the disease. A common feature of many autoimmune diseases in humans as well as in experimental animals is an increased incidence in females, mainly due to effect of sexual hormones on the immune system [102, 103].

1.13 Systemic lupus erythematosus

Systemic lupus erythematosus (SLE) is a prototypic systemic autoimmune disease that affects multiple organs [104]. Systemic autoimmune diseases are generally characterized by the development of multi-clonal T and B cell responses, presence of autoantibodies against a variety of ubiquitous self-antigens (such as anti-nuclear antibodies (ANAs)), deposition of immune complexes in tissue (often in kidneys), development of tissue inflammation, damage and fibrosis.

SLE is a multisystem disease affecting mainly the joints, skin, kidneys and brain. The disease is characterized by autoantibody production by dysregulated B cells, target organ infiltration by inflammatory T cells and aberrant immune cell activation due to abnormal antigen presenting cell (APC) function. The exact mechanisms of lupus development are not entirely understood [105]. The disease is usually set off by an imbalance in the immune system (Fig 9). This includes defects in the establishment of peripheral and central tolerance itself (for example impaired deletion of self-reactive clones), strong infections, impaired clearance of apoptotic cells, intake of certain drugs [106-109]. This leads to the emergence of self-reactive T cell and B cell clones, and to the production of both specific proinflammatory cytokines and autoantibodies. While aberrant T cells provide help to autoreactive B cells, they also infiltrate target organs, causing damage and inflammation, and are thus key players in SLE disease pathogenesis. Several mouse strains are prone to develop systemic lupus-like disease and are therefore used as model systems for the disease. These include NZBxNZW F1, NZM.2410 or MRL-lpr mice [110]. The molecular defects underlying the first two models are not entirely clarified, while in MRL-lpr mice deregulated FAS signaling leads to defective apoptosis of immunocompetent cells.
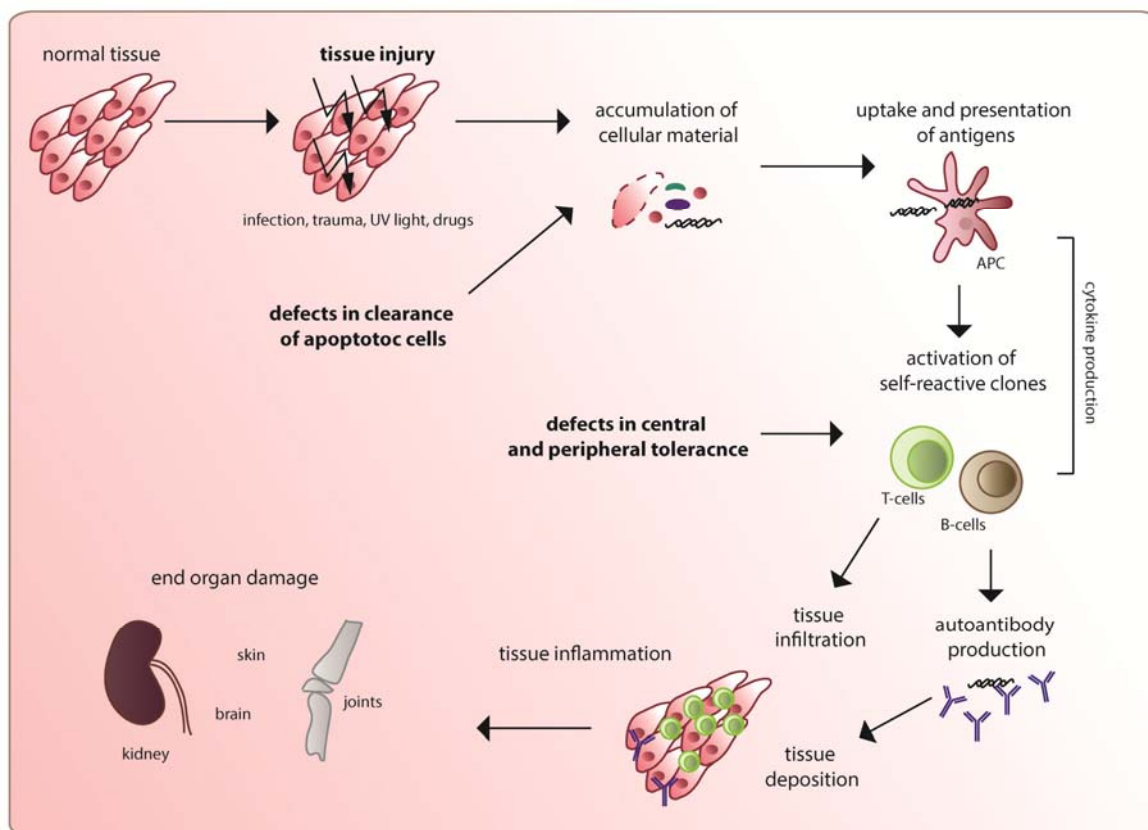
Fig 9. Model of development of autoimmune diseases. Autoimmune diseases progress through a series of steps. The initial impulse can come from different levels (highlighted in **bold**). The main triggers of autoimmunity are tissue injury, defects in clearance of dead cells and defects on tolerance establishment. They all come down to activation of self-reactive T and B cell clones, increased cytokine and autoantibody production, tissue inflammation and organ damage. APC, antigen-presenting cell.

1.14 Cell signaling and autoimmunity

Numerous efforts have been made to identify genomic susceptibility loci and signaling abnormalities leading to lupus exacerbation. More than 20 genes, implicated mostly in TLR/interferon signaling, adaptive immune response and immune complex clearance mechanisms, are associated with human SLE [111]. Lupus is also characterized by an imbalance in cytokine and chemokine production [112], and by a wide range of signaling anomalies. These include defects in TCR/BCR signaling resulting in chronic activation of lymphocytes, impaired apoptotic signaling, epigenetic mechanisms, such as defective DNA methylation, and aberrant gene regulation, such as defective alternative splicing [113]. These pathways may become valid drug targets to ameliorate the disease in patients [114]. The number of signaling abnormalities identified in SLE continues to grow, likely reflecting the complex nature of the disease.

AKT and ERK signaling cascades are one of the strong 'candidate' pathways in lupus pathogenesis. In general, increased AKT signaling and decreased ERK signaling are features of autoimmune diseases. These indications come from studies on lymphocytes obtained from patients suffering from SLE (also see below) [115, 116].

1.15 MAPK and PI3K/AKT pathways in autoimmunity – mouse models

PI3K/AKT pathway

Mouse models can provide us insight in the mechanisms of autoimmune disorders and a rational basis for the development of treatments [117].

Various murine models with increased PI3K/AKT pathway activity suffer from autoimmune diseases. Transgenic mice with T cell-restricted myristoylated AKT (myr-AKT) or gag-AKT expression suffer from accumulation of CD4+ T cells and B cells, resistance of T cells to apoptosis and features of autoimmunity, such as immune complex deposits in glomeruli [118, 119]. Mice with constitutively active PI3K in T cells have been also described and show expansion of CD4+ T cells and increased B cell activity. They also develop symptoms of autoimmunity including anti-dsDNA antibodies, renal disease with immunoglobulin deposits and tissue infiltrates [120]. PTEN$^{+/-}$ mice develop autoimmune disease associated with lymphadenopathy [73]. The autoimmune disease was characterized by positive ANAs test, glomerulonephritis with proteinaceous deposits and resistance to apoptosis induction in T cells. Similarly, T cell-specific loss of PTEN leads to defects in central and peripheral tolerance. Lck-Cre Pten$^{flox/-}$ mice have impaired negative thymic selection as well as defects in antigen-induced deletion of peripheral T cells, which leads to a lymphoproliferative autoimmune phenotype. In addition, these mice eventually also develop CD4+ T cell lymphomas [121]. A later study suggested that disruption of the PTEN gene in the T cell lineage causes both lymphomas and autoimmunity, but this is a result of distinct events in the development of T cells. Lymphomas in these mice originated from the thymus and could be prevented by thymectomy. Multiorgan autoimmunity was a consequence of defective T cell AICD in the periphery [122]. B cell-restricted deletion of PTEN results in changes of B cell homeostasis, autoantibody secretion and impaired apoptosis, all features of autoimmune disease [123, 124].

ERK pathway

Several reports exist that link ERK activity with lupus development. In general, decreased ERK signaling leads to establishment of autoimmunity. Treatment with

hydralazine, a drug that causes inhibition of ERK signaling, or with MEK inhibitors, resulted in anti-double-stranded DNA antibodies in a murine model of drug-induced lupus [125]. This might be due to an effect on DNA methylation and subsequent changes in expression of genes involved in lymphocyte activation and homeostasis [126]. Mice expressing inducible dominant negative MEK in T cells develop antibodies against dsDNA and other features of lupus that are common in humans [127].

The presented work provides mechanistic insights in the crossregulation of the MEK/ERK and AKT signaling via a MEK1/MAGI1/PTEN complex and its role in maintenance of peripheral tolerance.

II. SUBMITTED MANUSCRIPT

Title: **MEK1 is required for PTEN membrane recruitment, AKT regulation, and the maintenance of peripheral tolerance**

Authors: Katarina Zmajkovicova, Veronika Jesenberger, Federica Catalanotti, Christian Baumgartner, Gloria Reyes, and Manuela Baccarini

Submission procedure in Molecular Cell:

Submitted: 29.5.2012

Revised #1: 13.9.2012

Revised #2: 18.12.2012

Relevance and Contributions:

The manuscript provides novel mechanistic insights in the crossregulation of the MEK/ERK and AKT signaling via a MEK1/MAGI1/PTEN complex and its role in maintenance of peripheral tolerance.

K.Z. designed experiments, performed *in vitro* experiments, flow cytometry and wrote the manuscript. V.J. designed experiments, performed histological analysis, peripheral blood counts, *Critidia* assay and ELISAs and wrote the manuscript. F.C. and G.R. designed and performed experiments in Figure 1A-B, D-E and S1A-B. C.B. performed the colony forming assays. M.B designed experiments and wrote the manuscript.

MEK1 is required for PTEN membrane recruitment, AKT regulation, and the maintenance of peripheral tolerance

Katarina Zmajkovicova*, Veronika Jesenberger*, Federica Catalanotti[1], Christian Baumgartner, Gloria Reyes[2], and Manuela Baccarini

Department of Microbiology and Immunobiology, University of Vienna, Max F. Perutz Laboratories, Doktor-Bohr-Gasse 9, 1030 Vienna, Austria

Corresponding author: Manuela Baccarini; phone ++431 4277 54607; fax: ++431 4277 9546; email: manuela.baccarini@univie.ac.at

* equal contribution

[1] present address: Memorial Sloan-Kettering Cancer Center, Human Oncology and Pathogenesis Program, New York, NY 10065, USA

[2] present address: Department of Pharmacology, University of California San Diego, 9500 Gilman Drive, Department 0636, La Jolla, CA 92093-0636, USA

Highlights:

- A complex of MEK1, MAGI1, and PTEN regulates PIP_3 turnover and AKT signaling
- Ablation/inhibition of MEK1 blocks complex formation and PTEN membrane recruitment
- ERK-mediated MEK1 phosphorylation coordinates the timing of ERK and AKT signaling
- *In vivo*, MEK1 ablation induces AKT activation and a breach in peripheral tolerance

2.1 SUMMARY

The Raf/MEK/ERK and PI3K/AKT pathways are prominent effectors of oncogenic Ras. These pathways negatively regulate each other, but the mechanism involved is incompletely understood. We now identify MEK1 as an essential regulator of lipid/protein phosphatase PTEN, through which it controls phosphatidylinositol-3-phosphate accumulation and AKT signaling. MEK1 ablation stabilizes AKT activation and, in vivo, causes a lupus-like autoimmune disease and myeloproliferation. Mechanistically, MEK1 is necessary for PTEN membrane recruitment as part of a ternary complex containing the multidomain adaptor MAGI1. Complex formation is independent of MEK1 kinase activity but requires phosphorylation of T292 on MEK1 by activated ERK. Thus, inhibiting the ERK pathway reduces PTEN membrane recruitment, increasing phosphatidylinositol-3-phosphate accumulation and AKT activation. Our data offer a conceptual framework for the observation that activation of the PI3K pathway frequently mediate resistance to MEK inhibitors, and for the promising results obtained by combined MEK/PI3K inhibition in preclinical cancer models.

2.2 INTRODUCTION

The Raf/MEK/ERK pathway is amongst the most thoroughly studied downstream effectors of activated Ras (Wimmer and Baccarini, 2010). Deregulation of the pathway is implicated in both developmental disorders and cancer (Maurer et al., 2011; Schubbert et al., 2007). Consequently, numerous RAF and MEK inhibitors aimed at blocking ERK activation have been designed (Chapman and Miner, 2011; Poulikakos and Solit, 2011).

The dual specificity kinases MEK1 and 2 are activated by RAF and mediate phosphorylation of ERK1 and 2 (Roskoski, 2012). MEK1 and 2 are very similar but differ structurally in a proline-rich domain in the C-terminal half of the catalytic core, which in MEK1 contains the negative regulatory phosphorylation sites T286, targeted by Cdk5 mainly in postmitotic neurons; and T292, essential for the negative feedback regulation of MEK by ERK1 and 2 (Roskoski, 2012).

MEK1 and 2 also bind differentially to scaffolds such as MP1, which plays a role in ERK1 activation at late endosomes (Teis et al., 2002); and IQGAP1, which regulates adhesion/migration and promotes signaling from MEK1 to ERK and attenuates MEK2/ERK signaling (Roy et al., 2005).

Finally, disruption of the mek1 gene in vivo causes abnormal placenta development and lethality around embryonic day 9.5 (Bissonauth et al., 2006; Catalanotti et al., 2009; Giroux et al., 1999), while mek2-/- mice are normal (Belanger et al., 2003).

We have recently reported that MEK1 is essential for the regulation of the timing and strength of ERK signaling. By phosphorylating the T292 site in the proline-rich region of MEK1, ERK exerts negative feedback control on MEK1/MEK2 dimers. If MEK1 is absent, this control is disabled, leading to increased ERK signaling (Catalanotti et al., 2009).

Besides this negative feedback within the pathway, ERK can interfere with phosphatidylinositol-3 Kinase (PI3K)/AKT signaling, another major protumorigenic Ras effector (Liu et al., 2009; Song et al., 2012). In response to growth factors, PI3K converts phosphatidylinositol 4,5 diphosphate (PIP2) in the second messenger phosphatidylinositol 3,4,5 triphosphate (PIP3). AKT binds to PIP3 via its pleckstrin homology (PH) domain and translocates to the membrane, where it is activated by phosphorylation of T308 and S473. Tumor suppressor phosphatase and tensin homologue deleted on chromosome ten (PTEN) dephosphorylates PIP3, counteracting PI3K activity and restraining AKT activation (Liu et al., 2009; Song et al., 2012). Inhibition or silencing of MEK increases growth factor-stimulated AKT activation (Hoeflich et al., 2009; Ussar and Voss, 2004; Yu et al., 2002), a finding which was linked to ERK-mediated inhibition of PI3K recruitment to the EGF receptor via phosphorylation of the

adaptor GAB1 (Lehr et al., 2004; Zhang et al., 2002).

We show that MEK1 is required for the control of PIP3 accumulation at the cell membrane, which it regulates by ensuring the proper localization of PTEN in the context of a ternary complex with a multiprotein adaptor, MAGI1. MEK1 ablation deregulates the AKT pathway which, in vivo, induces a breach of peripheral self tolerance and myeloproliferation.

2.3 RESULTS

MEK1 is essential for the negative regulation of AKT signaling

We monitored the impact of MEK1 on AKT signaling in wild type (WT) and mek1 knockout (KO) mouse embryonic fibroblasts (MEFs; (Catalanotti et al., 2009)) stimulated with epidermal growth factor (EGF). Phosphorylation of AKT and its downstream effectors mTOR, GSK3β, and S6K was reproducibly enhanced in MEK1-deficient cells (Figure 1A, 1C). The increase in AKT phosphorylation was rescued by the re-expression of full-length MEK1 (Figure 1B). The levels of the membrane lipid PIP3, necessary for AKT activation (Liu et al., 2009), were significantly higher in KO MEFs than in control cells (Figure 1D & S1A-B). In contrast, PI3K expression and activity (Figure 1E & S1C) were comparable in WT and KO cells, as were PTEN expression and the EGF-induced dephosphorylation of the C-terminal residues which negatively regulate PTEN activity, its association with PDZ-containing proteins (Rahdar et al., 2009; Vazquez et al., 2001) and with PIP2 (Figure S1D). However, PTEN was hardly detectable at the membrane of KO MEFs, even after EGF stimulation (Figure 1F & S1E-F); and membrane-associated PTEN activity was greatly reduced (Figure 1G). Consistently, focal adhesion kinase (FAK), a membrane-associated PTEN protein substrate (Tamura et al., 1998; Yamada and Araki, 2001), was also hyperphosphorylated in KO cells (Figure S1G). MEK1 ablation did not impact the specific activity of membrane PTEN; in the cytosol, activity transiently increased at 5 min of EGF treatment (Figure 1G). PTEN can be regulated by a variety of posttranslational modifications and by the interaction with other proteins (Song et al., 2012); which of these mechanisms is responsible for this transient increase in cytosolic PTEN activity is currently unknown. Thus, MEK1 is required for correct membrane localization of PTEN and for limiting PIP3 accumulation and AKT activation.

mek1 KO mice develop myeloproliferation and autoimmune disease

To investigate the function of MEK1 in vivo, we used mice with epiblast-restricted mek1 ablation (mek1f/f; Sox2Cre mice (Catalanotti et al., 2009); referred to as KO mice). These animals, in particular the females, had a significantly decreased survival rate (Figure 2A). Increased numbers of circulating lymphocytes could be detected in the blood of 1-3 months (mo) old mice; this was exacerbated in old mek1 KO animals, in which it was accompanied by granulocytosis and thrombocytosis (Figure 2B). By 8-10 mo of age, 83% mek1 deficient females had developed severe splenomegaly (Figure 2C), hepatomegaly with lesser frequency (Figure 2D; observed in 45% of the animals) and, occasionally, lymphadenopathy. Liver and spleen showed effacement of architecture, extramedullary hematopoiesis, accumulation of atypical megakaryocytes, and fibrosis (Figure 2E and S2A). Splenomegaly correlated with a massive increase in immature Mac1+Gr1+ myeloid cells (Figure 2H), a population observed in pathological

conditions such as cancer and autoimmunity (Gabrilovich and Nagaraj, 2009). KO bone marrow and splenocytes isolated from young, unaffected animals gave rise to a significant higher number of colony forming units in semi-solid media, indicating a cell-autonomous phenotype (Figure S2B). In addition, KO spleens contained significantly increased numbers of T (CD3+) and B (CD19+) cells (Figure 2F). The CD4+/CD8+ ratio was normal, but more T- and B-cells were activated, as shown by the coexpression of the activation marker CD69 with CD3 and CD19 (Figure 2G). Despite the autoimmune disease, splenic Tregs were not decreased (not shown). A slight increase in activated T-cells was the only phenotype detected in the spleen of young KO mice (Figure S2C). In contrast to the marked phenotypic alterations in spleen and liver, KO thymi were normal in terms of cellularity and subset distribution (Supplementary Figure S2D).

Among the non-hematopoietic organs, KO lungs showed thickening of the interstitial alveolar spaces with vascular congestion (Figure S2E); however, the kidneys were the organs most severely affected. The tubules were dilated and filled with proteinaceous material, and the glomeruli displayed signs of focal proliferation and sclerosis reminiscent of glomerulonephritis, accompanied by the deposition of immunocomplexes in the glomeruli (Figure 3A-B). In addition, antibodies against dsDNA, a hallmark of lupus-like autoimmune diseases, were detected in the sera of 7 out of 7 KO 5-10 mo old females (Figure 3C; titer of 1:100 in 5 mice; 1:1000 in 2 mice). This correlated with a marked increase in the concentrations of serum immunoglobulins (IgG1, IgG2b, IgA) and in the frequency of IgA and IgG-producing B cells affected mice (Figure 3D-E). Circulating BAFF and IL-10 (Figure 3F), crucially implicated in the pathogenesis of lupus-like disease (Su et al., 2012), were also elevated; and the frequency of cells producing IL-10, GM-CSF, TGF-β and IFN-γ was elevated to varying degrees (Figure S3A). In all cases, the increase was most pronounced in CD4+ lymphocytes. IFNα, IL-3, IL-6, IL-17, IL-23 were tested but proved similar in WT and KO (not shown).

Thus, the KO mice are prone to develop both myeloproliferation and a lupus-like autoimmune disorder reminiscent of those reported for pten+/- (Di Cristofano et al., 1999), hematopoetic (Guo et al., 2008; Yilmaz et al., 2006) of T-cell-restricted PTEN KO (Liu et al., 2010; Suzuki et al., 2001) or constitutively active AKT transgenic mice (Kharas et al., 2010; Parsons et al., 2001).

mek1 ablation deregulates AKT activation and impairs activation-induced cell death

The AKT deregulation caused by PTEN mislocalization (Figures 1 & S1) could contribute to the phenotypes of mek1 KO mice. Indeed, AKT phosphorylation was detected to variable extents in KO kidneys, livers, lungs, spleen and lymphnodes (Figure 3A and S2F-G). In contrast, ERK phosphorylation, deregulated in cultured fibroblasts

and in some organs in vivo (Catalanotti et al., 2009), was not affected (Figure S2H). Given the poor conditions of these animals, however, it is impossible to distinguish whether this phosphorylation is cause or consequence of the phenotypes observed. We therefore investigated in more detail the spleen of young mek1 KO mice, which was normal but for a slight increase in the number of activated T-cells (Figure S2C). pAKT (Figure 3G) was increased and membrane PTEN was decreased (Figure 3H) in the KO samples. Increased pAKT was also observed in KO CD4+ T-cells stimulated with αCD3/CD28 (Figure 3I). KO CD4+ T-lymphocytes and B cells were less responsive to activation-induced cell death (AICD), a phenotype abrogated by a PI3K, but not by a MEK inhibitor (Figure 3J-K), and to Fas-induced apoptosis (Figure 3L). In contrast, other functions of CD4+ cells and B cells, such as their ability to proliferate and express the activation marker CD69 in response to T or B cell receptor stimulation were unaffected (Figure S3B-C), indicating that the resistance to activation-induced cell death (AICD) is the major cell-autonomous phenotype. KO MEFs were also resistant to various proapoptotic stimuli (Figure S3D-E). This is reminiscent of the impaired apoptosis observed in PTEN deficient lymphocytes (Buckler et al., 2008; Di Cristofano et al., 1999; Liu et al.; Suzuki et al., 2003) and fibroblasts (Stambolic et al., 1998).

A MEK1/MAGI-1/PTEN complex regulates PTEN membrane recruitment

To gain insight in PTEN regulation by MEK1, we tested whether MEK1 and PTEN interacted in cells. PTEN was present in MEK1 immunoprecipitates (IPs) from growth-factor stimulated fibroblasts (Figure 4A). Conversely, MEK1 but not MEK2 could be detected in PTEN IPs from WT cells, and interaction was enhanced upon growth factor stimulation (Figure 4B & D). Recombinant PTEN and MEK1 did not interact in vitro (Figure S4A), indicating a requirement for a scaffold protein which, since MEK1 impacts membrane localization of PTEN, should be involved in PTEN membrane recruitment. Membrane-Associated Guanylate Kinase (MAGUK) family member with Inverted domain structure-1 (MAGI1) is a PTEN binding partner which localizes to the plasma membrane, specifically in domains such as adherens junctions, which act as focal points for the regulation of PIP3 pools and therefore control the recruitment and activation of AKT by assembling signaling complexes involving E-cadherin, β-catenin, and PTEN (Bonifant et al., 2007; Kotelevets et al., 2005). MAGI1 contains six PDZ domains, a guanylate kinase (GUK) domain and two WW domains flanked by two PDZ domains (Dobrosotskaya et al., 1997); PTEN binds selectively to the second PDZ domain of MAGI1 (Kotelevets et al., 2005). Several isoforms and splice variants of MAGI1 are expressed in different cell types (Dobrosotskaya et al., 1997; Emtage et al., 2009; Kotelevets et al., 2005; Laura et al., 2002; Xu et al., 2008). MAGI1 in MEFs appeared as multiple bands, with a predominant band of approximately 100kD (MAGI1100, marked by an asterisk) and two

further bands of about 130 and 150kD. The 100kD isoform was selectively recruited to the membrane upon growth factor stimulation of WT cells, but MEK1 ablation prevented MAGI1 membrane translocation (Figure 4C). In addition, MAGI1100 was detected in PTEN IPs from WT, but not MEK1 KO MEF whole cell lysates and membrane fractions (Figure 4D & S4B), and the interaction between PTEN and MAGI1 could be restored by adding recombinant MEK1 to the KO lysates prior to PTEN immunoprecipitation (Figure 4E). MAGI1 was detectable in MEK1, but not in MEK2 IPs (Figure S4C-D). Thus, MEK1 is essential for the formation of a complex containing MAGI1 and PTEN, and for their membrane translocation upon growth factor stimulation. The kinetics of EGF-induced complex formation were similar to those of MEK1 phosphorylation on the ERK-dependent negative regulatory residue unique to MEK1 T292. pT292 MEK1 was enriched in PTEN immunoprecipitates, as assessed by densitometry (10% of total pT292 MEK1 vs. 0.7% of total MEK1 in PTEN IPs from EGF stimulated cells), while neither the activating RAF-dependent (S218 and S222) nor the PAK-dependent (S298) sites correlated well with binding (Figure 4D). Thus, T292 might work as a temporal switch, ensuring that ternary complex formation and membrane translocation occur after ERK activation.

MEK1 ablation decreases PTEN membrane localization and increases AKT phosphorylation in splenocytes (Figure 3G-H). MAGI1100 is expressed in spleen, and it is detectable, together with MEK1, in PTEN immunoprecipitates from WT, but not KO organs (Figure 4F). Therefore, the mechanism described for the MEFs operates also in the spleen. In line with the lack of phenotype and AKT activation in KO thymi (Figure S2D & G), MAGI1100 was not expressed in thymus, and MEK1 was absent in PTEN immunoprecipitates from this organ (Figure 4F).

In MEFs, MAGI1 is the most efficiently expressed MAGI protein (Figure S4E). Consistently, MAGI1 knockdown (KD) efficiently abrogated PTEN binding to MEK1 (Figure 4G), reduced PTEN membrane localization and increased AKT activation (Figure S4F-G). Thus, MAGI1 is the scaffold mediating the interaction between MEK1 and PTEN. The ternary complex was also found in human, rat and chicken cells (Figure S4H) and in monkey cells (Figure 5F), indicating that it represents an important conserved regulatory principle.

We next examined the interaction of MEK1 with selected MAGI1 domains expressed as myc-fusion proteins (Xu et al., 2008). The GUK and, to a greater extent, the two WW domains were detectable in MEK1 IPs, whereas the PTEN-binding PDZ domains were not (Figure 5A). Consistently, deletion of either the GUK or the WW domains reduced MAGI1 binding to MEK1, and deletion of both domains abolished it (Figure 5B). MEK1 was detectable in full length MAGI1, GUK and WW domains IPs.

GUK domains are phospho-peptide binding modules (Zhu et al., 2011), and WW motifs recognize proline-rich ligands, also in conjunction with S/T phosphorylation (Gao et al., 2009; Ingham et al., 2005; Macias et al., 2002). Mutating T292 in the proline-rich region of MEK1 to a nonphosphorylatable A (T292A) decreased, and a phosphomimetic (T292D) mutation increased, binding to MAGI1 and WW, but not GUK (Figure 5C-E). Thus, if the GUK domain is phosphosensitive, binding must depend on a different phosphorylation site. Mutation of the WW domains of MAGI1, in particular of WW2, strongly reduced MEK1 binding by a GUK-WW MAGI1 fragment or by full-length MAGI1 (Figure 5 F-G). Remarkably, a MAGI1 GUK-WW fragment, which binds to MEK1 but not to PTEN, strongly reduced the binding of endogenous MEK1 and MAGI1 to PTEN, reduced PTEN membrane recruitment, and triggered AKT hyperactivation (Figure 5H-I), mimicking the MEK1 KO. A MAGI1 GUK-WW2 domain mutant was less efficient in preventing MEK1/MAGI1 binding to PTEN and causing AKT activation (Figure 5H). The residual MEK1 binding/dominant negative activity of the MAGI1 GUK-WW2 domain mutant is likely due to the interaction of the MAGI1 GUK domain with other MEK1 binding sites (Figure 5A, B, D). Together, the data support the hypothesis that perturbations of the ternary complex PTEN/MAGI/MEK1 result in AKT activation.

MEK1 T292 phosphorylation controls complex formation

To further investigate the role of T292, we monitored complex formation in KO MEFs reconstituted with nonphosphorylatable T292A or phosphomimetic T292D MEK1 mutants. The mutants expressed at comparable levels, slightly lower than WT MEK1. MAGI1100 formed a complex with PTEN in WT and T292D cells, but not in KO or T292A cells; in addition, complex formation between MAGI1, PTEN and the phosphomimetic MEK1 T292D mutant was not regulated by growth factor treatment (Figure 6A).

Like KO MEFs, MEK1 T292A cells showed defective PTEN membrane recruitment, and PIP3 accumulation as well as AKT phosphorylation were increased above the levels observed in KO cells. The exact reasons for these differences between KO and reconstituted cells are unknown. In contrast, MEK1 T292D mutant cells displayed constitutive PTEN membrane recruitment, as well as low levels of PIP3 and AKT phosphorylation (Figure 6B-D). Consistent with this biochemical behavior, MEK1 T292A cells were resistant to TNFα-induced apoptosis (Figure S5A). Thus, T292 phosphorylation is a prerequisite for proper complex formation and for the regulation of the PIP3 pathway.

T292 is phosphorylated by ERK which might thus regulate the timing of PTEN membrane recruitment and AKT signaling. Indeed, MEK inhibitors blocked both ERK and T292 phosphorylation, concomitantly increasing AKT phosphorylation (Figure 6E & S5B) and PIP3 accumulation (Figure 6F) and, most importantly, reducing the binding of MEK1

and MAGI1100 to PTEN and of MAGI1100 to MEK1 (Figure 6G-H). In MEK1 T292D MEFs, MEK inhibition did not perturb the association of PTEN with MEK1 or MAGI1100 or AKT phosphorylation (Figure 6I-J); thus, phosphorylation of T292 is required, and MEK1 kinase activity is dispensable, for the interaction of MEK1 with MAGI100 and PTEN.

Two other MAGI family proteins, MAGI2 and 3, were also able to form complexes with MEK1. Consistent with the data obtained for MAGI1, chemical inhibition of T292 phosphorylation decreased the recruitment of MAGI2 and 3 to the membrane (Figure S5C-D).

2.4 DISCUSSION

A kinase-independent role for MEK1 in the regulation of PTEN function

We report the existence of a ternary complex between MEK1, MAGI1 and PTEN, mediating the translocation of PTEN to the membrane and therefore regulating the concentration of PIP3 and AKT activation. Both MEK1 and MAGI1 are necessary for complex formation, and PTEN will not bind to one component if the other is missing. The complex is held together by MAGI1, which contacts PTEN via its PDZ domain (Kotelevets et al., 2005) and MEK1. MAGI1 binds to MEK1 via its GUK and WW2 domains, but only binding to the WW domains is sensitive to the ERK-mediated phosphorylation of T292 in MEK1. The MAGI1 WW domains are very similar to the group Ib WW2 and WW3 domains of the ubiquitin ligase Nedd4L, whose binding to SMAD2 and 3 depends on the phosphorylation of a T in the linker region (Gao et al., 2009); the NEDD4 WW2 domain has been found to bind to proteins containing PR sequences in an unbiased proteomic screen (Ingham et al., 2005). T292 of MEK1 is embedded in such a PR containing sequence (PPRPRTPGRP in MEK1, SPRPRPPGRP in MEK2); in addition, the MEK1 sequence does not contain any other predicted WW binding sites. Since the proline-rich loop of MEK1 is disordered in all available crystal structures, it is not possible to model its interaction with the MAGI1 WW domains; and at this point it is not possible to distinguish whether phosphorylation creates a reversible MAGI1 binding site on MEK1 or rather induces exposure of another MAGI1 binding site through an allosteric mechanism.

Besides being essential for the assembly of the MEK1/MAGI/PTEN complex, pT292 is also required for the downregulation of MEK2-dependent ERK signaling, mediated by MEK1 in the context of a MEK1/MEK2 heterodimer (Catalanotti et al., 2009). Thus, phosphorylation of MEK1 T292 relays a negative feedback within the ERK pathway and initiates the deactivation of the PIP3/AKT pathway through the membrane localization of MAGI/PTEN, acting as a temporal switch for both cascades.

MEK1 has been reported to bind to another WW domain containing protein, namely the proapoptotic tumor suppressor WOX1, associated with the death of activated T cell leukemia. In this case, however, the WOX1/MEK1 complex dissociates upon ERK activation (Lin et al., 2011). Thus, ERK differentially regulates binding of MEK1 to WW domain containing proteins, and may negatively affect survival by promoting the translocation of WOX1 to the mitochondria (Lin et al., 2011) and the membrane recruitment of PTEN in the context of the MEK1/MAGI1/PTEN complex.

Our data show that MEK1 binding to the GUK and WW domains of MAGI1 promotes both complex formation between MAGI1 and PTEN and their membrane translocation. We do not know in detail how this is accomplished. One hypothesis is that

binding to MEK1 will cause a conformational change in MAGI1, exposing the PDZ domains necessary for PTEN binding [PDZ2, (Kotelevets et al., 2005)] and for the binding to membrane proteins such as Cadherins [PDZ4 and 5 (Kotelevets et al., 2005; Mizuhara et al., 2005; Xu et al., 2008)]. Intramolecular interactions between the SH3 and the GUK domain of other MAGUK proteins have been described, postulated to keep the proteins in an inactive, "closed" conformation (Montgomery et al., 2004). In MAGI, the WW domain replaces the SH3. It is conceivable that the WW domain may also be involved in intramolecular interactions which can be interrupted by MEK1 binding. Whatever the mechanism involved, MEK1 kinase activity is not required for complex formation and MEK1 binds to MAGI1 as a monomer or as a MEK1 dimer, but not as a heterodimer.

It is noteworthy that MEK1, but not PTEN, binds selectively to MAGI100, the only isoform translocated to the membrane in response to growth factors. Binding of PTEN to other MAGI1 isoforms may localize the phosphatase to other subcellular compartments, such as the nucleus (Dobrosotskaya et al., 1997; Laura et al., 2002), but it does not rescue membrane recruitment in the absence of MEK1. In addition, MAGI1100 is selectively expressed in organs and cells that are affected by MEK1 ablation (compare thymus and spleen in Figure 4F), where it correlates with the lack of PTEN membrane recruitment.

The possibility also exists that it is MEK1, rather than MAGI1, which mediates the membrane recruitment of the ternary complex. In this context, MEK reportedly binds to paxillin, and growth factor treatment induces the recruitment of Raf and ERK to this complex. Activated ERK phosphorylates paxillin on S83, promoting its association with activated FAK and PI3K and increasing cell spreading (Ishibe et al., 2004). The study did not differentiate between MEK1 and MEK2; however, our data would predict that in the absence of MEK1 at least a certain number of focal adhesions would fail to recruit MAGI/PTEN, resulting in the increased FAK phosphorylation, growth factor-induced migration, and cell spreading (Catalanotti et al., 2009) observed in the MEK1 KO fibroblasts.

Finally, some PTEN membrane binding, unaffected by EGF stimulation, can be observed in MEK1 KO fibroblasts (on average approx. 20% of the WT). It is conceivable that this binding is mediated by the N-terminal PIP2-binding motif of PTEN, which has been shown to be necessary for membrane association (Rahdar et al., 2009). Alternative binding mechanisms likely underlie the rather modest EGF-mediated membrane recruitment of PTEN and MEK1, compared with the robust increase of MAGI1; consistent with this, a strong increase in the amount of both MEK1 and MAGI1100 is observed in membrane PTEN IPs from stimulated cells, indicating that EGF causes the

preferential recruitment of the ternary complex to the membrane.

Together, these data define a novel kinase-independent function of MEK1 outside the canonical pathway, and provide new insight into PTEN regulation.

Biological implications of a disabled feedback

MEK1 KO mice succumb early to an autoimmune disease accompanied by extramedullary hematopoiesis. The latter phenotype has been observed in PTEN cell-type-restricted KO or AKT transgenic mice (Guo et al., 2008; Kharas et al., 2010; Yilmaz et al., 2006), and we could show that KO bone marrow and spleen from unaffected animals contain significantly higher numbers of colony forming units, indicating a cell-autonomous phenotype. At this point, however, the contribution of the MEK1 KO environment, with its lymphoid dysregulation and autoimmune disease, is unclear. Cell-type-restricted MEK1 ablation and transplantation experiments are planned to clarify this matter.

The autoimmune disease clearly correlates with a reduction in T-cell activation-induced cell death and with AKT activation in T cells and kidney. A similar phenotype can be achieved by genetic manipulations increasing PIP3/AKT signaling (Borlado et al., 2000; Di Cristofano et al., 1999; Liu et al., 2010; Parsons et al., 2001; Suzuki et al., 2001), but also by adoptive transfer of mouse T-lymphocytes treated ex vivo with MEK inhibitor (Deng et al., 2003) or T-cell restricted expression of a dominant negative MEK transgene (Sawalha et al., 2008). The latter treatments would mimic the MEK1 KO by reducing phosphorylation of the critical T292 residue in MEK1 and therefore PTEN membrane recruitment. Importantly, both reduced ERK activation (Gorelik and Richardson, 2010) and increased AKT signaling (Tang et al., 2009) have been observed in T cells from lupus patients. Together with our data, these results suggest that the activation of ERK and its cross-talk with the PI3K pathway are crucial players in the development of experimental and possibly clinical lupus-like autoimmune diseases.

The MEK1 KO does not phenocopy T-cell restricted PTEN deletion in two aspects: the breach of central tolerance (Suzuki et al., 2001) and the development of T-cell lymphomas (Liu et al., 2010). In both cases, the cells responsible for the phenotype originate in the thymus, which is not affected in the MEK1 KO mice. This lack of phenotype correlates with the lack of expression of MAGI100, and underscores the specific effect of MEK1 on this particular mechanism of PTEN regulation. In this context, it is important to consider that the impaired membrane localization of MAGI-1 in KO cells and organs might cause deregulation/mislocalization of one or more of its many interaction partners thereby playing a role in the phenotype of the MEK1 KO mice.

Is the regulation of PTEN by MEK1/MAGI relevant in the context of cancer? MAGI has been found mutated in human cancer genomes (Berger et al., 2011;

Pleasance et al., 2010), and it can suppress the growth of tumor xenografts (Zaric et al., 2012). Based on this, it is in principle possible that MEK1 may act as a tumor suppressor under certain conditions, as observed in a model of Myc-induced B cell lymphoma (Bric et al., 2009). More broadly, inhibition of the Raf/MEK/ERK pathway often causes activation of the AKT pathway in cancer (Hoeflich et al., 2009; Mirzoeva et al., 2009; Wee et al., 2009), due to the release of yet incompletely identified negative feedback loops. The use of Raf or MEK inhibitors may, by preventing the phosphorylation of T292 in MEK1, decrease PTEN membrane recruitment, increasing PIP3 concentrations and favoring the emergence of resistance mechanisms relying on the PI3K/AKT pathway. This would provide a mechanistic framework for the combined inhibition of these pathway, which is being increasingly advocate as the treatment of choice (Hoeflich et al., 2012; Sos et al., 2009; Villanueva et al., 2010).

2.5 REFERENCES

Belanger, L.F., Roy, S., Tremblay, M., Brott, B., Steff, A.M., Mourad, W., Hugo, P., Erikson, R., and Charron, J. (2003). Mek2 is dispensable for mouse growth and development. Mol Cell Biol *23*, 4778-4787.

Berger, M.F., Lawrence, M.S., Demichelis, F., Drier, Y., Cibulskis, K., Sivachenko, A.Y., Sboner, A., Esgueva, R., Pflueger, D., Sougnez, C*., et al.* (2011). The genomic complexity of primary human prostate cancer. Nature *470*, 214-220.

Bissonauth, V., Roy, S., Gravel, M., Guillemette, S., and Charron, J. (2006). Requirement for Map2k1 (Mek1) in extra-embryonic ectoderm during placentogenesis. Development *133*, 3429-3440.

Bonifant, C.L., Kim, J.S., and Waldman, T. (2007). NHERFs, NEP, MAGUKs, and more: interactions that regulate PTEN. J Cell Biochem *102*, 878-885.

Borlado, L.R., Redondo, C., Alvarez, B., Jimenez, C., Criado, L.M., Flores, J., Marcos, M.A., Martinez, A.C., Balomenos, D., and Carrera, A.C. (2000). Increased phosphoinositide 3-kinase activity induces a lymphoproliferative disorder and contributes to tumor generation in vivo. Faseb J *14*, 895-903.

Bric, A., Miething, C., Bialucha, C.U., Scuoppo, C., Zender, L., Krasnitz, A., Xuan, Z., Zuber, J., Wigler, M., Hicks, J*., et al.* (2009). Functional identification of tumor-suppressor genes through an in vivo RNA interference screen in a mouse lymphoma model. Cancer Cell *16*, 324-335.

Buckler, J.L., Liu, X., and Turka, L.A. (2008). Regulation of T-cell responses by PTEN. Immunol Rev *224*, 239-248.

Catalanotti, F., Reyes, G., Jesenberger, V., Galabova-Kovacs, G., de Matos Simoes, R., Carugo, O., and Baccarini, M. (2009). A Mek1-Mek2 heterodimer determines the strength and duration of the Erk signal. Nature structural & molecular biology *16*, 294-303.

Chapman, M.S., and Miner, J.N. (2011). Novel mitogen-activated protein kinase kinase inhibitors. Expert Opin Investig Drugs *20*, 209-220.

Deng, C., Lu, Q., Zhang, Z., Rao, T., Attwood, J., Yung, R., and Richardson, B. (2003). Hydralazine may induce autoimmunity by inhibiting extracellular signal-regulated kinase pathway signaling. Arthritis and rheumatism *48*, 746-756.

Di Cristofano, A., Kotsi, P., Peng, Y.F., Cordon-Cardo, C., Elkon, K.B., and Pandolfi, P.P. (1999). Impaired Fas response and autoimmunity in Pten+/- mice. Science *285*, 2122-2125.

Dobrosotskaya, I., Guy, R.K., and James, G.L. (1997). MAGI-1, a membrane-associated guanylate kinase with a unique arrangement of protein-protein interaction domains. J Biol Chem *272*, 31589-31597.

Emtage, L., Chang, H., Tiver, R., and Rongo, C. (2009). MAGI-1 modulates AMPA receptor synaptic localization and behavioral plasticity in response to prior experience. PLoS ONE *4*, e4613.

Gabrilovich, D.I., and Nagaraj, S. (2009). Myeloid-derived suppressor cells as regulators of the immune system. Nat Rev Immunol *9*, 162-174.

Gao, S., Alarcón, C., Sapkota, G., Rahman, S., Chen, P.-Y., Goerner, N., Macias, M.J., Erdjument-Bromage, H., Tempst, P., and Massagué, J. (2009). Ubiquitin Ligase Nedd4L Targets Activated Smad2/3 to Limit TGF-β Signaling. Molecular Cell *36*, 457-468.

Giroux, S., Tremblay, M., Bernard, D., Cardin-Girard, J.F., Aubry, S., Larouche, L., Rousseau, S., Huot, J., Landry, J., Jeannotte, L*., et al.* (1999). Embryonic death of Mek1-deficient mice reveals a role for this kinase in angiogenesis in the labyrinthine region of the placenta. Curr Biol *9*, 369-372.

Gorelik, G., and Richardson, B. (2010). Key role of ERK pathway signaling in lupus. Autoimmunity *43*, 17-22.

Guo, W., Lasky, J.L., Chang, C.J., Mosessian, S., Lewis, X., Xiao, Y., Yeh, J.E., Chen, J.Y., Iruela-Arispe, M.L., Varella-Garcia, M*., et al.* (2008). Multi-genetic events collaboratively contribute to Pten-null leukaemia stem-cell formation. Nature *453*, 529-533.

Hoeflich, K.P., Merchant, M., Orr, C., Chan, J., Den Otter, D., Berry, L., Kasman, I., Koeppen, H., Rice, K., Yang, N.-Y*., et al.* (2012). Intermittent Administration of MEK Inhibitor GDC-0973 plus PI3K Inhibitor GDC-0941 Triggers Robust Apoptosis and Tumor Growth Inhibition. Cancer Research *72*, 210-219.

Hoeflich, K.P., O'Brien, C., Boyd, Z., Cavet, G., Guerrero, S., Jung, K., Januario, T., Savage, H., Punnoose, E., Truong, T*., et al.* (2009). In vivo antitumor activity of MEK and phosphatidylinositol 3-kinase inhibitors in basal-like breast cancer models. Clin Cancer Res *15*, 4649-4664.

Ingham, R.J., Colwill, K., Howard, C., Dettwiler, S., Lim, C.S.H., Yu, J., Hersi, K., Raaijmakers, J., Gish, G., Mbamalu, G*., et al.* (2005). WW Domains Provide a Platform for the Assembly of Multiprotein Networks. Molecular and Cellular Biology *25*, 7092-7106.

Ishibe, S., Joly, D., Liu, Z.X., and Cantley, L.G. (2004). Paxillin serves as an ERK-regulated scaffold for coordinating FAK and Rac activation in epithelial morphogenesis. Mol Cell *16*, 257-267.

Kharas, M.G., Okabe, R., Ganis, J.J., Gozo, M., Khandan, T., Paktinat, M., Gilliland, D.G., and Gritsman, K. (2010). Constitutively active AKT depletes hematopoietic stem cells and induces leukemia in mice. Blood *115*, 1406-1415.

Kotelevets, L., van Hengel, J., Bruyneel, E., Mareel, M., van Roy, F., and Chastre, E. (2005). Implication of the MAGI-1b/PTEN signalosome in stabilization of adherens junctions and suppression of invasiveness. Faseb J *19*, 115-117.

Laura, R.P., Ross, S., Koeppen, H., and Lasky, L.A. (2002). MAGI-1: a widely expressed, alternatively spliced tight junction protein. Exp Cell Res *275*, 155-170.

Lehr, S., Kotzka, J., Avci, H., Sickmann, A., Meyer, H.E., Herkner, A., and Muller-Wieland, D. (2004). Identification of major ERK-related phosphorylation sites in Gab1. Biochemistry *43*, 12133-12140.

Lin, H.P., Chang, J.Y., Lin, S.R., Lee, M.H., Huang, S.S., Hsu, L.J., and Chang, N.S. (2011). Identification of an In Vivo MEK/WOX1 Complex as a Master Switch for Apoptosis in T Cell Leukemia. Genes & cancer *2*, 550-562.

Liu, P., Cheng, H., Roberts, T.M., and Zhao, J.J. (2009). Targeting the phosphoinositide 3-kinase pathway in cancer. Nature reviews *8*, 627-644.

Liu, X., Karnell, J.L., Yin, B., Zhang, R., Zhang, J., Li, P., Choi, Y., Maltzman, J.S., Pear, W.S., Bassing, C.H*., et al.* (2010). Distinct roles for PTEN in prevention of T cell lymphoma and autoimmunity in mice. J Clin Invest *120*, 2497-2507.

Macias, M.J., Wiesner, S., and Sudol, M. (2002). WW and SH3 domains, two different scaffolds to recognize proline-rich ligands. FEBS Lett *513*, 30-37.

Maurer, G., Tarkowski, B., and Baccarini, M. (2011). Raf kinases in cancer-roles and therapeutic opportunities. Oncogene *30*, 3477-3488.

Mirzoeva, O.K., Das, D., Heiser, L.M., Bhattacharya, S., Siwak, D., Gendelman, R., Bayani, N., Wang, N.J., Neve, R.M., Guan, Y*., et al.* (2009). Basal subtype and MAPK/ERK kinase (MEK)-phosphoinositide 3-kinase feedback signaling determine susceptibility of breast cancer cells to MEK inhibition. Cancer Res *69*, 565-572.

Mizuhara, E., Nakatani, T., Minaki, Y., Sakamoto, Y., Ono, Y., and Takai, Y. (2005). MAGI1 recruits Dll1 to cadherin-based adherens junctions and stabilizes it on the cell surface. J Biol Chem *280*, 26499-26507.

Montgomery, J.M., Zamorano, P.L., and Garner, C.C. (2004). MAGUKs in synapse assembly and function: an emerging view. Cell Mol Life Sci *61*, 911-929.

Parsons, M.J., Jones, R.G., Tsao, M.S., Odermatt, B., Ohashi, P.S., and Woodgett, J.R. (2001). Expression of active protein kinase B in T cells perturbs both T and B cell homeostasis and promotes inflammation. J Immunol *167*, 42-48.

Pleasance, E.D., Cheetham, R.K., Stephens, P.J., McBride, D.J., Humphray, S.J., Greenman, C.D., Varela, I., Lin, M.L., Ordonez, G.R., Bignell, G.R.*, et al.* (2010). A comprehensive catalogue of somatic mutations from a human cancer genome. Nature *463*, 191-196.

Poulikakos, P.I., and Solit, D.B. (2011). Resistance to MEK Inhibitors: Should We Co-Target Upstream? Sci Signal *4*, pe16-.

Rahdar, M., Inoue, T., Meyer, T., Zhang, J., Vazquez, F., and Devreotes, P.N. (2009). A phosphorylation-dependent intramolecular interaction regulates the membrane association and activity of the tumor suppressor PTEN. Proceedings of the National Academy of Sciences *106*, 480-485.

Roskoski, R., Jr. (2012). MEK1/2 dual-specificity protein kinases: structure and regulation. Biochem Biophys Res Commun *417*, 5-10.

Roy, M., Li, Z., and Sacks, D.B. (2005). IQGAP1 is a scaffold for mitogen-activated protein kinase signaling. Mol Cell Biol *25*, 7940-7952.

Sakurai, A., Fukuhara, S., Yamagishi, A., Sako, K., Kamioka, Y., Masuda, M., Nakaoka, Y., and Mochizuki, N. (2006). MAGI-1 is required for Rap1 activation upon cell-cell contact and for enhancement of vascular endothelial cadherin-mediated cell adhesion. Mol Biol Cell *17*, 966-976.

Sanchez, T., Thangada, S., Wu, M.-T., Kontos, C.D., Wu, D., Wu, H., and Hla, T. (2005). PTEN as an effector in the signaling of antimigratory G protein-coupled receptor. Proceedings of the National Academy of Sciences of the United States of America *102*, 4312-4317.

Sawalha, A.H., Jeffries, M., Webb, R., Lu, Q., Gorelik, G., Ray, D., Osban, J., Knowlton, N., Johnson, K., and Richardson, B. (2008). Defective T-cell ERK signaling induces interferon-regulated gene expression and overexpression of methylation-sensitive genes similar to lupus patients. Genes and immunity *9*, 368-378.

Schubbert, S., Shannon, K., and Bollag, G. (2007). Hyperactive Ras in developmental disorders and cancer. Nat Rev Cancer *7*, 295-308.

Song, M.S., Salmena, L., and Pandolfi, P.P. (2012). The functions and regulation of the PTEN tumour suppressor. Nat Rev Mol Cell Biol *13*, 283-296.

Sos, M.L., Fischer, S., Ullrich, R., Peifer, M., Heuckmann, J.M., Koker, M., Heynck, S., Stückrath, I., Weiss, J., Fischer, F.*, et al.* (2009). Identifying genotype-dependent efficacy of single and combined PI3K- and MAPK-pathway inhibition in cancer. Proceedings of the National Academy of Sciences *106*, 18351-18356.

Stambolic, V., Suzuki, A., de la Pompa, J.L., Brothers, G.M., Mirtsos, C., Sasaki, T., Ruland, J., Penninger, J.M., Siderovski, D.P., and Mak, T.W. (1998). Negative Regulation of PKB/Akt-Dependent Cell Survival by the Tumor Suppressor PTEN. Cell *95*, 29-39.

Su, D.L., Lu, Z.M., Shen, M.N., Li, X., and Sun, L.Y. (2012). Roles of pro- and anti-inflammatory cytokines in the pathogenesis of SLE. Journal of biomedicine & biotechnology *2012*, 347141.

Suzuki, A., Kaisho, T., Ohishi, M., Tsukio-Yamaguchi, M., Tsubata, T., Koni, P.A., Sasaki, T., Mak, T.W., and Nakano, T. (2003). Critical roles of Pten in B cell homeostasis and immunoglobulin class switch recombination. J Exp Med *197*, 657-667.

Suzuki, A., Yamaguchi, M.T., Ohteki, T., Sasaki, T., Kaisho, T., Kimura, Y., Yoshida, R., Wakeham, A., Higuchi, T., Fukumoto, M.*, et al.* (2001). T cell-specific loss of Pten leads to defects in central and peripheral tolerance. Immunity *14*, 523-534.

Tamura, M., Gu, J., Matsumoto, K., Aota, S., Parsons, R., and Yamada, K.M. (1998). Inhibition of cell migration, spreading, and focal adhesions by tumor suppressor PTEN. Science *280*, 1614-1617.

Tang, H., Tan, G., Guo, Q., Pang, R., and Zeng, F. (2009). Abnormal activation of the Akt-GSK3β signaling pathway in peripheral blood T cells from patients with systemic lupus erythematosus Cell Cycle *8*, 2789-2793.

Teis, D., Wunderlich, W., and Huber, L.A. (2002). Localization of the MP1-MAPK scaffold complex to endosomes is mediated by p14 and required for signal transduction. Dev Cell *3*, 803-814.

Ussar, S., and Voss, T. (2004). MEK1 and MEK2, different regulators of the G1/S transition. J Biol Chem *279*, 43861-43869.

Vazquez, F., Grossman, S.R., Takahashi, Y., Rokas, M.V., Nakamura, N., and Sellers, W.R. (2001). Phosphorylation of the PTEN Tail Acts as an Inhibitory Switch by Preventing Its Recruitment into a Protein Complex. Journal of Biological Chemistry *276*, 48627-48630.

Villanueva, J., Vultur, A., Lee, J.T., Somasundaram, R., Fukunaga-Kalabis, M., Cipolla, A.K., Wubbenhorst, B., Xu, X., Gimotty, P.A., Kee, D.*, et al.* (2010). Acquired resistance to BRAF inhibitors mediated by a RAF kinase switch in melanoma can be overcome by cotargeting MEK and IGF-1R/PI3K. Cancer Cell *18*, 683-695.

Wee, S., Jagani, Z., Xiang, K.X., Loo, A., Dorsch, M., Yao, Y.M., Sellers, W.R., Lengauer, C., and Stegmeier, F. (2009). PI3K pathway activation mediates resistance to MEK inhibitors in KRAS mutant cancers. Cancer Res *69*, 4286-4293.

Wimmer, R., and Baccarini, M. (2010). Partner exchange: protein-protein interactions in the Raf pathway. Trends in Biochemical Sciences *35*, 660-668.

Xu, Z., Peng, A.W., Oshima, K., and Heller, S. (2008). MAGI-1, a candidate stereociliary scaffolding protein, associates with the tip-link component cadherin 23. J Neurosci *28*, 11269-11276.

Yamada, K.M., and Araki, M. (2001). Tumor suppressor PTEN: modulator of cell signaling, growth, migration and apoptosis. J Cell Sci *114*, 2375-2382.

Yilmaz, O.H., Valdez, R., Theisen, B.K., Guo, W., Ferguson, D.O., Wu, H., and Morrison, S.J. (2006). Pten dependence distinguishes haematopoietic stem cells from leukaemia-initiating cells. Nature *441*, 475-482.

Yu, C.F., Liu, Z.X., and Cantley, L.G. (2002). ERK negatively regulates the epidermal growth factor-mediated interaction of Gab1 and the phosphatidylinositol 3-kinase. J Biol Chem *277*, 19382-19388.

Zaric, J., Joseph, J.M., Tercier, S., Sengstag, T., Ponsonnet, L., Delorenzi, M., and Ruegg, C. (2012). Identification of MAGI1 as a tumor-suppressor protein induced by cyclooxygenase-2 inhibitors in colorectal cancer cells. Oncogene *31*, 48-59.

Zhang, S.Q., Tsiaras, W.G., Araki, T., Wen, G., Minichiello, L., Klein, R., and Neel, B.G. (2002). Receptor-specific regulation of phosphatidylinositol 3'-kinase activation by the protein tyrosine phosphatase Shp2. Mol Cell Biol *22*, 4062-4072.

Zhu, J., Shang, Y., Xia, C., Wang, W., Wen, W., and Zhang, M. (2011). Guanylate kinase domains of the MAGUK family scaffold proteins as specific phospho-protein-binding modules. Embo J *30*, 4986-4997.
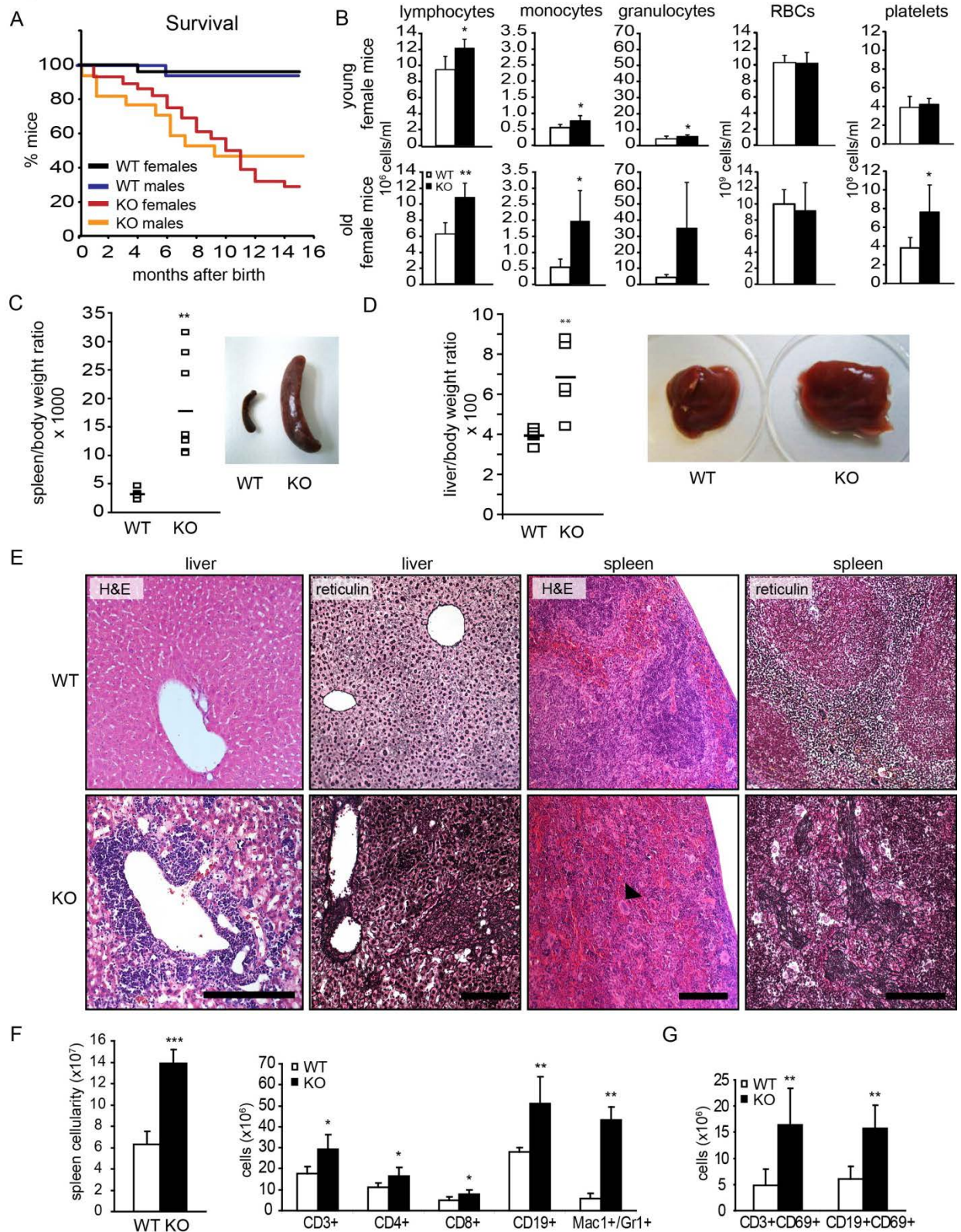
Figure 1
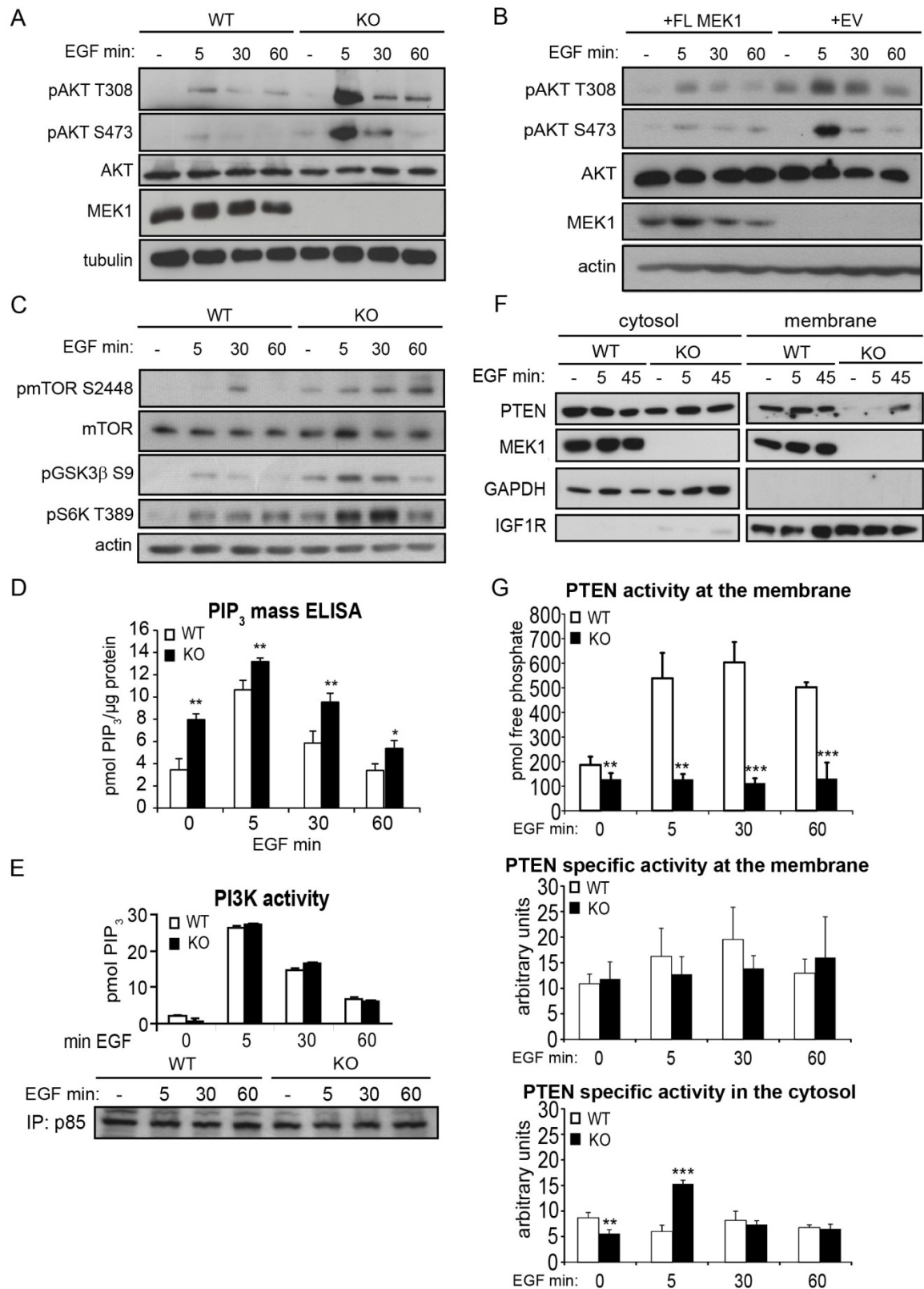
Figure 1 - MEK1 ablation promotes PIP$_3$ signaling by preventing PTEN membrane translocation. A-C, WT and KO MEFs (**A**), and KO MEFs reconstituted with full length MEK1 (+FL MEK1) or empty vector (+EV) (**B**) were stimulated with EGF and lysed at the indicated time points. Proteins and phosphorylated proteins were detected by immunoblotting as indicated. **D,** ELISA measurement of cellular PIP$_3$ in MEFs upon EGF stimulation. **E,** PI3K activity in p85 IPs from untreated or EGF-stimulated MEFs was assessed by ELISA. The amount of PIP$_3$ was normalized to the amount of immunoprecipitated p85. **F,** Extracts of starved or EGF-stimulated MEFs separated into cytosolic and membrane fractions. The presence of PTEN, MEK1, GAPDH (cytosolic marker) and IGF1R (plasma membrane marker) was assessed by immunoblotting. **G,** PTEN activity in membrane and cytosol fractions of EGF-stimulated MEFs. In the middle and bottom panels, arbitrary units were calculated by dividing pmoles of release phosphate by the amount of immunoprecipitated PTEN determined by the densitometry of western blots, and represent the mean ± SD of three experiments. *< 0.05; ** < 0.01; *** < 0.001. See Figure S1.

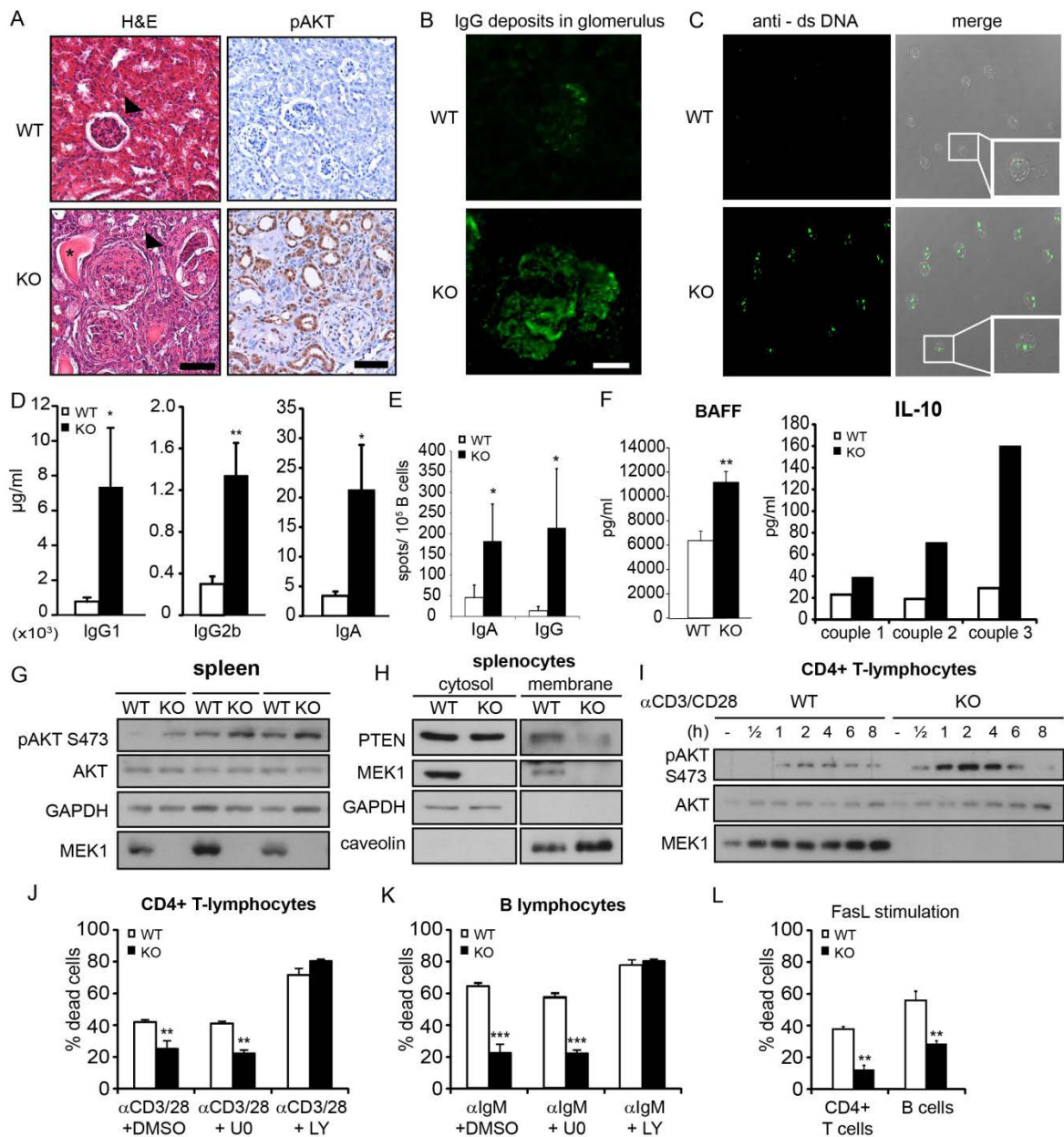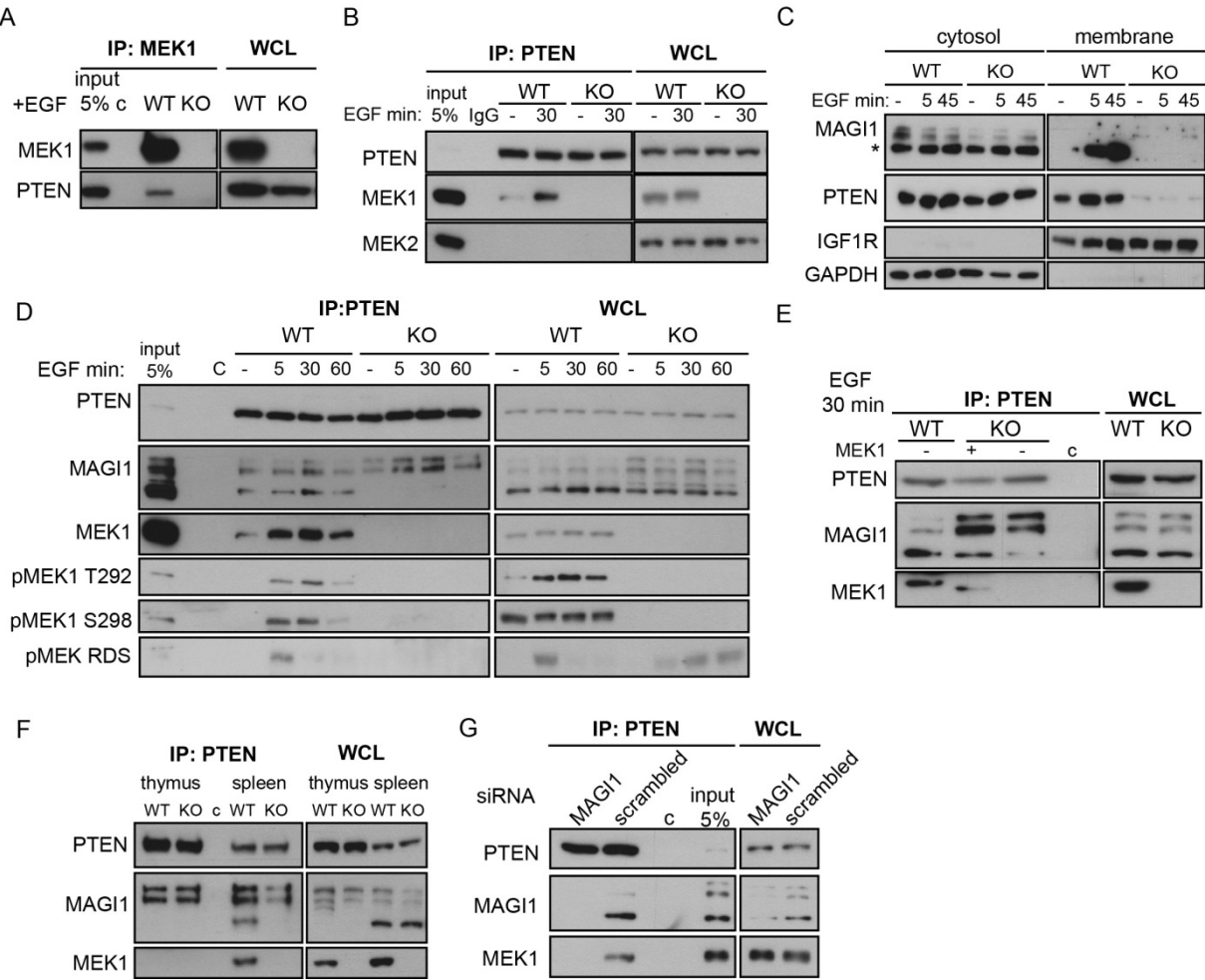Figure 2

Figure 2 – Myeloproliferation and lymphocyte activation in MEK1 KO mice. A, Survival of female (n=28) and male (n=17) KO mice monitored over a 15-mo period. **B,** Peripheral blood cell counts of young (1-3 mo) and old (8-12 mo) female KO mice and sex-matched WT littermates. Values represent mean ± SD (n=5). **C-D,** Spleno- and hepatomegaly in MEK1 KO mice. The plots show the weight of spleens (C; n=6) and livers (D; n=5) isolated from affected mice (n=6). **E,** Effacement of tissue architecture, extramedullary hematopoiesis (H&E staining; arrowhead = giant megakaryocyte) and fibrosis in KO livers and spleens. Scale bar 200µm. **F-G,** Increased Mac1$^+$/Gr1$^+$ cells and activated lymphocytes in spleens of affected KO mice (age 5-12 mo, n=5), detected by FACS analysis of lineage-specific and activation-induced markers (G; CD69). Values represent mean ± SD (n=5). * < 0.05; ** < 0.01; *** < 0.001. See Figure S2.
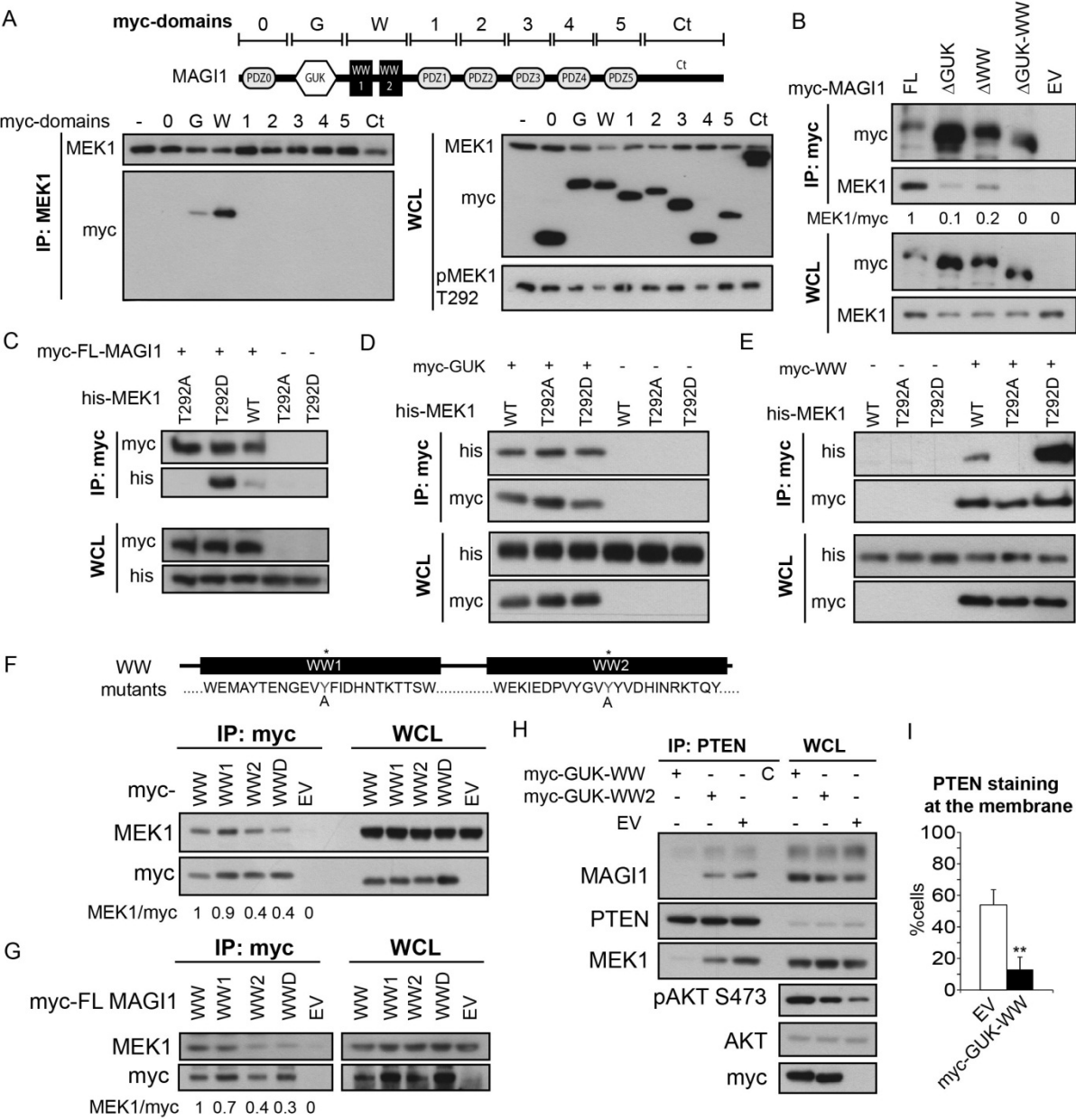
Figure 3

Figure 3 - *mek1* ablation leads to systemic autoimmune disease. A, Enlarged glomeruli (arrows), tubules filled with proteinaceous material (asterisk), and increased pAKT in KO kidneys. Scale bar 100µm. **B,** Immune complex deposition in the glomerulus of a 10 mo-old KO female visualized by mouse IgG antibodies (green). Scale bar 30µm. **C,** dsDNA autoantibodies detected in the serum of KO mice (5-10 mo, n=7) by *Crithidia luciliae* kinetoplast staining. **D,** IgG1, IgG2b, IgA levels in the sera of 8-10 mo-old mice (n=3) assessed by ELISA. **E,** Frequency of B cells secreting IgA and IgG in 8-10 mo-old mice determined by ELISpot (n=4). **F**, BAFF and IL-10 serum levels determined as in D. **G,** AKT phosphorylation and expression of AKT, MEK1, and GAPDH (loading control) were determined in lysates of 8 week-old WT and KO spleens. **H,** PTEN, MEK1, GAPDH (cytosolic marker), and caveolin (membrane marker) detected by immunoblotting in subcellular fractions of freshly isolated WT and KO splenocytes. **I,** Splenic CD4+ T-cells stimulated with αCD3 and αCD28 (3 µg/ml each). .The indicated proteins were visualized by immunoblotting. **J-L,** Survival of CD4+ T-cells and B cells in response to AICD and FasL induced cell death. Values represent mean ± SD. $* < 0.05$; $** < 0.01$; $*** < 0.001$. See Figure S3.
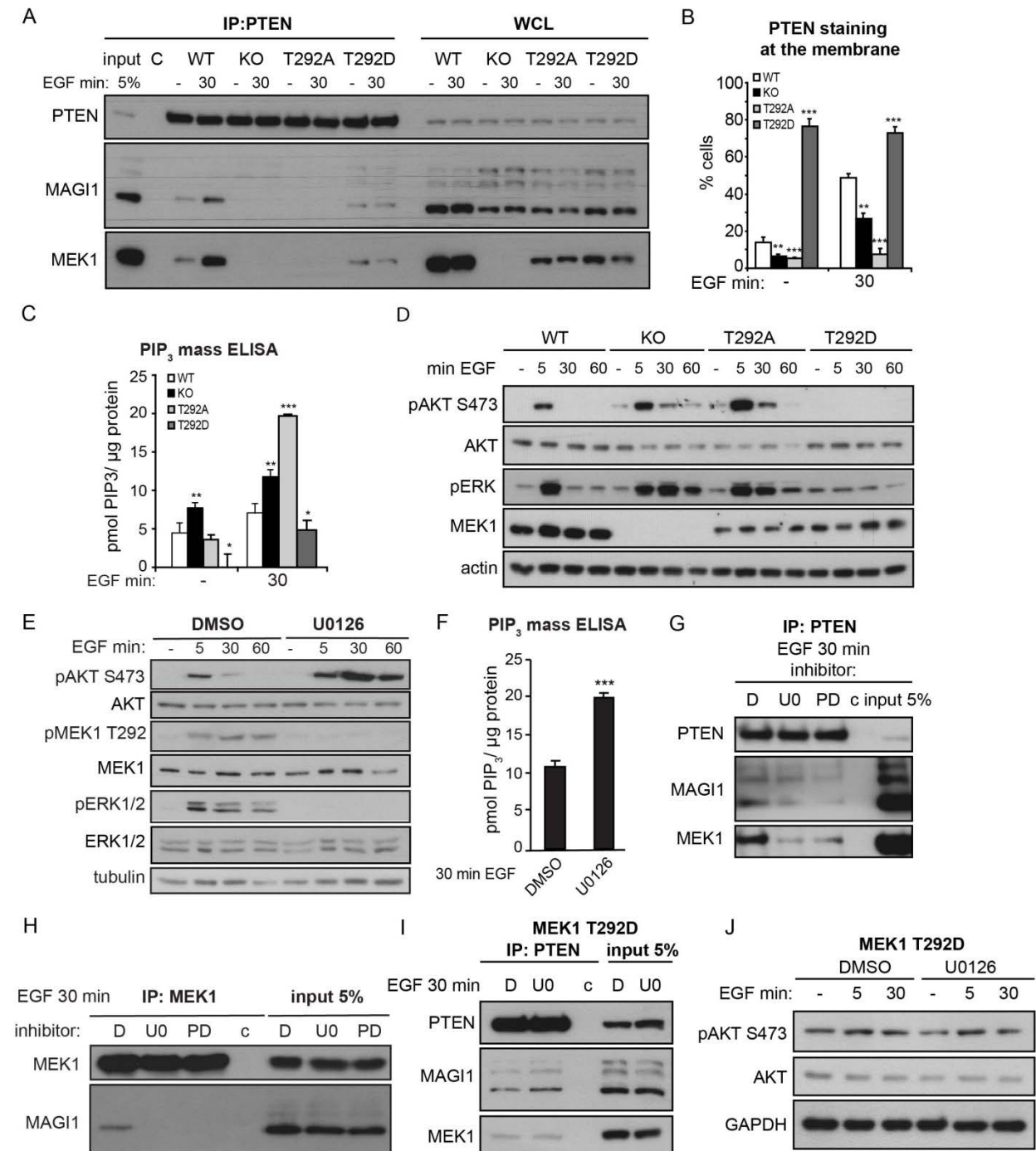
Figure 4

Figure 4 – A MEK1/MAGI1/PTEN ternary complex regulates MAGI1 and PTEN membrane recruitment. A-B, MEK1 (A) or PTEN (B) IPs prepared from EGF-stimulated WT and KO MEFs. MEK1, MEK2, and PTEN were detected by immunoblotting. WCL, whole cell lysates; c, unspecific binding to beads or isotype control antibody (IgG). **C,** Translocation of $MAGI1_{100}$ (*) and PTEN to the membrane. MAGI1, PTEN, IGF1R (membrane marker) and GAPDH (cytosolic marker) detected by immunoblotting of cytosol and membrane fractions of EGF-stimulated MEFs. **D,** PTEN, MAGI1, MEK1, and pMEK1 (pS298, pT292, and Raf-dependent sites, pRDS) detected by immunoblotting in WCL and PTEN IPs from EGF-stimulated MEFs. **E,** PTEN was immunoprecipitated from EGF stimulated (30 min) WT and KO MEFs. 1 µg of recombinant MEK1 (rMEK1) was added to the KO lysate as indicated. rMEK1 lacks 34 N-terminal amino acids and runs faster than endogenous MEK1. **F,** WCL and PTEN IPs from WT and KO thymocytes and splenocytes immunoblotted with PTEN, MAGI1, and MEK1 antibodies. **G,** WT MEFs transfected with siRNA against MAGI1 or control siRNA (scrambled). PTEN, MAGI1, and MEK1 were detected by immunoblotting of WCL and PTEN IPs from EGF-stimulated cells (30 min) MEFs. * < 0.05; ** < 0.01; *** < 0.001 See Figure S4.

Figure 5

Figure 5 – Structure-function analysis of MEK1/MAGI1 complexes. COS7 cells continuously growing in the presence of serum were transiently transfected with the indicated constructs. **A,** myc-tagged MAGI1 domains (schematically depicted in the upper panel) in endogenous MEK1 IPs and WCL were detected by immunoblot. **B**, myc-tagged MAGI1 and His-tagged MEK1 were detected in myc-tag IPs and WCL of cells transfected with myc-tagged MAGI1 deletion mutants and His-tagged MEK1. **C-E,** myc tagged MAGI1 proteins and His-tagged MEK1 were detected in myc-tag IP and WCL of cells transfected with His-tagged WT and mutant MEK1 and myc-tagged full-length MAGI1 (C), GUK (D) or WW (E) domains. Lysates were subjected to immunoblotting with His and myc antibodies. **F-G,** myc-tagged MAGI1 proteins and endogenous MEK1 were detected by immunoblotting in myc-tag IPs and cell lysates of cells transfected with WT and mutant WW domains of MAGI1 (1,2, and D, double mutant; F) or full-length MAGI1 bearing the same mutations (G). EV, empty vector. **H-I,** COS7 cells transfected with a plasmid encoding the WT or mutated GUK-WW (H) domains of MAGI1 or EV were subjected to PTEN IP. The indicated antigens were detected by immunoblotting (H). PTEN membrane localization was assessed by immunofluorescence (I; n=3). The numbers in B, F and G indicate the ratio between MEK1:myc-MAGI1 proteins, measured by densitometry. The MEK1:WT myc-MAGI1 ratio is set as 1.

Figure 6

Figure 6 – T292 phosphorylation, but not MEK1 kinase activity, promotes MEK1/MAGI1/PTEN binding and decreases PIP$_3$ pathway activation. A, WT, KO and MEK1 mutant fibroblasts were stimulated with EGF. PTEN, MAGI1 and MEK1 in endogenous PTEN IPs and WCL were detected by immunoblotting. **B-D,** MEK1 WT, KO and mutant fibroblasts were stimulated with EGF. PTEN membrane recruitment was determined by immunofluorescence. The plot in **B** depicts the percentage of cells (mean ±SD of 3 experiments) showing membrane PTEN. The plot in **C** shows PIP$_3$ levels, determined by ELISA. **D**, pAKT pERK, AKT, MEK, and tubulin (loading control) were detected by immunoblotting. **E-F,** WT MEFs were pretreated with MEK inhibitors or DMSO and stimulated with EGF. **E**, Phosphorylation and expression of AKT, ERK, MEK1 and tubulin (loading control) were determined by immunoblotting. **F,** intracellular PIP$_3$ levels in WT MEFs pretreated with U0126 or DMSO and stimulated with EGF.were measured by ELISA. **G-H,** WT fibroblasts pretreated with DMSO or MEK inhibitors (U0126, PD0325901) and stimulated with EGF were subjected to PTEN (**G**) or MEK1 IP (**H**). PTEN, MAGI1, and MEK1 were detected by immunoblotting. c, Non-specific binding to the beads. **I-J,** T292D MEK1 mutant MEFs were treated with U0126 or DMSO and stimulated with EGF. PTEN, MEK1 and MAGI1 in PTEN IPs (**I**) and pAKT, AKT and GAPDH (loading control) in WCL (**J**) were visualized by immunoblotting. In J, c represents non-specific binding to the beads. * < 0.05; ** < 0.01; *** < 0.001. See Figure S5.

2.7 SUPPLEMENTARY MATERIAL

Supplementary Figures

Figure S1 - Impact of *mek1* ablation on PIP_3 signaling (linked to Figure 1).

Figure S2 - Phenotypes of MEK1 KO mice (linked to Figure 2).

Figure S3 - *mek1* ablation leads to systemic autoimmune disease (linked to Figure 3).

Figure S4 - MEK1 interacts with PTEN via MAGI, and MAGI plays a role in PTEN membrane recruitment and AKT phosphorylation (linked to Figure 4).

Figure S5 - T292 phosphorylation, but not MEK1 kinase activity, promotes MEK1/MAGI1/PTEN binding and decreases PIP_3 pathway activation (linked to Figure 6).

Figure S1
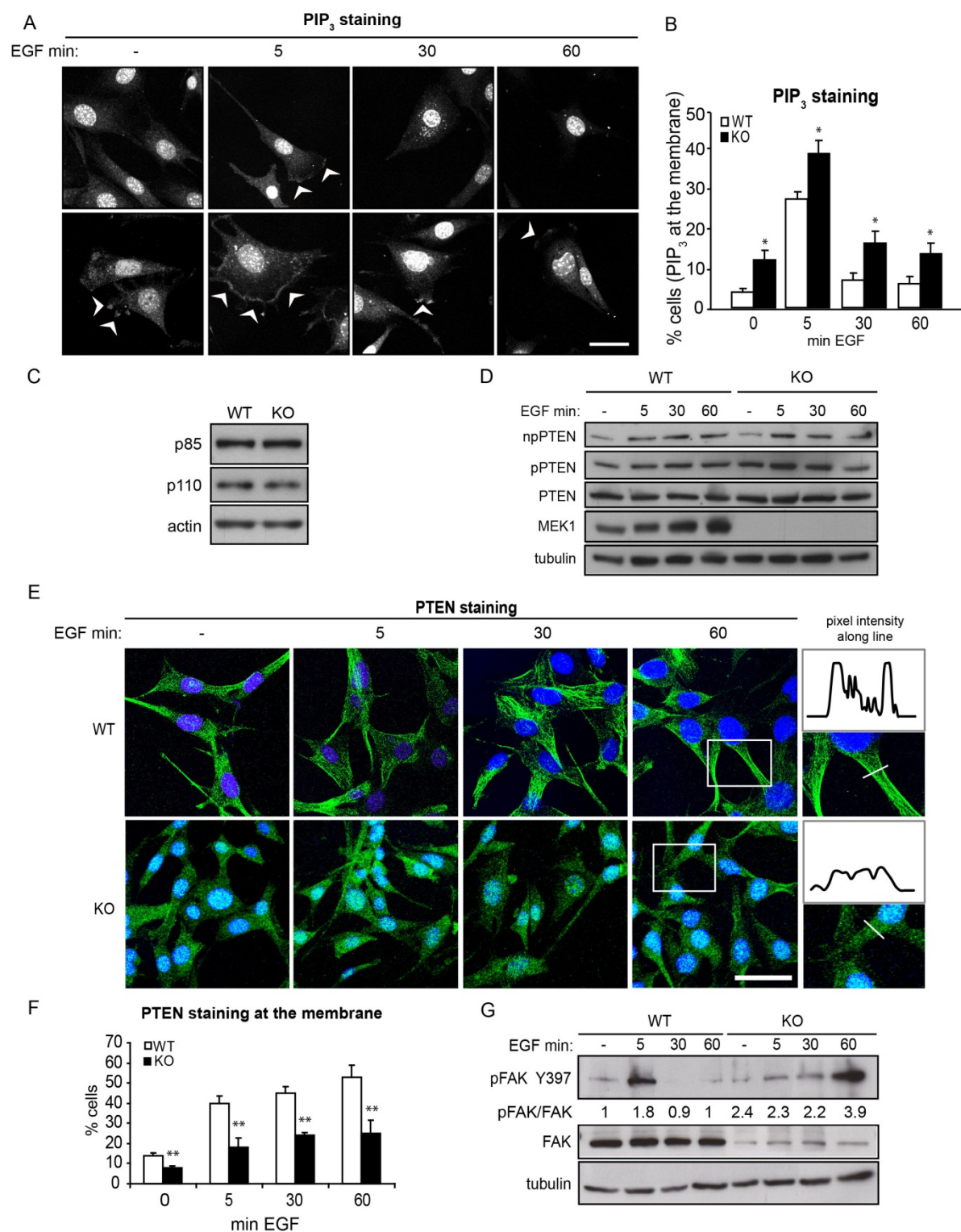
Figure S1 – Impact of *mek1* ablation on PIP$_3$ signaling. A-B, Increased accumulation of PIP$_3$ at the membrane of KO cells upon EGF stimulation. WT and KO MEFs were stimulated with EGF for the indicated times. After fixation, cells were stained with a PIP$_3$ antibody. The arrows indicate accumulation of PIP$_3$ at the leading edge of the cells. Quantification of PIP$_3$ staining is shown in (B). A minimum of 100 cells per slide were counted. The graph shows mean of three experiments ± SD. * < 0.05; ** < 0.01; *** < 0.001. Scale bar 30 µm. **C,** Expression of PI3K subunits is equal in WT and KO MEFs. Whole cell lysates from WT and KO MEFs were immunoblotted with the indicated antibodies. Actin is shown as a loading control. **D,** PTEN expression and phosphorylation is not altered in KO MEFs. To assess PTEN expression and phosphorylation (residues S380, T382 and T383; pPTEN = phosphorylated PTEN; npPTEN = non-phosphorylated), WT and KO whole cell lysates prepared at different times after EGF stimulation and the indicated antigens were detected by immunoblotting. Tubulin is shown as a loading control. **E-F,** inefficient PTEN membrane recruitment in EGF-stimulated KO MEFs. Cells were fixed at the indicated time points and stained with a PTEN antibody (green). Nuclei were visualized by DAPI (blue). Scale bar=30 µm. Left panels show the PTEN staining intensity along the indicated lines. **F,** Quantification of cells with membrane localization of PTEN was performed by counting at least 300 cells per experimental condition. The plot represents the mean of three independent experiments ± SD. * < 0.05; ** < 0.01; *** < 0.001. **G,** Phosphorylation of FAK Y397 is increased in KO MEFs. WT and KO whole cell lysates prepared at different times after EGF stimulation and the indicated antigens were detected by immunoblotting. Tubulin is shown as a loading control. The quantification was performed in ImageJ. pFAK values were divided by total FAK values. Numbers represent values relative to the unstimulated WT sample, arbitrarily set to 1. In the KO, FAK phosphorylation increases at 6o min after EGF stimulation, even if some PTEN reaches the membrane at this stage. However, the amount of PTEN localized to the KO membrane is low (20% of the WT at the 45 min time point) and doesn't even reach the amount of membrane PTEN observed in the unstimulated WT cells. This would allow the accumulation of the phosphorylated form of. It is also possible that the KO impairs the recruitment of PTEN to membrane domains, such as adherens junctions, in which FAK is enriched, resulting in a disproportionate increase of FAK phosphorylation.
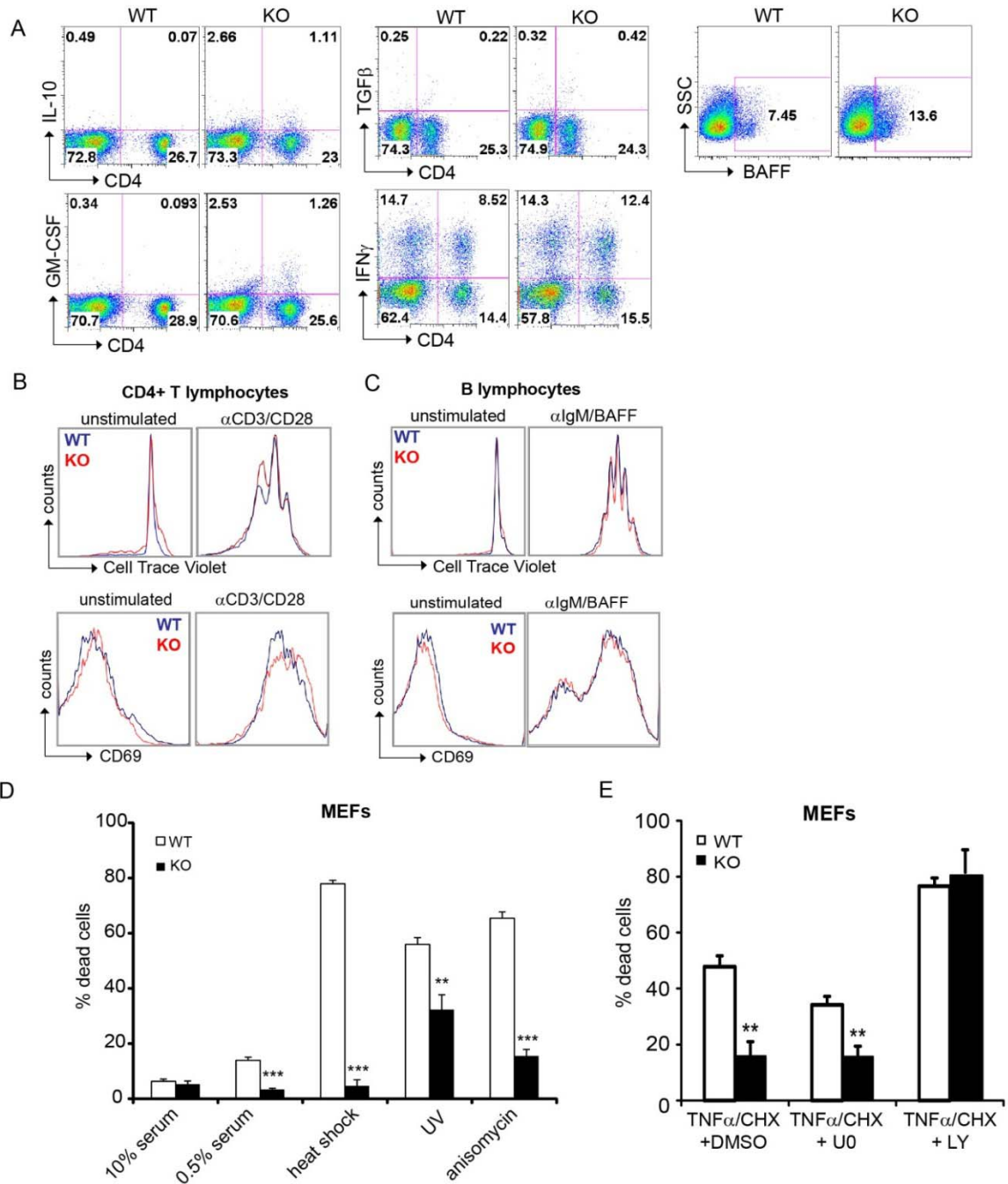
Figure S2
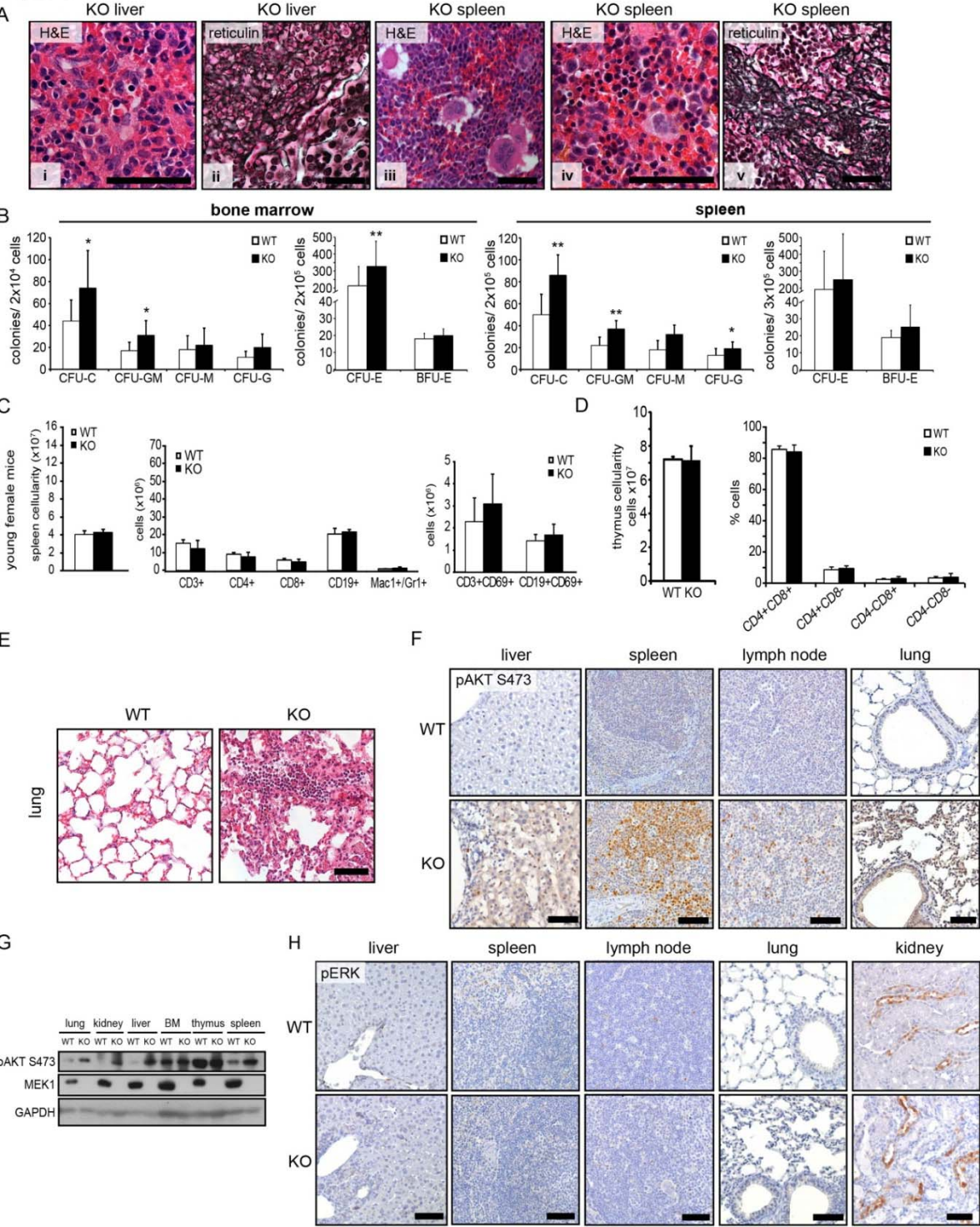
Figure S2 – Phenotypes of MEK1 KO mice – A, Extramedullary hematopoiesis in KO liver (panel i, H&E) and spleen (iv, H&E), accumulation of atypical megakaryocytes in KO spleen (iii, H&E), and fibrosis in liver (ii, reticulin stain) and spleen (v, reticulin stain) are shown at higher magnification. Scale bar 30µm. **B,** Colony forming units from bone marrow and spleen were determined in young mice (5-8 weeks, n=5). CFU-C= total myeloid colonies, CFU-GM= granulocyte/monocyte colony forming units, CFU-G= granulocyte colony forming units, CFU-M= monocyte colony forming units, BFU-E= burst forming units, CFU-E= colony forming units erythroid. Values represent mean ± SD. **C,** Normal spleen cellularity and splenocyte subsets in young female mice (age 1-3 months, n=5), detected by FACS analysis of lineage-specific and activation-induced markers (CD69). Values represent mean ± SD of 5 mice. **D,** Normal thymic development in *mek1*-deficient mice. Cellularity and composition of thymi isolated from 8 week-old WT and KO females (n =6). Thymocytes were stained for the indicated lineage-specific surface markers and analyzed by FACS. Values represent mean ± SD. **E,** Thickening of interstitial alveolar spaces and vascular congestion in H&E stained lung section from a representative 1 year old couple. Scale bar 200µm. **F-G,** AKT phosphorylation in *mek1* KO organs. **F,** Livers, spleens, lymph nodes, and lungs, were dissected, sectioned and stained with an antibody against pAKT S473 (n=3). Representative sections from a 1 year old couple are shown. Scale bar 100µm. **G,** Western blot analysis of organ lysates isolated from a representative 11 month-old mouse and a sex-matched littermate. **H**, Livers, spleens, lymph nodes, lungs and kidneys were dissected, sectioned and stained with an antibody against pERK (n=3). Representative sections from a 1 year old couple are shown. Scale bar 100µm.

Figure S3

Figure S3 - *mek1* ablation leads to systemic autoimmune disease. A, Cytokine profiles of splenocytes from 8-10 months old mice. Total splenocytes were stimulated in vitro. Cell positive for CD4 and the indicated cytokines were detected by FACS. Plots show one representative littermate pair out of three. **B-C,** Proliferation (upper panels) and expression of the activation marker CD69 (lower panels) was monitored in CD4+ T cells and B cells activated in vitro. Histograms show the results of one representative experiment out of three independent experiments. **D-E,** WT and KO MEFs were grown in medium containing 10% FCS or exposed to different apoptotic stimuli: starvation in 0.5% FCS, heat shock for 30 min at 42°C, UV irradiation 780 J/m^2, anisomycin (10µg/ml), or TNFα (10ng/ml)/cycloheximide (5µg/ml) for 16 hours. Values represent means ± SD from triplicate samples. One representative experiment is shown. In **E,** WT and KO MEFs were pretreated for 1 hour with UO126 (10 µM), LY294002 (50 µM) or DMSO (vehicle). Cell death was measured by FACS (PI). Results are normalized to spontaneous cell death, values represent mean ± SD. * < 0.05; ** < 0.01; *** < 0.001.

Figure S4
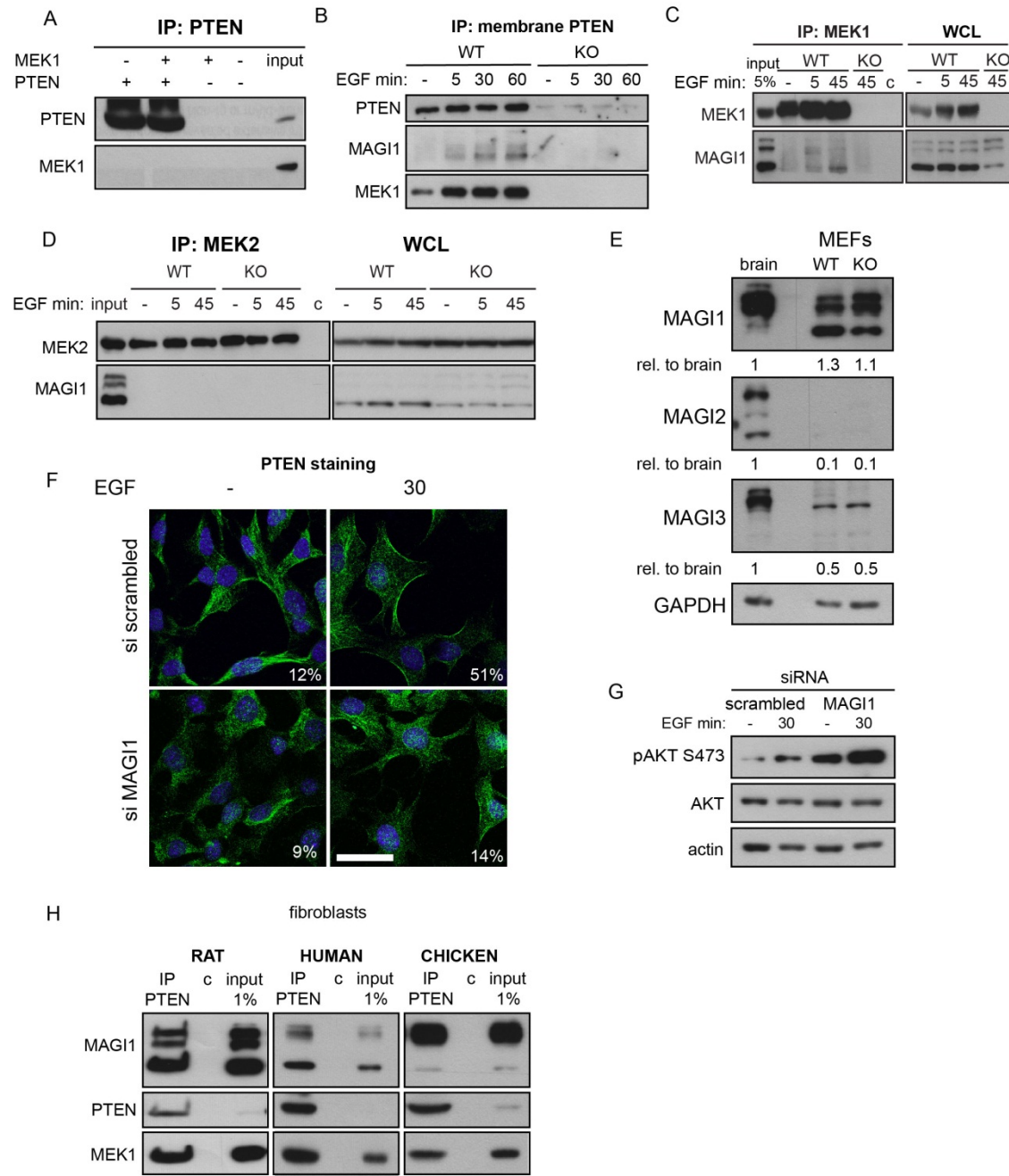
Figure S4 - MEK1 interacts with PTEN via MAGI, and MAGI plays a role in PTEN membrane recruitment and AKT phosphorylation. **A,** MEK1 does not interact with PTEN directly. Recombinant purified MEK1 (1µg) and PTEN (1 µg) were co-incubated prior to PTEN immunoprecipitation and immunoblotting with the indicated antibodies. **B,** EGF stimulation increases the amount of $MAGI1_{100}$ and MEK1 co-immunoprecipitated with membrane PTEN. PTEN was immunoprecipitated from the membrane fraction of EGF-stimulated MEFs. PTEN, MEK1 and MAGI1 were detected by immunoblotting.   **C-D,** MEK1, but not MEK2, binds to MAGI1. MEK1 (C) or MEK2 (D) were immunoprecipitated from EGF-stimulated WT and KO MEFs. MAGI1 coimmunoprecipitation was examined by immunoblotting. c, unspecific binding to beads. **E,** MAGI1 is the main MAGI protein expressed in WT and KO MEFs. Immunoblot comparing the amounts of MAGI1, MAGI2, and MAGI3 expressed in MEFs and with those present in brain lysates, which contain all three and are therefore used as a reference. The numbers represent the ratio between the amount of MAGI proteins contained in the MEF and brain lysates, normalized for GAPDH content (loading control; all determined by densitometry). All three MAGI1 isoforms were taken into account in this calculation. **F-G,** Knockdown of MAGI1 impairs PTEN membrane translocation and induces AKT activation. WT MEFs transfected with siRNA against MAGI-1 or control siRNA (scrambled) were starved, stimulated with EGF for 30 min and stained for PTEN (green) and DNA (DAPI, blue) (F; Scale bar 30 µm). The percentage of cells showing PTEN membrane localization is shown in the insets. In G, whole cell lysates were immunoblotted with phosphospecific AKT antibodies and AKT antibodies to determine the degree of AKT phosphorylation. Actin is shown as a loading control. **H,** Primary fibroblasts from rat, human and chicken continuously growing in the presence of 10% serum were lysed and subjected to PTEN IP. c, control for unspecific binding to the beads.

Figure S5
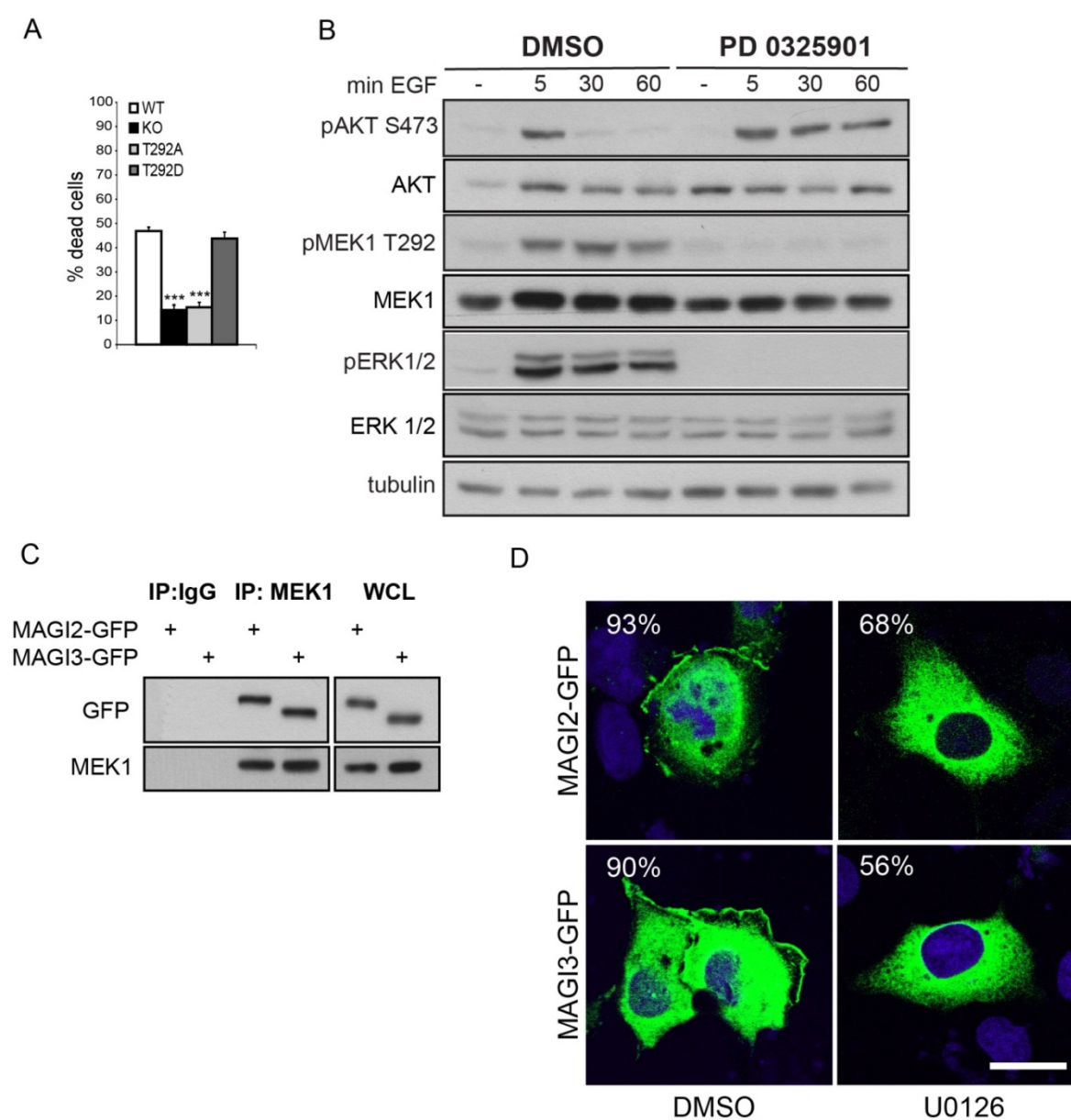
Figure S5 - T292 phosphorylation, but not MEK1 kinase activity, promotes MEK1/MAGI1/PTEN binding and decreases PIP$_3$ pathway activation. A, WT, KO and MEK1 mutants expressing MEFs were treated with TNFα (10ng/ml)/cycloheximide (5µg/ml) for 16 hours. Cell death was analyzed by propidium iodide staining. **B,** WT MEFs were pretreated with PD0325901 or DMSO (vehicle) and stimulated with EGF for the indicated times. Whole cell lysates were subjected to immunoblot analysis with the indicated antibodies. Tubulin is shown as a loading control. **C-D**, MAGI2 and 3 interact with MEK1 and their membrane localization is affected by chemical inhibition of MEK1 T292 phosphorylation. COS7 cells were transfected with MAGI2-GFP and MAGI-3-GFP plasmids. Immunoprecipitation was performed using a MEK1 or an irrelevant (IgG) antibody. In D, membrane of MAGI2 and 3 was determined in cells treated with the MEK inhibitor U0126 or with the vehicle DMSO. The percentage of cells showing MAGI2 or MAGI3 membrane localization is shown in the insets.

III. ADDITIONAL RESULTS

3.1 PTEN localization in WT and MEK1 KO mouse embryonic fibroblasts

Figures 1F and S1E-F in the Manuscript show a defect in the membrane translocation of PTEN in MEK1 KO fibroblasts. The IF studies suggest that PTEN also accumulates in the nucleus in the KO fibroblasts. Nuclear PTEN plays role in maintaining genomic integrity [67]. While the mechanism of nuclear import has been described in previous studies alternatively as passive diffusion or active transport [128, 129], the precise mode of PTEN nuclear export remains unknown. MEK1 contains a nuclear export signal and it has been implicated in the nuclear export of ERK and PPARγ [13]. It would therefore be interesting to investigate whether MEK1 is involved in the nuclear shuttling of PTEN.

To this aim, we performed fractionation experiments to determine the levels of PTEN in the nuclear fractions after EGF stimulation (Fig 10). We did not find any apparent accumulation of PTEN in the KO nuclear fractions after EGF stimulation. It is possible that the accumulation seen with PTEN immunofluorescence is artifactual and does not represent a real nuclear localization of PTEN.
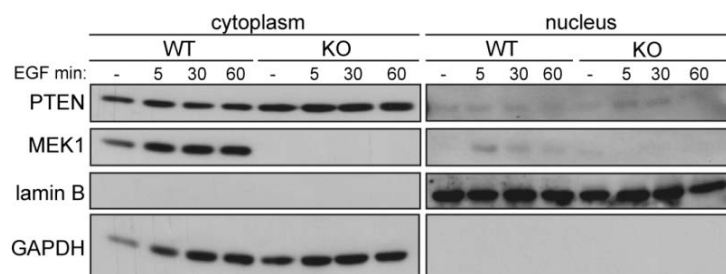
Figure 10. WT and KO MEFs were starved and stimulated with EGF. The cells were then separated into cytoplasmic and nuclear fractions by differential lysis and centrifugation. The fractions were analyzed by immunoblotting. Lamin B was used as a nuclear marker and GAPDH as a cytoplasmic marker.

Another observation made in the PTEN IF studies was localization of the phosphatase to unknown fibrillar structures in the cytoplasm of WT MEFs. By double staining with components of the cytoskeleton we could show that PTEN colocalizes with tubulin, but this colocalization is absent in the KO MEFs (Fig 11A). This was not due to defects in the microtubular cytoskeleton itself (Fig 11B). The interaction of PTEN with tubulin was confirmed in immunoprecipitation (Fig 11C), and complex formation was diminished in the KO cells. Treatment of WT MEFs with nocodazole, a microtubule destabilizing agent, resulted in mislocalization of PTEN similar to that observed in KO

MEFs (Fig 11D). However, nocodazole didn't result in increased AKT signaling as expected (Fig 11E). This is most likely because microtubules regulate PI3K localization [130] and also because they are generally implicated in the correct assembly of signaling complexes and signal transduction through their interaction with multiple kinases and phosphatases [131]. This is probably also the reason for the decreased ERK activation observed after nocodazole treatment.
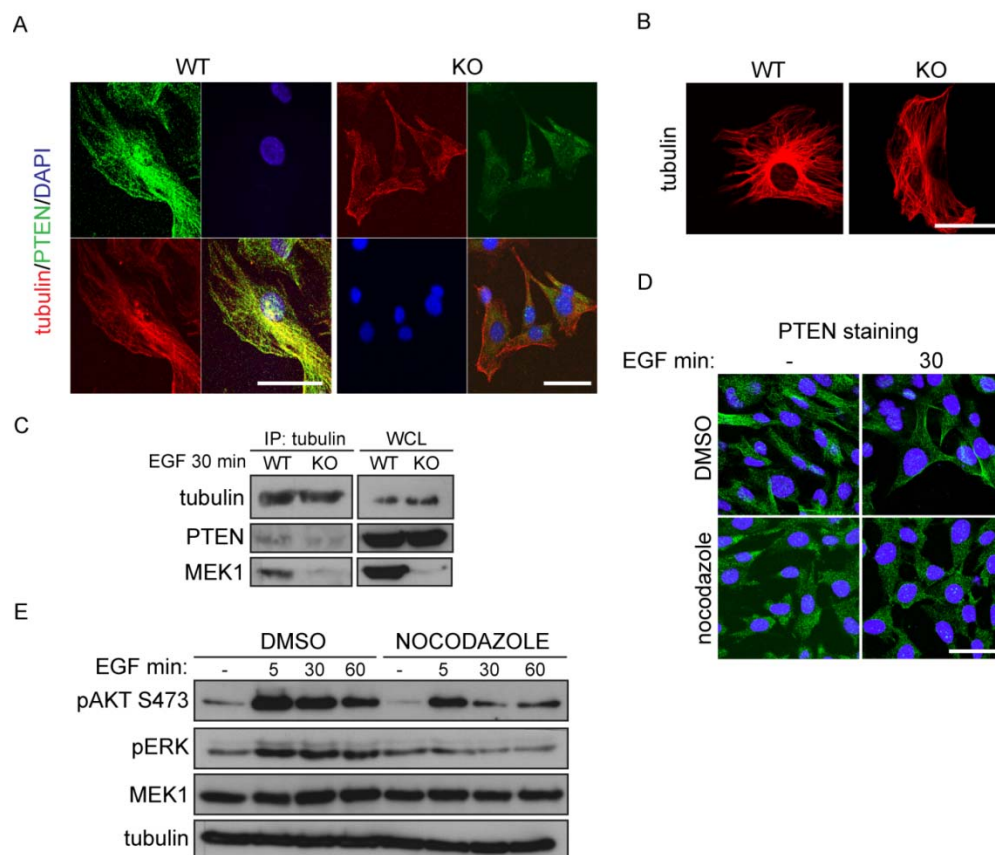
Figure 11. A, WT and KO MEFs were stimulated with EGF for 30 min, fixed and stained for PTEN and tubulin. Nuclei were visualized by DAPI (blue). Scale bar 30 μm. **B**, Microtubules in WT and KO MEFs were visualized by staining for tubulin. Scale bar 30 μm. **C,** WT and KO MEFs were stimulated with EGF for 30 min and the whole-cell lysates were subjected to tubulin IP. Samples were analyzed by immunoblotting. **D**, WT MEFs were pretreated 10 min with DMSO or 10 μM nocodazole and stimulated with EGF. The cells were then fixed and stained for PTEN. The nuclei were visualized by DAPI (blue). Scale bar 30 μm. **E,** WT MEFs were pretreated 10 min with DMSO or 10 μM nocodazole and stimulated with EGF for the indicated times. Whole cell lysates were subjected to western-blot analysis.

PTEN is known to interact with microtubule-associated serine-threonine kinases (MAST205, MAST2/3) [132, 133]. The biological implications of this complex are not yet fully understood. One possibility is that microtubules are involved in the transport of PTEN to the membrane. However, to date only one active transport mechanism for

PTEN has been reported. Van Diepen and coauthors have discovered that in neurons PTEN can directly associate with myosinV, a motor protein which mediates its transport to the membrane [134]. Thus, the possible role of microtubules and MEK1 in the translocation of PTEN remains to be addressed. We don't know yet whether MEK1 is solely necessary for MEK1/MAGI1/PTEN complex formation or whether it is actively contributing to the transport process itself, for example by loading the complex on microtubules, or by driving the interaction with the membrane-associated proteins. The latter is well possible, since MEK1 can directly interact with paxillin, which is normally located at the junctional complexes [23].

3.2 Characterization of MAGI1

In the manuscript, we have identified multiple isoforms of MAGI1 protein. Only the $MAGI1_{100}$ isoform formed a complex with MEK1 and PTEN. The exact character of the isoform, however, remains unknown. MAGI protein encoding genes generally produce various splice variants [82]. It is plausible that $MAGI1_{100}$ is a shorter splice variant of MAGI1. The possibility also exists that $MAGI1_{100}$ is produced by proteolytic cleavage [135], or that other unknown posttranslational modifications are involved.

We analyzed the expression of the different isoforms in various mouse tissues (Fig 12A). The isoform expression pattern differs between tissues. This may diversify MAGI1 signaling. For example, one would expect a greater impact of MEK1 deletion in tissues with higher relative $MAGI1_{100}$ expression. This is true in thymocytes and splenocytes. In thymocytes, which completely lack $MAGI1_{100}$, we didn't see any perturbations in AKT signaling (Fig 12A, 12B). Conversely, splenocytes expressing relatively high levels of a $MAGI1_{100}$ have hyperactivated AKT pathway (Fig 12A, Figures 2G and S2G in the Manuscript).
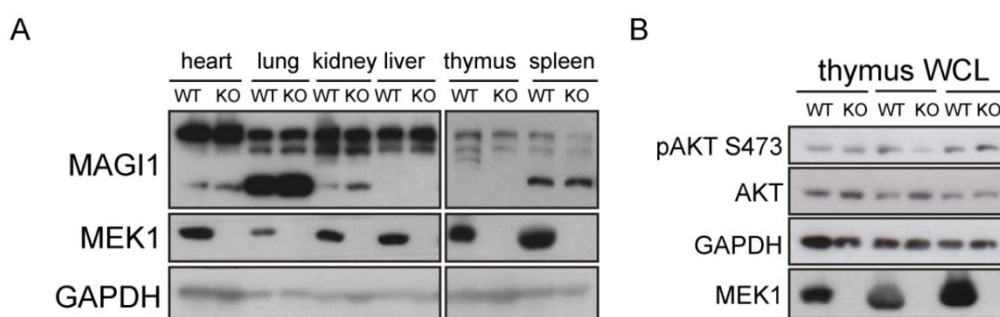
Figure 12. A, Tissue lysates from WT and KO littermate mice were analyzed by immunoblotting. **B,** Lysates from thymi of 3 littermate female mice (8 weeks old) were analyzed by immunoblotting.

We also investigated the localization of MAGI1 within the cell. Immunofluorescence showed that MAGI1 accumulates at the membrane in WT MEFs, while in the KO cells it is more randomly localized (Fig 13A). These data confirm the fractionation experiments in the Manuscript (Fig 4C in the Manuscript). Several studies describe MAGI proteins as components of junctional complexes [42, 76]. Indeed MAGI1 colocalized with paxillin in WT MEFs (Fig 13B), a protein found in cellular junctions. The colocalization was diminished in the KO fibroblasts. Once again, these data suggest that MEK1 via its interaction with paxillin [23] can bring MAGI1 to complexes localized at cellular junctions.
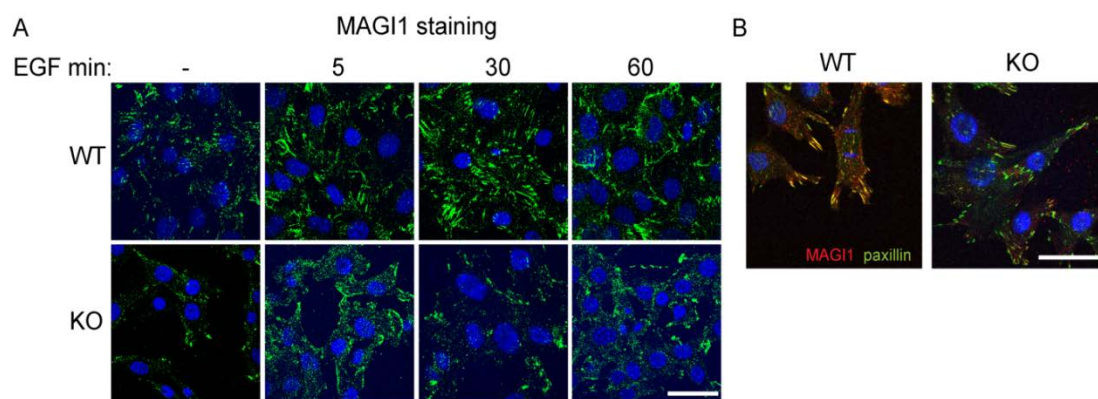
Figure 13. WT and KO MEFs were starved and stimulated with EGF. After fixation, the cells were stained with MAGI1 antibody **(A)** or double stained with MAGI1 and paxillin antibodies **(B)**. Nuclei are visualized by DAPI (blue). Scale bar 30 µm.

However, the IF analysis is complicated by simultaneous staining of all isoforms of MAGI1. At the moment, it is not technically possible to stain specifically $MAGI1_{100}$. Isoform-specific antibodies would be necessary to address this problem.

3.3 Role of MEK1 S298 phosphorylation in the crosstalk to AKT pathway

We have described the regulatory role of MEK1 T292 phosphorylation in the complex formation between WW domain of MAGI1 and MEK1 in the Manuscript. T292 is not the only prosphorylation site within the proline-rich domain. S298 is phosphorylated in MEK1, and not in MEK2, by PAK1. It is therefore necessary to address the question of whether this phosphorylation also has an impact on AKT signaling and MEK1/MAGI1/PTEN complex formation.

To this aim, we created stable monoclonal MEF cell lines expressing phosphomimetic S298D and unphosphorylatable S298A forms of MEK1 at this residue. We investigated the kinetics of AKT activation in these mutants in comparison to KO

MEFs. S298A mutation resulted in increased and prolonged AKT signaling (Fig 14A). This effect was confirmed by PIP3 ELISA (Fig 14B). PTEN recruitment to the membrane was impaired in the S298A mutant (Fig 14C) as well as the PTEN/MAGI1/MEK1 complex formation (Fig 14D). The effect on PTEN recruitment is not as strong as in the T292A mutant (Fig 6B in Manuscript), which may be due to residual T292 phosphorylation of the S298A mutant (data not shown). The S298D mutant had a peak of AKT signaling at 5 min of EGF stimulation, followed by fast downregulation; a pattern usually seen in the WT MEFs. However the interpretation of this set of experiments is complicated by the fact that S298A mutant MEK1 is expressed at much lower levels than the S298D mutant and the cells tend to lose its expression when cultured. It is therefore questionable to what degree this may affect the AKT signaling.
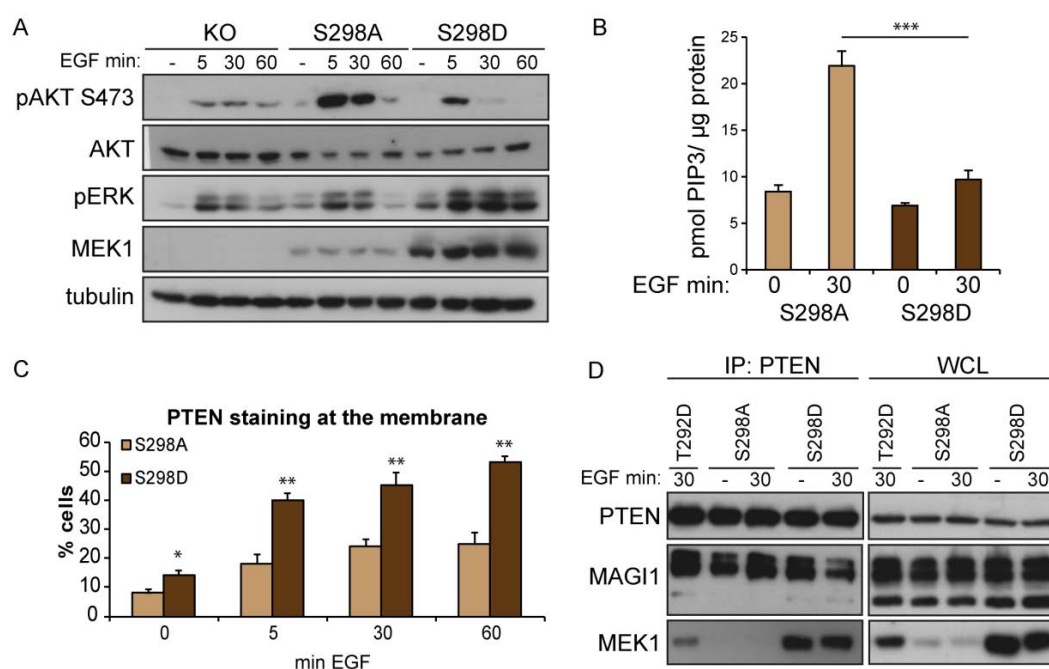
Figure 14. A, KO MEFs and MEFs stably expressing MEK1 S298A or MEK1 S298D mutants were starved and stimulated with EGF. Whole-cell lysates were subjected to immunoblotting. **B,** MEFs stably expressing MEK1 S298A or MEK1 S298D mutants were starved and stimulated with EGF. Total levels of PIP_3 were analyzed by ELISA. **C,** MEFs stably expressing MEK1 S298A or MEK1 S298D mutants were starved and stimulated with EGF. Cells with membrane-localized PTEN were counted. See the manuscript for details on the PTEN staining and quantification. **D,** MEFs stably expressing MEK1 S298A or MEK1 S298D mutants were starved and stimulated with EGF. Cellular lysates were subjected to PTEN immunoprecipitation and analyzed with immunoblotting.

S298 phosphorylation is a prerequisite for proper MEK1/ERK activation and therefore also for T292 phosphorylation (see Fig 14A and [15]). Therefore it is hard to distinguish whether the effect on AKT signaling and complex formation is due to the impact on T292 phosphorylation or whether this is an independent regulatory mechanism. To address this question, double mutants have to be tested; for example T292A/S298A, T292D/S298A and T292D/S298A.

3.4 Effects of MEK1 KO in the thymus

The thymus is the organ where T cell development is accomplished and central tolerance is established through negative selection. Interestingly, the thymus was not affected by MEK1 deletion in terms of AKT signaling (Fig 12B and Fig S2G in Manuscript). This might be due to the absence of the MAGI1$_{100}$ isoform and therefore of the MAGI100/PTEN/MEK1 regulatory mechanism (Fig 12A and Fig 4F in the Manuscript). The development of T cells is normal in WT and KO mice (Fig S2D in the Manuscript). We also analyzed whether there were differences in the negative selection of the thymocytes. The KO thymocytes responded to TCR stimulation *in vitro* with similar levels of AKT activation (Fig 15A) and with a rate of cell death very similar to that of the WT thymocytes (Fig 15B); thus, we concluded that the negative selection in these mice is normal.
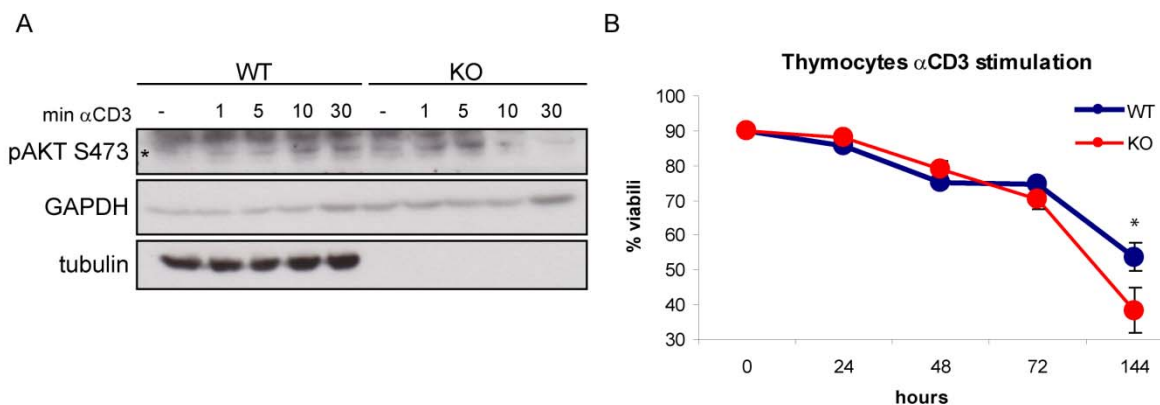
Figure 15. A, Total thymocytes isolated from 8 week-old WT and KO mice were starved for 2 hours and then stimulated with 10 µg/ml of αCD3 antibody for the indicated times. Whole-cell lysates were analyzed by western blot. The asterisk indicates the pAKT band. **B,** Total thymocytes isolated from 8 week-old WT and KO mice were stimulated with 1 µg/ml of αCD3 antibody and the viability was assessed at the indicated times by PI staining and flow cytometric analysis. n=3

3.5 Effects of MEK1 KO in the spleen

Defects in the engulfment and clearance of apoptotic cells can result in autoimmune response [136]. PTEN has been also implicated in this process by negatively regulating engulfment of apoptotic cells via Rac GTPase [137]. We tested whether the accumulation of apoptotic cells could be the initial stimulus promoting autoimmunity in the MEK1 KO mice. Flow cytometric analysis of apoptosis in freshly isolated splenocytes did not reveal any significant differences between WT and MEK1 KO mice (Fig 16A).
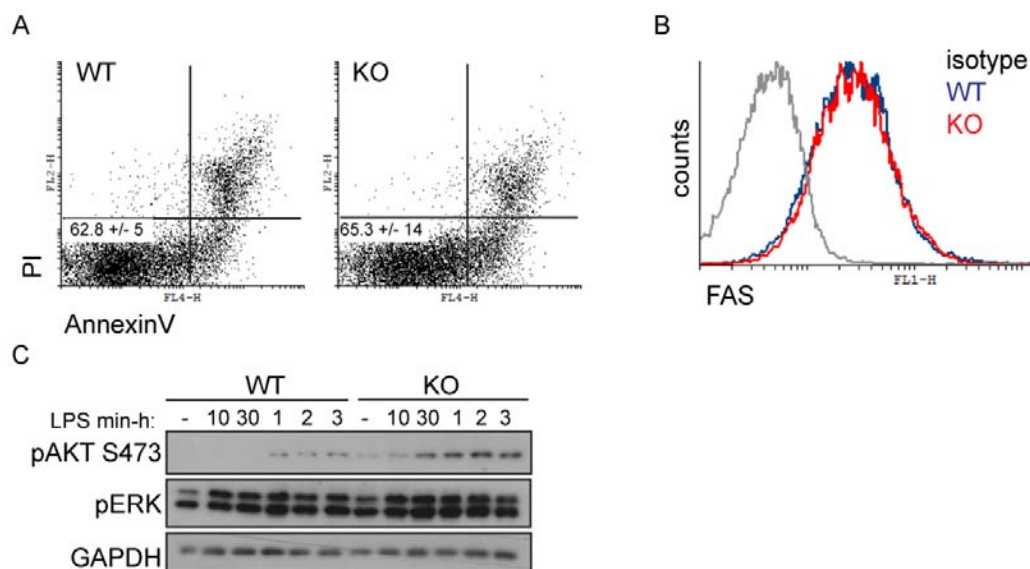
Figure 16. A, Splenocytes freshly isolated from 8 week-old female WT and KO littermates were stained with PI and APC-AnnexinV, followed by flow cytometry. n=3, a dot-plot from a representative couple is shown with quantification of viable cells from all 3 couples. **B,** Splenocytes freshly isolated from 8 week-old female WT and KO littermates were stained with FITC-linked antibody against FAS and analyzed by flow cytometry. The specificity of the staining was controlled by a FITC-linked isotype antibody. **C**, Purified splenic B cells were starved for 2 hours and then stimulated with 10 µg/ml of LPS for the indicated times. Whole-cell lysates were analyzed by immunoblotting.

PTEN deregulation as a result of MEK1 loss could lead to altered FAS expression and/or responsiveness [73]. FAS is a death receptor localized on the cell surface, whose activation by FAS ligand (FASL) leads to apoptosis induction. Impaired FAS signaling results in systemic autoimmunity [138]. The expression of FAS on freshly isolated splenocytes was analyzed by flow cytometry (Fig 16B). We didn't find any differences in the total splenocyte population. However, it is possible that FAS expression is deregulated only in a subset of immune cells in the KO. To ascertain this, it would be necessary to perform a more detailed analysis of FAS and FASL expression on

different cell lineages. Alternatively, despite the normal FAS levels, the expression of the ligand FASL can be also altered. This can be easily analyzed by surface staining and flow cytometry.

We show deregulated AKT signaling in CD4+ T cells in response to TCR stimulation (Fig 3I in the Manuscript). We also analyzed AKT activation in B cells, since the survival of MEK1 KO B cells is enhanced after αIgM and FASL stimulation compared to WT controls (Figures 3K-L in the Manuscript). One possible reason for this could be again the deregulation of AKT signaling. PTEN deletion in B cells activates the pathway in B cells and affects the B cell survival and homeostasis [123, 124].

Somewhat surprising, AKT activation was very similar in WT and KO splenic B cells after BCR stimulation by αIgM antibodies for short time (up to 30 min, data not shown). However after LPS stimulation, the KO B cells responded with stronger AKT and ERK activation (Fig 16C).

IV. FINAL CONCLUSIONS AND OUTLOOK

4.1 Significance of the study

The presented work elucidates in detail a novel mechanism of crosstalk between the RAF/MEK/ERK and PI3K/AKT signaling cascades mediated by MEK1. We report that MEK1 negatively regulates AKT pathway in the context of a MEK1/MAGI1/PTEN complex. MEK1 interacts with the GUK and WW domains of MAGI1 and complex formation is stimulated by phosphorylation of T292 in the proline-rich domain of MEK1, which regulates the binding to the WW domain. The MEK1/MAGI1/PTEN complex regulates PTEN recruitment to the membrane and in this way it maintains the homeostasis of PIP_3 levels, AKT activity and downstream outputs of AKT signaling such as survival. *In vivo*, MEK1 maintains peripheral lymphocyte tolerance by controlling apoptosis via the AKT pathway (Fig 17).
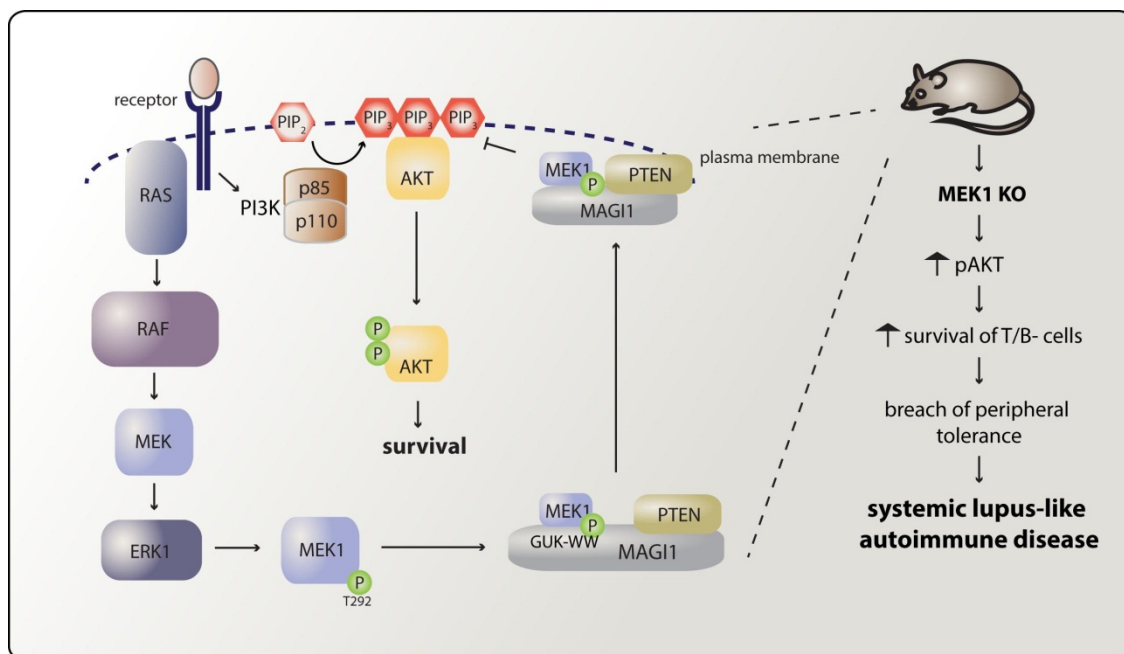
Fig 17. The working model depicts the mechanism of the crosstalk between MEK1 and AKT signaling as well the consequences of MEK1 knockout (KO) *in vivo*. MEK1 is phosphorylated by ERK on T292. This form of MEK1 facilitates the formation and membrane localization of the MEK1/MAGI1/PTEN complex, which inhibits AKT signaling. The result of MEK1 KO in vivo is increased AKT signaling, which promotes the survival of T- and B-cells and ultimately leads to breach in peripheral tolerance and symptoms of systemic lupus-like autoimmune disease.

The significance of this work can be summarized in four major aspects:

1.   First, it is noteworthy that the regulatory mechanism is specific for the MEK1 isoform. The two isoforms have long been perceived only as upstream activators of ERK with equal functions in cellular signaling. Increasing amount of evidence from *in vivo* and *in vitro* studies has changed this point of view [1, 11, 12]. It is now clear that MEK kinase isoforms diversify and fine-tune the signaling not only within their own MAPK pathway, but also in crosstalk to parallel cascades [139]. In addition, we identified the role of phosphorylation on the T292 residue unique to MEK1 as a regulator of both ERK and AKT signaling.

2.   Next, the study provides novel evidence about the communication between the RAF/MEK/ERK and PI3K/AKT pathways. Both cascades influence each other at multiple points of signal transduction, both positively and negatively [139]. Yet the role of MEK kinases in this interplay has not been elucidated in detail before. This is surprising considering how much effort is recently invested in MEK inhibitor development. It is well known that crosstalk leads to activation of compensatory signaling and allows tumor cells to evade inhibitor-induced cell death [35]. Our results suggest that inhibition of MEK with small molecules might result in triggering AKT signaling through dysfunction of PTEN, which may in turn lead to emergence of resistance to inhibitor treatment.

3.   Based on our results that MEK1 positively regulates PTEN, one of the most prominent tumor suppressors, we can speculate that MEK1 can also act as tumor suppressor under certain circumstances. This exciting possibility has been already suggested in a study by Bric *et al.* [140]. The authors identified MEK1 in a loss of function screen for genes that modulate Myc-induced tumorigenesis in a model of Burkitt lymphoma. This study emphasizes the concept that many genes can act as either pro- or antioncogenic, depending on genetic or cellular context. MEK1 was found to act as context-dependent tumor suppressor whose action was revealed in Myc-expressing cells. The effect is seemingly paradoxical, since MEK1 usually transmits oncogenic signals downstream of RAS [141]. Nevertheless, this dual function of MEK1 needs to be studied in more detail because of its implications for the MEK inhibitor drug discovery and treatment.

4.   Last but not least, our study identifies an important isoform-specific role of MEK1 *in vivo* in the homeostasis of the immune system. The deletion of MEK1 is lethal during early embryogenesis, but epiblast-restricted conditional MEK1 KO mice are viable [1]. MEK2 can apparently compensate for MEK1 isoform in most of the tissues except placenta. Thus, MEK1 is essential for the trophoblast development but dispensable for

normal epiblast development. However, our results indicate that MEK1 is required postnatally for the maintenance of homeostasis, in particular in the hematopoietic compartment.

4.2 Outlook for future studies on MEK1
In vitro

It remains unclear how MEK1 is involved in the transport of PTEN to the membrane. Very little is known about the transport mechanisms of PTEN [134] and MEK1 and therefore it would be interesting to pursue this question. We have several preliminary indications that microtubules are involved in this process. First, it would be necessary to determine whether the transport involves the whole MEK1/MAGI1/PTEN complex, or the complex forms only at the membrane and the proteins are recruited separately. We already know that the complex can be found in the membrane fraction (fig). Whether the complex is already formed in the cytosol or on the cytoskeleton needs to be addressed by further experiments. These will include for example immunoprecipitations from the cytosolic and cytoskeletal fractions or interaction studies between the isolated components of cytoskeleton and the members of the complex. If the complex is transported as a whole, the next question would be which of the proteins makes contact with the structures (microtubules, motor proteins or vesicles) that then mediate the transport process itself.

In our study we analyzed the mode of interaction between MEK1 and MAGI1. We have narrowed down the interaction region in MAGI1 to GUK and WW domains. We also know that T292 phosphorylation in the proline-rich domain in MEK1 regulates the binding to the WW domains. Most of our data were obtained from interaction studies performed with endogenous proteins from cellular lysates. At this moment we cannot exclude that the interaction between MEK1 and MAGI1 is indirect, since the WW domain interaction studies were performed by immunoprecipitating ectopically expressed proteins from whole cell lysates. To confirm direct binding, it would be necessary to express and purify recombinant MAGI1, GUK and WW domains and perform pull-down experiments with purified MEK1. The regulatory role of T292 phosphorylation in the binding between WW domains and MEK1 can be further analyzed by affinity studies between MEK1 phosphopeptides and purified WW domains.

In our study, we didn't identify the precise character of the MAGI1 isoforms with an apparent size difference on SDS-PAGE. MAGI protein encoding genes give raise to multiple splice variants with different molecular weights [82]. Isoforms resulting from

proteolytic cleavage have been also reported [135]. It is also possible, that other posttranslational modifications such as glycosylation result in the apparent differences in the molecular weight. Yet, we don't know which of the mechanisms mentioned above operates to produce the $MAGI1_{100}$ isoform. One option would be to isolate cDNA from MEFs and by designing suitable primers identify the sequence spliced in these cells. Possible posttranslational modifications can be addressed with treatment of cells with appropriate inhibitors (e.g. tunicamycin for glycosylation).

A more provocative question is whether MEK1 functions as a kinase towards MAGI1. ERK1/2 are the only substrates of MEK kinases known until now. Our results show that the kinase activity of MEK1 is dispensable for the complex formation between MEK1, MAGI1 and PTEN. However, this does not exclude the possibility that MEK1 can phosphorylate MAGI1. Multiple phosphorylation sites were found in MAGI1 in phosphoproteomic studies (www.phosphosite.org). Two of them, Y373 and Y858 were also experimentally verified and the phosphatase was identified (PTPRZ) [142]. It is not yet clear whether this phosphorylation induce conformational changes within the protein that affect binding to its interaction partners, or protein stability and turnover. Y373 is located in the second WW domain of MAGI1, a domain that binds to MEK1. Could the WW domain be a substrate of MEK1? Experiments addressing this intriguing possibility include verifying the functional consequences of MAGI1 phosphorylation, kinase assays with constitutively active MEK1 and purified WW domains and further validation *in vivo*, for example by developing Y373 phospho-specific antibodies and their application on MEK1 KO cell lysates.

In vivo

The ablation of MEK1 in the whole organism leads to significantly decreased survival of mice accompanied by a complex immunopathology comprising extramedullary hematopoiesis, myeloproliferation, inflammation, and lupus-like autoimmune disease. Thus, MEK1 clearly plays role in the homeostasis of the hematopoietic system. However, in our system it is not possible to distinguish whether these phenotypes are independent from each other or they should be viewed as a complex linked pathology. The mice used in this study lack MEK1 in all tissues, therefore it not possible to make conclusion about the role of MEK1 in different hematopoietic lineages as well as in the environment. To circumvent this problem, mating of the *Mek1^{f/f}* mice with lineage-restricted Cre would be necessary.

To characterize the myeloproliferative phenotype of the MEK1 KO mice in more detail, we need to distinguish between cell-autonomous roles of MEK1 in hematopoietic

stem and/or progenitor cells from the consequences of MEK1 ablation in the environment (i.e. hematopoietic niche, inflammatory environment). Both extramedullary hematopoeisesis and myeloproliferation are not necessarily cell-intrinsic properties but can be reactive conditions to altered environment (autoimmune disease) [143, 144]. To address this issue, detailed phenotypic analysis of bone marrow and peripheral cell populations, *in vitro* experiments and transplantation experiments would be helpful.

We have already started performing *in vitro* colony-forming cell (CFC) assays in semisolid medium to compare the number of hematopoietic progenitors present in the bone marrow and spleen. The first experiments had promising results and showed increased number of myeloid and erythroid progenitors (Fig S2B in the Manuscript). The reasons for this may be various, including increased number or proliferation of progenitors. These preliminary data highlight the need for detailed phenotypic, functional and morphological analysis of the hematopoietic compartment in the bone marrow. If the myeloproliferation that we see in aged MEK1 KO mice is a real myeloproliferative disease, it should be transplantable. The possible ways to test this are classical bone marrow transplantations to irradiated recipients or, less time consuming, CFU-S (colony-forming unit spleen) experiments.

As suggested above, MEK1 can function as tumor suppressor under certain conditions [140]. On the other hand, MEK1 KO mice don't develop any tumors during their life. Inspired by the study of Bric *et al.*, we plan to investigate a potential suppressor role of MEK1 in leukemia by combining MEK1 ablation with the expression of retrovirally encoded oncogenes and monitoring the latency of leukemogenesis.

The major challenge is to identify the mechanisms by which is MEK1 operating *in vivo in* different tissues. Besides canonical ERK signaling and the newly identified crosstalk to the AKT pathway, there might be novel partners/targets. To identify them, we need to employ unbiased approaches, for example comparing the gene expression signatures of WT and MEK1 KO cell populations using genomic arrays. This approach might give us completely novel insights about the role of MEK1 in cell signaling.

V. EXPERIMENTAL PROCEDURES

Mice

Generation of the *mek1^{f/f}; Sox2Cre* mice was described previously [1] Mice were maintained on a mixed Sv129/Bl6 background.

Cell culture

Immortalized WT and KO mouse embryonic fibroblasts (MEFs) and stable KO clones re-expressing WT and mutant MEK1 [1] were cultured in DMEM plus 10% (v/v) FCS (PAA) and penicilin/streptomycin and starved in 0.5% (v/v) FCS overnight prior to treatment with EGF (2 ng/ml, Biomedical Technologies). Primary human, chicken and rat fibroblasts were maintained in the same media. Primary mouse lymphocytes were grown in RPMI 1640 (PAA) containing 10% FCS, 1 mM sodium pyruvate (Sigma-Aldrich), 1% non-essential aminoacids (Sigma-Aldrich), 50 µM β-ME , 10 mM N-acetylcysteine, 20 mM HEPES (Sigma) and penicillin/streptomycin at density 0.5-1 million cells/ml. Inhibitors (10 nM PD0325901, Sigma-Aldrich; 10 µM U0126 and 50 µM LY294002, Cell Signaling) were added 1 hour before stimulation.

Plasmid constructs and cloning

myc-MAGI1, myc-tagged MAGI1 domains, MAGI2-GFP and MAGI3-GFP plasmids were provided from Zhigang Xu. MAGI1 deletion mutants were obtained by site-directed mutagenesis of full length myc-MAGI1 [145] using the indicated primers and Phusion Hot Start II polymerase (Finnzymes). The myc-GUK-WW construct was generated by amplifying the relevant fragment of the full length MAGI1 plasmid using the indicated primers and followed by recloning into pcDNA3.1 plasmid. QuikChange Site-Directed Mutagenesis Kit (Stratagene) was used to introduce point mutations in WW domains. All constructs were verified by sequencing to harbor the correct mutation.

ΔGUK	
5'-CTACCTCTTTCTGCAGAG-3'	5'- AAGGGGTCTCCAGATCATCTACCTCTTTCTGCAGAG-3'
5'-CTGGAACCGTTGGTTGAG-3'	5'-ATGATCTGGAGACCCCTTCTGGAACCGTTGGTTGAG-3'
Δ WW	
5'-CTAGAAGCCAAACGGAAG-3'	5'-CCTGAAAACTGGGAGATGCTAGAAGCCAAACGGAAG-3'
5'-TAGAGGACCTAAATTATC-3'	5'-CATCTCCCAGTTTTCAGGTAGAGGACCTAAATTATC-3'

ΔGUK-WW	
5'-CTAGAAGCCAAACGGAAG -3'	5'-AAGGGGTCTCCAGATCATCTAGAAGCCAAACGGAAG-3'
5'-CTGGAACCGTTGGTTGAG-3'	5'-ATGATCTGGAGACCCCTTCTGGAACCGTTGGTTGAG-3'
myc-GUK-WW	
5'-CTAGCTAGCATGGCATCAATGCAGAAGCTGATCTCAGAGGAGGACCTGAGGCTCAACAAGGACCTACG-3'	5'-CGCGGATCCTTAATGGGAAGGAGCAACAGGAG-3'
WW1 mutation Y-A	
5'-CCTATACTGAAAATGGAGAAGTCGCTTTCATAGACCACAACACG-3'	5'-CGTGTTGTGGTCTATGAAAGCGACTTCTCCATTTTCAGTATAGG-3'
WW2 mutation Y-A	
5'-CCCTGTCTACGGTGTCGCCTATGTAGACCACATCAACAGG-3'	5'-CCTGTTGATGTGGTCTACATAGGCGACACCGTAGACAGGG-3'

PCR mix

template (100 ng/ µl)	1 µl	template	0.5 µl
5x High fidelity buffer	10 µl	5x polymerase buffer	10 µl
10 mM dNTPs	1 µl	10 mM dNTPs	1 µl
2U/µl Phusion polymerase	0.5 µl	Turbo polymerase	1 µl
primers 10 µM	4x 2.5 µl	Primers 10 µM	2x 0.5 µl
autoclaved ddH$_2$O	27.5µl	ddH$_2$O	36.5 µl
total/1 reaction	50 µl		50 µl

Transfections

COS7 cells were cultured in DMEM plus 10% FCS and penicilin/streptomycin in 10 cm culture dish. Prior to transfection, the medium was replaced by DMEM 0% FCS with penicilin/streptomycin. 5-10 µg of plasmid was mixed with 500 µl of pure DMEM and TurboFect (Fermentas), incubated for 15 min and applied dropwise to the cells. After 5

hours, the medium was replaced with fresh DMEM plus 10% FCS and penicilin/streptomycin. MEFs were transfected with 30 nM MAGI1 siRNA duplexes [83] or non-targeting pool (D-001810-10-05, Dharmacon) using Lipofectamine RNAiMAX (Invitrogen).

Whole cell lysates, Immunoprecipitations and pull downs

Cells were washed 2x with ice-cold PBS, lysed in a buffer containing 20 mM TrisHCl pH 7.4, 137 mM NaCl, 1 mM $CaCl_2$, 1 mM $MgCl_2$, 1% NP-40, 1mM Na_3VO_4, 50 mM NaF, 2 mM PMSF and protein inhibitor cocktail (Roche) incubated 15 min on ice and centrifuged 15 min at 15000 rpm. Immunoprecipitates (IPs) were prepared by adding the appropriate antibodies (MEK1, MEK2; BD Transduction Labs; myc tag, E. Ogris, MFPL, Vienna; PTEN, Santa Cruz; all 1:100) to the whole cell lysates (500 µg – 2 mg of total protein). After incubation with the antibodies for 5 hours, protein A-sepharose (GE Healthcare) or protein G-agarose (Thermo Scientific) beads were added to the IPs and incubated for 1 more hour. Then, the beads were washed 3 times with lysis buffer and the proteins were eluted by adding Laennli protein loading dye. Pulldown experiments were carried out in IP buffer plus 0.1% BSA, using purified recombinant PTEN (Calbiochem) and MEK1 (gift of I. Moarefi, Crelux GmbH).

Protein electrophoresis and western blotting

Whole cell lysates and IPs were analyzed by SDS-PAGE (10% gels). Proteins were blotted over night on nitrocellulose membranes Hybond-C Extra (Amersham Biosciences) by wet blotting in Tris-Glycine buffer containing methanol. The membranes were blocked in 5% milk TBST, washed with TBST and incubated with primary antibodies for 3 hours at room temperature or over night at 4 ºC. After washing with TBST, the blots were incubated with secondary HRP-linked antibodies for 1 hour at room temperature. A list of primary and secondary antibodies is included below:

antigen	dilution	diluent	Species	Cat. no	company
AKT,	1/1000	3%BSA TBST	rabbit	9272	Cell Signaling
pAKT S473	1/1000	3%BSA TBST	rabbit	9271	Cell Signaling
pAKT T308	1/1000	3%BSA TBST	Rabbit	9275	Cell Signaling
p85	1/1000	3%BSA TBST	Rabbit	4292	Cell Signaling
p110α	1/1000	3%BSA TBST	rabbit	4254	Cell Signaling
MEK1	1/1000	5% milk TBST	mouse	2352	Cell Signaling
pMEK S218/222	1/1000	3%BSA TBST	rabbit	9121	Cell Signaling
pMEK1 S298	1/1000	3%BSA TBST	rabbit	9128	Cell Signaling
PTEN	1/1000	3%BSA TBST	rabbit	9552	Cell Signaling
pPTEN 380/382/383	1/1000	3%BSA TBST	rabbit	9549	Cell Signaling
npPTEN 380/382/383	1/500	3%BSA TBST	rabbit	9569	Cell Signaling
pERK	1/1000	3%BSA TBST	rabbit	9101	Cell Signaling
ERK	1/1000	3%BSA TBST	rabbit	9102	Cell Signaling
pmTOR S2448	1/1000	3%BSA TBST	rabbit	2971	Cell Signaling
mTOR	1/1000	3%BSA TBST	rabbit	2983	Cell Signaling
pGSK3β S9	1/1000	3%BSA TBST	rabbit	9336	Cell Signaling
pS6K T389	1/1000	3%BSA TBST	rabbit	9234	Cell Signaling
IGF1R	1/1000	3%BSA TBST	rabbit	3027	Cell Signaling
GAPDH	1/5000	5% milk TBST	rabbit	abs16	Millipore
myc tag	1/2000	3%BSA TBST	rabbit	2278	Cell Signaling
MAGI1	1/500	3%BSA TBST	mouse	Sc-100326	Santa Cruz
MAGI2	1/500	3%BSA TBST	rabbit	Ab111692	Millipore
MAGI3	1/500	3%BSA TBST	rabbit	Ab9878	Abcam
actin	1/2000	3%BSA TBST	goat	sc-1616	Santa Cruz
FAK	1/200	3%BSA TBST	rabbit	sc-558	Santa Cruz
pFAKY397	1/1000	3%BSA TBST	mouse	611806	BD Transduction Laboratories
caveolin	1/1000	3%BSA TBST	rabbit	610060	BD Transduction Laboratories
MEK2	1/1000	3%BSA TBST	mouse	610236	BD Transduction Laboratories
tubulin	1/5000	5% milk TBST	mouse	T9026	Sigma
pMEK1 T292	1/1000	3%BSA TBST	rabbit	07-852	Upstate
his tag	1/1000	3%BSA TBST	rabbit	600-401-382	Rockland
GFP	1/2000	3%BSA TBST	mouse	11814460001	Roche
Secondary antibodies					
α-mouse	1/2000	5% milk TBST		NA931V	GE-Healthcare
α-rabbit	1/4000	5% milk TBST		NA934V	GE-Healthcare
α-goat	1/5000	5% milk TBST		sc-2020	Santa Cruz

Membranes were developed using SuperSignal West Pico/Femto Chemiluminescent Substrate (Thermo Scientific) and Amersham Hyperfilm (GE Healthcare).

Subcellular Fractionation

Subcellular fractionation was performed using commercial kits (Subcellular Fractionation Kit for cultured cells from Thermo Scientific was used for MEFs and ProteoJet membrane protein extraction kit from Fermentas was used for splenocytes). Hypotonic lysis with differential centrifugation was used to produce cytoplasmic and membrane fractions for PTEN phosphatase assay (for details see Biochemical assays).

Biochemical assays, ELISA

PIP$_3$ levels were measured by PIP$_3$ mass ELISA (Echelon). PI3K activity was assessed with a PI3K ELISA Kit (Echelon). Phosphatase activity in PTEN IPs was monitored as described [146]. Briefly, cells were washed with ice-cold TBS and lysed in hypotonic buffer. After homogenization, the lysates were centrifuged at 700 g for 5 min. The supernatant was then ultracentrifuged at 45000rpm for 30 min. The supernatant (cytosol) and pellet (cellular membranes resuspended in PTEN lysis buffer (25 mM Tris pH8, 150 mM NaCl, 1% NP-40, 1mM EDTA, 5% glycerol) were then subjected to PTEN IP. Immunoisolated PTEN was then incubated with 20 μM PIP$_3$ (Echelon) in PTEN assay buffer (10 mM Hepes pH 7.2, 150 mM NaCl, 10 mM DTT) for 2 hours at 37 ºC. The amount of released phosphate was measured by Malachite green phosphatase assay (Echelon). Serum antibodies, BAFF and IL-10 were detected by ELISA (Life Diagnostics, Inc.; and R&D Systems).

Blood analysis and flow cytometry

Peripheral blood cell counts were acquired using the V-Sight hematology analyzer (A. Menarini Diagnostics). Freshly isolated splenocytes were stained with antibodies against CD19, CD3e, CD4, CD8a, Mac1, Gr-1, CD69, B220, CD5, CD21, CD23, IgM, IgD and BAFF (details of the antibodies are listed below). For the analysis of intracellular cytokine expression, total splenocytes were stimulated with Cell Stimulation Cocktail with protein transport inhibitors (eBioscience) and LPS (5 ng/ml, Sigma) for 6 hours. Cells were then stained with αCD4, fixed, permeabilized (BD Cytofix/Cytoperm kit), blocked with 5% FCS and stained with cytokine-specific antibodies (see list below). Cells were analyzed by FACSCalibur and FACSAria (*BectonDickinson*) and FlowJo software.

Antibodies used for flow cytometry:

antigen	dilution	fluorochrome	company	cat. number
CD3e	1/100	PerCP	BD Pharmingen	
CD4	1/100	FITC	BD Pharmingen	553047
CD4	1/100	APC	BD Pharmingen	553051
CD5	1/100	APC	eBioscience	17-0051-81
CD8a	1/100	PE	BD Pharmingen	553032
CD19	1/100	FITC	eBioscience	11-0193-82
CD21	1/100	FITC	eBioscience	11-0211-81
CD23	1/100	APC	eBioscience	50-0232-80
CD69	1/100	PE	BD Pharmingen	553237
B220	1/100	PE	BD Pharmingen	553090
Mac1/CD11b	1/100	FITC	BD Pharmingen	553310
FAS	1/100	FITC	BD Pharmingen	15404
Gr-1	1/100	PE	BD Pharmingen	553128
FOXP3	1/500	APC	eBioscience	17-5773-80
RORγT	1/500	PercP-eFluor 710	eBioscience	46-6981
GATA3	1/500	PE	eBioscience	12-9966-41
T-bet	1/500	PE-Cy™7	eBioscience	25-5825-80
IgM	1/100	FITC	eBioscience	11-5890-81
IgD	1/100	APC	eBioscience	17-5993-80
BAFF	1/100	FITC	LifeSpan Biosciences	LS-C18645
IFNα	1/100	FITC	PBL Interferon source	22100-3
IFNγ	1/100	PE	BD Pharmingen	554412
TGFβ	1/100	APC	LifeSpan Biosciences	LS-c39831
GM-CSF	1/100	FITC	eBioscience	11-7331-41
IL-3	1/100	PE	BD Pharmingen	554383
IL-6	1/100	PE	BD Pharmingen	554401
IL-10	1/100	FITC	eBioscience	11-7101-71
IL-17	1/100	APC	BioLegend	506915
IL-23	1/100	APC	eBioscience	50-7023-80

Cell sorting

Splenic CD4+ T- and B-cells were purified using MACS negative selection kits (MiltenyiBiotec; purity approx. 95% as determined by flow cytometry with CD4 and CD19 antibodies). Cells were subsequently subjected to proliferation, *in vitro* activation and cell death assays.

Proliferation assays

Expression of CD69 was assessed after 4 days of stimulation with α-IgM (5 µg/ml, Jackson ImmunoResearch) and BAFF (10 ng/ml,R&D) in the case of B cells and 1 µg/ml CD3 and CD28 in the case of CD4+ T cells. Proliferation of B and CD4+ T lymphocytes was analyzed by staining with Cell Trace Violet (Invitrogen) on day 1 and flow cytometric analysis after 4 days of activation with the same stimuli.

Cell death assays

In T cells, AICD was induced with αCD3/CD28 (1 µg/ml and 0.5 µg/ml, both BD Pharmingen) for 72 hours, followed by 16 hours stimulation with αCD3 (10 µg/ml). B cells were treated with soluble α-IgM Fab$_2$ fragment (0.1 µg/ml, Jackson ImmunoResearch) and analyzed 24 hours later. FasL (100ng/ml, Adipogen) induced apoptosis was monitored 6 hours after the treatment. Cell death was measured by annexinV-APC/propidium iodide staining (eBiosciences). MEFs were grown in medium containing 10% FCS and were exposed to different apoptotic stimuli: starvation in 0.5% FCS, heat shock for 30 min at 42°C, UV irradiation 780 J/m2, anisomycin (10µg/ml), or TNFα (10ng/ml)/cycloheximide (5µg/ml) for 16 hours. Cell death was determined by propidium iodide staining and flow cytometry.

ELISPOT

ELISpot assays were performed with IgA and IgG ELISpot kits (Mabtech) and MACS-sorted B cells.

Colony forming assays

Colony forming assays were performed as described (Miller et al., 2008). Briefly, total bone marrow cells or total splenocytes were seeded in semisolid media (StemCell Technologies) containing 10 ng/ml rmIL-3, 50 ng/ml rmSCF (both from StemCell Technologies) and 10 ng/ml rhIL-6 (eBioscience) for determination of CFU-C or in media containing 3U/ml EPO for counting CFU-E and BFU. We counted myeloid colonies

(CFU-GM, CFU-M and CFU-G) and immature BFU-E on day 7; mature CFU-E were counted on day 2.

Immunofluorescence

MEFs were fixed with ice-cold methanol for 5 min and washed extensively with PBS. Cells were blocked with 3% FCS in PBS for 30 min and then stained with α-PTEN (1/40, Santa Cruz) over night at 4 ºC, washed and incubated with goat α-mouse Alexa488 secondary antibody (1/500, Invitrogen). MEFs were fixed in 4% PFA, permeabilized with saponin and stained with α-PIP3-FITC antibody (Echelon). Slides were mounted with Vectashield with DAPI (Vector Laboratories). The frequency of membrane recruitment was established by counting cells in five to ten microscopic fields per experimental condition (300 cells) in at least three independent experiments. Images were acquired with the upright point scanning confocal microscope Zeiss LSM-510 Meta. The following lasers were used: Laser Diode 405nm; 25mW (violet) and Argon 458, 477, 488, 514nm; 30mW (blue). Images were acquired with 63x/1.40 plan-apochromat Oil, DIC III objective and Zeiss ZEN 2009, v 5,5.0,443 software running on Windows7-64-bit PC.

Histology and immunohistochemistry

H&E staining and immunohistochemistry were carried out as described in detail below. Reticular fibers were visualized by Gomori staining. Frozen kidney sections were examined as described in [73].

Fixation and processing of tissue

- wash 2x with cold PBS
- fix o/n in fresh 4% PFA in PBS
- wash with PBS
- o/n in 70% EtOH
- embed in paraffin
- cut 5 μm sections

Deparaffination and Rehydration

- 2x15 min xylene
- 2x10 min 100% EtOH

- 2x10 min 90% EtOH
- 1x5 min ddH$_2$O
- 1x5 min PBS

Blocking activity of endogenous peroxidase

- 1x10 min, RT: 125 ml MetOH + 117.5 ml ddH2O+ 7.5 ml 30% H$_2$O$_2$
- briefly rinse in tap-water
- 1x5 min ddH$_2$O

Antigen-Retrieval

- 1x citrate buffer pH 6.0: 2x45 min steamer, cool 30 min
- wash with PBS

Blocking

- add 120 µl blocking solution: PBS/5% NGS 60min RT

Primary antibody

- in PBS/5% NGS, at least 150 µl, 4° o.n.

pAkt (3787, Cell Signaling) 1/25

pErk (4376, Cell Signaling) 1/100

- wash 3x5 min PBS

Secondary-Antibody

- 120 µl, 30 min RT, DAKO Labeled Polymer-HRP α-rabbit
- wash 3x 5 min with PBS
- prepare DAB (3 tablets in 150 ml 200 mM Tris pH 7.4 and add 750 µl of [150 µl 30% H$_2$O$_2$ +1350 µl H$_2$O])
- wash 3x 5 min with PBS
- 5-8 min DAB solution, observe signal formation and wash 2x 5 min ddH$_2$O

Counterstain:

- filtered hematoxylin (1:3), 10-20 sec
- 1x5 min ddH$_2$O, 1x10 min running water

<u>Dehydration and mounting</u>

- 2x10 min 90% EtOH
- 2x10 min 100% EtOH
- 2x10 min xylene
- mount with Entellan

Statistical analysis

Unless otherwise indicated, values are expressed as mean (±SD) of at least three independent experiments. *p* values were calculated with the two-tailed Student's t test. A *p* value ≤ 0.05 is considered statistically significant.

VI. REFERENCES

1.	Catalanotti, F., et al., *A Mek1-Mek2 heterodimer determines the strength and duration of the Erk signal.* Nat Struct Mol Biol, 2009. **16**(3): p. 294-303.
2.	Qi, M. and E.A. Elion, *MAP kinase pathways.* J Cell Sci, 2005. **118**(Pt 16): p. 3569-72.
3.	Schlessinger, J., *Cell signaling by receptor tyrosine kinases.* Cell, 2000. **103**(2): p. 211-25.
4.	Yoon, S. and R. Seger, *The extracellular signal-regulated kinase: multiple substrates regulate diverse cellular functions.* Growth Factors, 2006. **24**(1): p. 21-44.
5.	Marshall, C.J., *Specificity of receptor tyrosine kinase signaling: transient versus sustained extracellular signal-regulated kinase activation.* Cell, 1995. **80**(2): p. 179-85.
6.	Wimmer, R. and M. Baccarini, *Partner exchange: protein-protein interactions in the Raf pathway.* Trends Biochem Sci, 2010. **35**(12): p. 660-8.
7.	Shaul, Y.D. and R. Seger, *The MEK/ERK cascade: from signaling specificity to diverse functions.* Biochim Biophys Acta, 2007. **8**(26): p. 19.
8.	Rusconi, P., E. Caiola, and M. Broggini, *RAS/RAF/MEK inhibitors in oncology.* Curr Med Chem, 2012. **19**(8): p. 1164-76.
9.	Aoki, Y., et al., *The RAS/MAPK syndromes: novel roles of the RAS pathway in human genetic disorders.* Hum Mutat, 2008. **29**(8): p. 992-1006.
10.	Roskoski, R., Jr., *MEK1/2 dual-specificity protein kinases: structure and regulation.* Biochem Biophys Res Commun, 2012. **417**(1): p. 5-10.
11.	Belanger, L.F., et al., *Mek2 is dispensable for mouse growth and development.* Mol Cell Biol, 2003. **23**(14): p. 4778-87.
12.	Giroux, S., et al., *Embryonic death of Mek1-deficient mice reveals a role for this kinase in angiogenesis in the labyrinthine region of the placenta.* Curr Biol, 1999. **9**(7): p. 369-72.
13.	Burgermeister, E., et al., *Interaction with MEK causes nuclear export and downregulation of peroxisome proliferator-activated receptor gamma.* Mol Cell Biol, 2007. **27**(3): p. 803-17.
14.	Zheng, C.F. and K.L. Guan, *Activation of MEK family kinases requires phosphorylation of two conserved Ser/Thr residues.* Embo J, 1994. **13**(5): p. 1123-31.
15.	Slack-Davis, J.K., et al., *PAK1 phosphorylation of MEK1 regulates fibronectin-stimulated MAPK activation.* J Cell Biol, 2003. **162**(2): p. 281-91.
16.	Park, E.R., S.T. Eblen, and A.D. Catling, *MEK1 activation by PAK: a novel mechanism.* Cell Signal, 2007. **19**(7): p. 1488-96.
17.	Brunet, A., G. Pages, and J. Pouyssegur, *Growth factor-stimulated MAP kinase induces rapid retrophosphorylation and inhibition of MAP kinase kinase (MEK1).* FEBS Lett, 1994. **346**(2-3): p. 299-303.
18.	Xu, B., et al., *The N-terminal ERK-binding site of MEK1 is required for efficient feedback phosphorylation by ERK2 in vitro and ERK activation in vivo.* J Biol Chem, 1999. **274**(48): p. 34029-35.
19.	Sharma, P., et al., *Phosphorylation of MEK1 by cdk5/p35 down-regulates the mitogen-activated protein kinase pathway.* J Biol Chem, 2002. **277**(1): p. 528-34.
20.	Kubota, Y., et al., *Oncogenic Ras abrogates MEK SUMOylation that suppresses the ERK pathway and cell transformation.* Nat Cell Biol, 2011. **13**(3): p. 282-91.
21.	Brown, M.D. and D.B. Sacks, *Protein scaffolds in MAP kinase signalling.* Cell Signal, 2009. **21**(4): p. 462-9.
22.	Kortum, R.L. and R.E. Lewis, *The molecular scaffold KSR1 regulates the proliferative and oncogenic potential of cells.* Mol Cell Biol, 2004. **24**(10): p. 4407-16.
23.	Ishibe, S., et al., *Phosphorylation-dependent paxillin-ERK association mediates hepatocyte growth factor-stimulated epithelial morphogenesis.* Mol Cell, 2003. **12**(5): p. 1275-85.
24.	Roy, M., Z. Li, and D.B. Sacks, *IQGAP1 is a scaffold for mitogen-activated protein kinase signaling.* Mol Cell Biol, 2005. **25**(18): p. 7940-52.
25.	Song, X., et al., *How does arrestin assemble MAPKs into a signaling complex?* J Biol Chem, 2009. **284**(1): p. 685-95.
26.	Tohgo, A., et al., *beta-Arrestin scaffolding of the ERK cascade enhances cytosolic ERK activity but inhibits ERK-mediated transcription following angiotensin AT1a receptor stimulation.* J Biol Chem, 2002. **277**(11): p. 9429-36.
27.	Meng, D., et al., *MEK1 binds directly to betaarrestin1, influencing both its phosphorylation by ERK and the timing of its isoprenaline-stimulated internalization.* J Biol Chem, 2009. **284**(17): p. 11425-35.

28. Schaeffer, H.J., et al., *MP1: a MEK binding partner that enhances enzymatic activation of the MAP kinase cascade.* Science, 1998. **281**(5383): p. 1668-71.

29. Teis, D., W. Wunderlich, and L.A. Huber, *Localization of the MP1-MAPK scaffold complex to endosomes is mediated by p14 and required for signal transduction.* Dev Cell, 2002. **3**(6): p. 803-14.

30. Wunderlich, W., et al., *A novel 14-kilodalton protein interacts with the mitogen-activated protein kinase scaffold mp1 on a late endosomal/lysosomal compartment.* J Cell Biol, 2001. **152**(4): p. 765-76.

31. Teis, D., et al., *p14-MP1-MEK1 signaling regulates endosomal traffic and cellular proliferation during tissue homeostasis.* J Cell Biol, 2006. **175**(6): p. 861-8.

32. Maiga, O., et al., *Identification of mitogen-activated protein/extracellular signal-responsive kinase kinase 2 as a novel partner of the scaffolding protein human homolog of disc-large.* Febs J, 2011. **278**(15): p. 2655-65.

33. Shaul, Y.D. and R. Seger, *The MEK/ERK cascade: from signaling specificity to diverse functions.* Biochim Biophys Acta, 2007. **1773**(8): p. 1213-26.

34. Matallanas, D., et al., *Raf family kinases: old dogs have learned new tricks.* Genes Cancer, 2011. **2**(3): p. 232-60.

35. Sos, M.L., et al., *Identifying genotype-dependent efficacy of single and combined PI3K- and MAPK-pathway inhibition in cancer.* Proc Natl Acad Sci U S A, 2009. **106**(43): p. 18351-6.

36. Hoeflich, K.P., et al., *Intermittent administration of MEK inhibitor GDC-0973 plus PI3K inhibitor GDC-0941 triggers robust apoptosis and tumor growth inhibition.* Cancer Res, 2012. **72**(1): p. 210-9.

37. Gedaly, R., et al., *The role of PI3K/mTOR inhibition in combination with sorafenib in hepatocellular carcinoma treatment.* Anticancer Res, 2012. **32**(7): p. 2531-6.

38. Menges, C.W. and D.J. McCance, *Constitutive activation of the Raf-MAPK pathway causes negative feedback inhibition of Ras-PI3K-AKT and cellular arrest through the EphA2 receptor.* Oncogene, 2008. **27**(20): p. 2934-40.

39. Sunayama, J., et al., *Crosstalk between the PI3K/mTOR and MEK/ERK pathways involved in the maintenance of self-renewal and tumorigenicity of glioblastoma stem-like cells.* Stem Cells, 2010. **28**(11): p. 1930-9.

40. Hayashi, H., et al., *Down-regulation of the PI3-kinase/Akt pathway by ERK MAP kinase in growth factor signaling.* Genes Cells, 2008. **13**(9): p. 941-7.

41. Lu, Y., et al., *Kinome siRNA-phosphoproteomic screen identifies networks regulating AKT signaling.* Oncogene, 2011. **30**(45): p. 4567-77.

42. Fruman, D.A., R.E. Meyers, and L.C. Cantley, *Phosphoinositide kinases.* Annu Rev Biochem, 1998. **67**: p. 481-507.

43. Alessi, D.R. and P. Cohen, *Mechanism of activation and function of protein kinase B.* Curr Opin Genet Dev, 1998. **8**(1): p. 55-62.

44. Hennessy, B.T., et al., *Exploiting the PI3K/AKT pathway for cancer drug discovery.* Nat Rev Drug Discov, 2005. **4**(12): p. 988-1004.

45. Leslie, N.R., et al., *Understanding PTEN regulation: PIP2, polarity and protein stability.* Oncogene, 2008. **27**(41): p. 5464-76.

46. Li, J., et al., *PTEN, a putative protein tyrosine phosphatase gene mutated in human brain, breast, and prostate cancer.* Science, 1997. **275**(5308): p. 1943-7.

47. Steck, P.A., et al., *Identification of a candidate tumour suppressor gene, MMAC1, at chromosome 10q23.3 that is mutated in multiple advanced cancers.* Nat Genet, 1997. **15**(4): p. 356-62.

48. Maehama, T. and J.E. Dixon, *The tumor suppressor, PTEN/MMAC1, dephosphorylates the lipid second messenger, phosphatidylinositol 3,4,5-trisphosphate.* J Biol Chem, 1998. **273**(22): p. 13375-8.

49. Stambolic, V., et al., *Negative regulation of PKB/Akt-dependent cell survival by the tumor suppressor PTEN.* Cell, 1998. **95**(1): p. 29-39.

50. Liliental, J., et al., *Genetic deletion of the Pten tumor suppressor gene promotes cell motility by activation of Rac1 and Cdc42 GTPases.* Curr Biol, 2000. **10**(7): p. 401-4.

51. Tamura, M., et al., *Inhibition of cell migration, spreading, and focal adhesions by tumor suppressor PTEN.* Science, 1998. **280**(5369): p. 1614-7.

52. Khan, S., et al., *PTEN promoter is methylated in a proportion of invasive breast cancers.* Int J Cancer, 2004. **112**(3): p. 407-10.

53. Eng, C., *PTEN: one gene, many syndromes.* Hum Mutat, 2003. **22**(3): p. 183-98.

54.   Yu, J., et al., *PTEN regulation by Akt-EGR1-ARF-PTEN axis.* Embo J, 2009. **28**(1): p. 21-33.
55.   Chappell, W.H., et al., *Increased protein expression of the PTEN tumor suppressor in the presence of constitutively active Notch-1.* Cell Cycle, 2005. **4**(10): p. 1389-95.
56.   Meng, F., et al., *MicroRNA-21 regulates expression of the PTEN tumor suppressor gene in human hepatocellular cancer.* Gastroenterology, 2007. **133**(2): p. 647-58.
57.   Tay, Y., et al., *Coding-independent regulation of the tumor suppressor PTEN by competing endogenous mRNAs.* Cell, 2011. **147**(2): p. 344-57.
58.   Okumura, K., et al., *PCAF modulates PTEN activity.* J Biol Chem, 2006. **281**(36): p. 26562-8.
59.   Wang, X., et al., *NEDD4-1 is a proto-oncogenic ubiquitin ligase for PTEN.* Cell, 2007. **128**(1): p. 129-39.
60.   Trotman, L.C., et al., *Ubiquitination regulates PTEN nuclear import and tumor suppression.* Cell, 2007. **128**(1): p. 141-56.
61.   Huang, J., et al., *SUMO1 modification of PTEN regulates tumorigenesis by controlling its association with the plasma membrane.* Nat Commun, 2012. **3**(911).
62.   Lee, S.R., et al., *Reversible inactivation of the tumor suppressor PTEN by H2O2.* J Biol Chem, 2002. **277**(23): p. 20336-42.
63.   Vazquez, F., et al., *Phosphorylation of the PTEN tail regulates protein stability and function.* Mol Cell Biol, 2000. **20**(14): p. 5010-8.
64.   Vazquez, F., et al., *Phosphorylation of the PTEN tail acts as an inhibitory switch by preventing its recruitment into a protein complex.* J Biol Chem, 2001. **276**(52): p. 48627-30.
65.   Rahdar, M., et al., *A phosphorylation-dependent intramolecular interaction regulates the membrane association and activity of the tumor suppressor PTEN.* Proc Natl Acad Sci U S A, 2009. **106**(2): p. 480-5.
66.   Tolkacheva, T., et al., *Regulation of PTEN binding to MAGI-2 by two putative phosphorylation sites at threonine 382 and 383.* Cancer Res, 2001. **61**(13): p. 4985-9.
67.   Planchon, S.M., K.A. Waite, and C. Eng, *The nuclear affairs of PTEN.* J Cell Sci, 2008. **121**(Pt 3): p. 249-53.
68.   Song, M.S., L. Salmena, and P.P. Pandolfi, *The functions and regulation of the PTEN tumour suppressor.* Nat Rev Mol Cell Biol, 2012. **13**(5): p. 283-96.
69.   Di Cristofano, A., et al., *Pten is essential for embryonic development and tumour suppression.* Nat Genet, 1998. **19**(4): p. 348-55.
70.   Podsypanina, K., et al., *Mutation of Pten/Mmac1 in mice causes neoplasia in multiple organ systems.* Proc Natl Acad Sci U S A, 1999. **96**(4): p. 1563-8.
71.   Alimonti, A., et al., *Subtle variations in Pten dose determine cancer susceptibility.* Nat Genet, 2010. **42**(5): p. 454-8.
72.   Wang, H., et al., *Allele-specific tumor spectrum in pten knockin mice.* Proc Natl Acad Sci U S A, 2010. **107**(11): p. 5142-7.
73.   Di Cristofano, A., et al., *Impaired Fas response and autoimmunity in Pten+/- mice.* Science, 1999. **285**(5436): p. 2122-5.
74.   Garcia-Cao, I., et al., *Systemic elevation of PTEN induces a tumor-suppressive metabolic state.* Cell, 2012. **149**(1): p. 49-62.
75.   Wu, Y., et al., *Interaction of the tumor suppressor PTEN/MMAC with a PDZ domain of MAGI3, a novel membrane-associated guanylate kinase.* J Biol Chem, 2000. **275**(28): p. 21477-85.
76.   Kotelevets, L., et al., *Implication of the MAGI-1b/PTEN signalosome in stabilization of adherens junctions and suppression of invasiveness.* Faseb J, 2005. **19**(1): p. 115-7.
77.   Wu, X., et al., *Evidence for regulation of the PTEN tumor suppressor by a membrane-localized multi-PDZ domain containing scaffold protein MAGI-2.* Proc Natl Acad Sci U S A, 2000. **97**(8): p. 4233-8.
78.   Mizuhara, E., et al., *MAGI1 recruits Dll1 to cadherin-based adherens junctions and stabilizes it on the cell surface.* J Biol Chem, 2005. **280**(28): p. 26499-507.
79.   Patrie, K.M., *Identification and characterization of a novel tight junction-associated family of proteins that interacts with a WW domain of MAGI-1.* Biochim Biophys Acta, 2005. **15**(1): p. 131-44.
80.   Dobrosotskaya, I., R.K. Guy, and G.L. James, *MAGI-1, a membrane-associated guanylate kinase with a unique arrangement of protein-protein interaction domains.* J Biol Chem, 1997. **272**(50): p. 31589-97.

81. Hirao, K., et al., *A novel multiple PDZ domain-containing molecule interacting with N-methyl-D-aspartate receptors and neuronal cell adhesion proteins.* J Biol Chem, 1998. **273**(33): p. 21105-10.

82. Laura, R.P., et al., *MAGI-1: a widely expressed, alternatively spliced tight junction protein.* Exp Cell Res, 2002. **275**(2): p. 155-70.

83. Sakurai, A., et al., *MAGI-1 is required for Rap1 activation upon cell-cell contact and for enhancement of vascular endothelial cadherin-mediated cell adhesion.* Mol Biol Cell, 2006. **17**(2): p. 966-76.

84. Mino, A., et al., *Membrane-associated guanylate kinase with inverted orientation (MAGI)-1/brain angiogenesis inhibitor 1-associated protein (BAP1) as a scaffolding molecule for Rap small G protein GDP/GTP exchange protein at tight junctions.* Genes Cells, 2000. **5**(12): p. 1009-16.

85. Tanemoto, M., et al., *MAGI-1a functions as a scaffolding protein for the distal renal tubular basolateral K+ channels.* J Biol Chem, 2008. **283**(18): p. 12241-7.

86. Xu, Z., et al., *MAGI-1, a candidate stereociliary scaffolding protein, associates with the tip-link component cadherin 23.* J Neurosci, 2008. **28**(44): p. 11269-76.

87. Patrie, K.M., et al., *The membrane-associated guanylate kinase protein MAGI-1 binds megalin and is present in glomerular podocytes.* J Am Soc Nephrol, 2001. **12**(4): p. 667-77.

88. Wegmann, F., et al., *Endothelial adhesion molecule ESAM binds directly to the multidomain adaptor MAGI-1 and recruits it to cell contacts.* Exp Cell Res, 2004. **300**(1): p. 121-33.

89. Patrie, K.M., et al., *Interaction of two actin-binding proteins, synaptopodin and alpha-actinin-4, with the tight junction protein MAGI-1.* J Biol Chem, 2002. **277**(33): p. 30183-90.

90. Hirabayashi, S., et al., *JAM4, a junctional cell adhesion molecule interacting with a tight junction protein, MAGI-1.* Mol Cell Biol, 2003. **23**(12): p. 4267-82.

91. Hirabayashi, S., et al., *MAGI-1 is a component of the glomerular slit diaphragm that is tightly associated with nephrin.* Lab Invest, 2005. **85**(12): p. 1528-43.

92. Banerji, S., et al., *Sequence analysis of mutations and translocations across breast cancer subtypes.* Nature, 2012. **486**(7403): p. 405-9.

93. Berger, M.F., et al., *The genomic complexity of primary human prostate cancer.* Nature, 2011. **470**(7333): p. 214-20.

94. Zaric, J., et al., *Identification of MAGI1 as a tumor-suppressor protein induced by cyclooxygenase-2 inhibitors in colorectal cancer cells.* Oncogene, 2012. **31**(1): p. 48-59.

95. Pleasance, E.D., et al., *A comprehensive catalogue of somatic mutations from a human cancer genome.* Nature, 2010. **463**(7278): p. 191-6.

96. Green, D.R., N. Droin, and M. Pinkoski, *Activation-induced cell death in T cells.* Immunol Rev, 2003. **193**: p. 70-81.

97. von Boehmer, H. and F. Melchers, *Checkpoints in lymphocyte development and autoimmune disease.* Nat Immunol, 2010. **11**(1): p. 14-20.

98. Hsieh, C.S., H.M. Lee, and C.W. Lio, *Selection of regulatory T cells in the thymus.* Nat Rev Immunol, 2012. **12**(3): p. 157-67.

99. Melchers, F., *The pre-B-cell receptor: selector of fitting immunoglobulin heavy chains for the B-cell repertoire.* Nat Rev Immunol, 2005. **5**(7): p. 578-84.

100. Wardemann, H. and M.C. Nussenzweig, *B-cell self-tolerance in humans.* Adv Immunol, 2007. **95**: p. 83-110.

101. Chen, C., et al., *Immunoglobulin heavy chain gene replacement: a mechanism of receptor editing.* Immunity, 1995. **3**(6): p. 747-55.

102. Ahmed, S.A., et al., *Gender and risk of autoimmune diseases: possible role of estrogenic compounds.* Environ Health Perspect, 1999. **5**: p. 681-6.

103. Rubtsov, A.V., et al., *Genetic and hormonal factors in female-biased autoimmunity.* Autoimmun Rev, 2010. **9**(7): p. 494-8.

104. Mills, J.A., *Systemic lupus erythematosus.* N Engl J Med, 1994. **330**(26): p. 1871-9.

105. Singh, R.R., *SLE: translating lessons from model systems to human disease.* Trends Immunol, 2005. **26**(11): p. 572-9.

106. Rubin, R.L., *Drug-induced lupus.* Toxicology, 2005. **209**(2): p. 135-47.

107. Jadali, Z. and S.M. Alavian, *Autoimmune diseases co-existing with hepatitis C virus infection.* Iran J Allergy Asthma Immunol, 2010. **9**(4): p. 191-206.

108. Nagata, S., R. Hanayama, and K. Kawane, *Autoimmunity and the clearance of dead cells.* Cell, 2010. **140**(5): p. 619-30.

109. Kanta, H. and C. Mohan, *Three checkpoints in lupus development: central tolerance in adaptive immunity, peripheral amplification by innate immunity and end-organ inflammation.* Genes Immun, 2009. **10**(5): p. 390-6.

110. Andrews, B.S., et al., *Spontaneous murine lupus-like syndromes. Clinical and immunopathological manifestations in several strains.* J Exp Med, 1978. **148**(5): p. 1198-215.

111. Lee, H.S. and S.C. Bae, *What can we learn from genetic studies of systemic lupus erythematosus? Implications of genetic heterogeneity among populations in SLE.* Lupus, 2010. **19**(12): p. 1452-9.

112. Yu, S.L., et al., *Immunopathological roles of cytokines, chemokines, signaling molecules, and pattern-recognition receptors in systemic lupus erythematosus.* Clin Dev Immunol, 2012. **715190**: p. 23.

113. Moulton, V.R. and G.C. Tsokos, *Abnormalities of T cell signaling in systemic lupus erythematosus.* Arthritis Res Ther, 2011. **13**(2): p. 207.

114. Perl, A., *Emerging new pathways of pathogenesis and targets for treatment in systemic lupus erythematosus and Sjogren's syndrome*: Curr Opin Rheumatol. 2009 Sep;21(5):443-7.

115. Deng, C., et al., *Decreased Ras-mitogen-activated protein kinase signaling may cause DNA hypomethylation in T lymphocytes from lupus patients.* Arthritis Rheum, 2001. **44**(2): p. 397-407.

116. Tang, H., et al., *Abnormal activation of the Akt-GSK3beta signaling pathway in peripheral blood T cells from patients with systemic lupus erythematosus.* Cell Cycle, 2009. **8**(17): p. 2789-93.

117. Fernandez, D., et al., *Rapamycin reduces disease activity and normalizes T cell activation-induced calcium fluxing in patients with systemic lupus erythematosus.* Arthritis Rheum, 2006. **54**(9): p. 2983-8.

118. Rathmell, J.C., et al., *Activated Akt promotes increased resting T cell size, CD28-independent T cell growth, and development of autoimmunity and lymphoma.* Eur J Immunol, 2003. **33**(8): p. 2223-32.

119. Parsons, M.J., et al., *Expression of active protein kinase B in T cells perturbs both T and B cell homeostasis and promotes inflammation.* J Immunol, 2001. **167**(1): p. 42-8.

120. Borlado, L.R., et al., *Increased phosphoinositide 3-kinase activity induces a lymphoproliferative disorder and contributes to tumor generation in vivo.* Faseb J, 2000. **14**(7): p. 895-903.

121. Suzuki, A., et al., *T cell-specific loss of Pten leads to defects in central and peripheral tolerance.* Immunity, 2001. **14**(5): p. 523-34.

122. Liu, X., et al., *Distinct roles for PTEN in prevention of T cell lymphoma and autoimmunity in mice.* J Clin Invest, 2010. **120**(7): p. 2497-507.

123. Suzuki, A., et al., *Critical roles of Pten in B cell homeostasis and immunoglobulin class switch recombination.* J Exp Med, 2003. **197**(5): p. 657-67.

124. Anzelon, A.N., H. Wu, and R.C. Rickert, *Pten inactivation alters peripheral B lymphocyte fate and reconstitutes CD19 function.* Nat Immunol, 2003. **4**(3): p. 287-94.

125. Deng, C., et al., *Hydralazine may induce autoimmunity by inhibiting extracellular signal-regulated kinase pathway signaling.* Arthritis Rheum, 2003. **48**(3): p. 746-56.

126. Oelke, K. and B. Richardson, *Decreased T cell ERK pathway signaling may contribute to the development of lupus through effects on DNA methylation and gene expression.* Int Rev Immunol, 2004. **23**(3-4): p. 315-31.

127. Sawalha, A.H., et al., *Defective T-cell ERK signaling induces interferon-regulated gene expression and overexpression of methylation-sensitive genes similar to lupus patients.* Genes Immun, 2008. **9**(4): p. 368-78.

128. Chung, J.H., M.E. Ginn-Pease, and C. Eng, *Phosphatase and tensin homologue deleted on chromosome 10 (PTEN) has nuclear localization signal-like sequences for nuclear import mediated by major vault protein.* Cancer Res, 2005. **65**(10): p. 4108-16.

129. Liu, F., et al., *PTEN enters the nucleus by diffusion.* J Cell Biochem, 2005. **96**(2): p. 221-34.

130. Khandani, A., et al., *Microtubules regulate PI-3K activity and recruitment to the phagocytic cup during Fcgamma receptor-mediated phagocytosis in nonelicited macrophages.* J Leukoc Biol, 2007. **82**(2): p. 417-28.

131. Gundersen, G.G. and T.A. Cook, *Microtubules and signal transduction.* Curr Opin Cell Biol, 1999. **11**(1): p. 81-94.

132. Valiente, M., et al., *Binding of PTEN to specific PDZ domains contributes to PTEN protein stability and phosphorylation by microtubule-associated serine/threonine kinases.* J Biol Chem, 2005. **280**(32): p. 28936-43.
133. Terrien, E., et al., *Interference with the PTEN-MAST2 interaction by a viral protein leads to cellular relocalization of PTEN.* Sci Signal, 2012. **5**(237): p. 2002941.
134. van Diepen, M.T., et al., *MyosinV controls PTEN function and neuronal cell size.* Nat Cell Biol, 2009. **11**(10): p. 1191-6.
135. Ivanova, S., et al., *Cellular localization of MAGI-1 caspase cleavage products and their role in apoptosis.* Biol Chem, 2007. **388**(11): p. 1195-8.
136. Munoz, L.E., et al., *The role of defective clearance of apoptotic cells in systemic autoimmunity.* Nat Rev Rheumatol, 2010. **6**(5): p. 280-9.
137. Mondal, S., et al., *PTEN negatively regulates engulfment of apoptotic cells by modulating activation of Rac GTPase.* J Immunol, 2011. **187**(11): p. 5783-94.
138. Cohen, P.L. and R.A. Eisenberg, *The lpr and gld genes in systemic autoimmunity: life and death in the Fas lane.* Immunol Today, 1992. **13**(11): p. 427-8.
139. Aksamitiene, E., A. Kiyatkin, and B.N. Kholodenko, *Cross-talk between mitogenic Ras/MAPK and survival PI3K/Akt pathways: a fine balance.* Biochem Soc Trans, 2012. **40**(1): p. 139-46.
140. Bric, A., et al., *Functional identification of tumor-suppressor genes through an in vivo RNA interference screen in a mouse lymphoma model.* Cancer Cell, 2009. **16**(4): p. 324-35.
141. de Vries-Smits, A.M.M., et al., *Involvement of p21ras in activation of extracellular signal-regulated kinase 2.* Nature, 1992. **357**(6379): p. 602-604.
142. Fujikawa, A., et al., *Consensus substrate sequence for protein-tyrosine phosphatase receptor type Z.* J Biol Chem, 2011. **286**(43): p. 37137-46.
143. Kogan, S.C., et al., *Bethesda proposals for classification of nonlymphoid hematopoietic neoplasms in mice.* Blood, 2002. **100**(1): p. 238-45.
144. Cripps, J.G. and J.D. Gorham, *MDSC in autoimmunity.* Int Immunopharmacol, 2011. **11**(7): p. 789-93.
145. Chiu, J., et al., *Site-directed, Ligase-Independent Mutagenesis (SLIM): a single-tube methodology approaching 100% efficiency in 4 h.* Nucleic Acids Research, 2004. **32**(21): p. e174.
146. Sanchez, T., et al., *PTEN as an effector in the signaling of antimigratory G protein-coupled receptor.* Proceedings of the National Academy of Sciences of the United States of America, 2005. **102**(12): p. 4312-4317.

CURRICULUM VITAE

First name	Katarina
Last name	Zmajkovicova
Date of birth	8.12.1985
Nationality	Slovak
Address	Kamenarska 3
	82104 Bratislava
	Slovakia

Contact   Zmajkovicova.katarina@gmail.com
+421 904 004 021
+43 676 4755000

Education

2009-2013   PhD in Molecular Biology
Universitat Wien, Austria

2007-2009   Master in Biomedical Sciences – graduated with 'Magna cum laude'
Katholieke Universiteit Leuven, Belgium

2004-2007   Bachelor in Biology
Comenius University, Bratislava, Slovakia

Research experience

2009-2013   Doctoral thesis 'Role of MEK1 in the crosstalk between signaling cascades'
MAPK signaling, Laboratory of Manuela Baccarini, Max F Perutz Laboratories, Vienna, Austria

2008-2009   Master thesis 'TRN-SR2 as a cellular cofactor of HIV infection'
Laboratory of Molecular Virology and Gene Therapy, Division of Molecular Medicine, Katholieke Universiteit Leuven, Belgium

2008   Lab rotations, Neurobiology and Gene Therapy (Prof. Veerle Baekelandt), Laboratory of Molecular Genetics of Human Malignancies (Prof. Maria Debiec-Rychter),

2006-2007   Bachelor thesis, Laboratory of Molecular Oncology, Cancer Research Institute, Slovak Academy of Sciences, Bratislava, Slovakia

Publications	De Houwer S., Demeulemeester J., Thys W, Taltynov O., <u>Zmajkovicova K.</u>, Christ F. and Debyser Z. (2012) **Identification of Residues in the C-terminal Domain of HIV-1 Integrase That Mediate Binding to the Transportin-SR2 Protein**, *J. Biol. Chem.* 287: 34059-34068
	<u>Zmajkovicova K</u>., Jesenberger V., Catalanotti F., Baumgartner C., Reyes G. and Baccarini M. **MEK1 is required for PTEN membrane recruitment, AKT regulation, and the maintenance of peripheral tolerance**, *Molecular Cell*, in revision

Congresses/awards

2012	PTEN Pathways&Targets, Cold Spring Harbor, USA; poster presentation
2012	Winner of the 'Young Oncologist Award' award for young doctoral researcher in the field of oncology, Slovakia
2011	Hallmarks and Horizons of Cancer, Lausanne, Switzerland; poster presentation

Technical skills

Cell culture	isolation and cultivation of various cell lines and primary cells, transfections, viral vector production, viral transductions, cell death assays, ELISpot
Mice handling	basic maintenance and breeding of mice, isolation of organs and peripheral blood
FACS	flow cytometric analysis of surface and intracellular antigens
Microscopy	light micrscopy and confocal microscopy, immunofluorescence
Histology	isolation, fixation and embedding of tissue, paraffin and frozen sections, basic histological and immunostainings
Protein biochemistry	western blot, immunoprecipitation, pull-down, enzymatic assays, ELISA
DNA methods	PCR, qPCR, cloning, site-directed mutagenesis
Computer skills	MS-Office, Adobe Illustator, Adobe Photoshop, ImageJ, FlowJo, Lasergene

Teaching experience

2011-2012   Supervision of diploma student Christian Baumgartner

2012   Immunology practicum, University of Vienna

Language skills

Slovak   mother tongue
English   fluent, FCE certificate
German   advanced, KMK Stufe II certificate
Dutch   advanced, Level 5 certificate from KULeuven
Spanish   basic